

Republic of Yemen

Emirate International University

Engineering and IT Faculty

Oil and Gas Engineering



الجمهورية اليمنية

الجامعة الإماراتية الدولية

كلية الهندسة وتقنية المعلومات

قسم هندسة النفط والغاز

**EMIRATES INTERNATIONAL UNIVERSITY
FACULTY OF ENGINEERING AND INFORMATION
TECHNOLOGY
OIL AND GAS ENGINEERING DEPARTMENT**

**WELL TEST ANALYSIS TO CHARACTERIZE QISHAN CLASTIC
MEMBER RESERVOIR IN SHARYOOF FIELD BLOCK-(53)**

**A PROJECT SUBMITTED IN PARTIAL FULFILLMENT OF THE
REQUIREMENTS FOR THE BACHELOR DEGREE OF OIL AND GAS
ENGINEERING**

DONE BY:

**RIYADH ALI NASSER SHAYA
HASHEM ABDULLAH AL-WASHALI
ALI ABDULHAMEED ALI GHURAB
HAFEDH ABDULLAH NASSER SHAYA
SULIMAN AHMED MOHAMMED AL-NTAIAH**

SUPERVISOR:

Eng. Mohammed Abbas

SANA'A

June-2024

DECLARATION

We hereby declare that this Bachelor's Project is the result of our own work, except for quotations and summaries which have been duly acknowledged.

Name:	Riyadh Ali Nasser Shaya	Signature	Date
Matric. Number:	2020070260		
Name:	Hashem Abdullah Al-washali	Signature	Date
Matric. Number:	2019060918		
Name:	Ali Abdulhameed Ali Ghurab	Signature	Date
Matric. Number:	2020070268		
Name:	Hafedh Abdullah Nasser Shaya	Signature	Date
Matric. Number:	2020070349		
Name:	Suliman Ahmed Mohammed Al-ntaiah	Signature	Date
Matric. Number:	2020071279		

APPROVAL

This is to certify that the project titled (**Well Test Analysis to Characterize Qishan Clastic Member Reservoir in Sharyoof Field Block-(53)**) has been read and approved for meeting part of the requirements and regulations governing the award of the Bachelor of Engineering (Oil and Gas) degree of Emirates International University, Sana'a, Yemen.

Project Supervisor: Eng. Mohammed Abbas

Date:

Signature:

ABSTRACT

Reservoir characterization is a process of describing variations in rock and fluid properties related to the reservoir. Well testing may provide important information related to reservoir pressure, reservoir size, distance from well to boundaries, type of boundaries (permeable/impermeable), heterogeneities in reservoir, flow rates, formation condition, productivity index. The main reservoir characterizations are very important to understand and identify the flow behavior of the reservoir such initial reservoir pressure, porosity, average permeability, water saturation, net pay zone, oil viscosity, formation transmissibility, formation conductivity, formation mobility, and the radius of investigation,

In this study Qishn Clastic reservoir in Sharyoof field Block 53 Masila basin, characterized by well test analysis approach using model's interpretation and petrophysical analysis to better understand the reservoir fluid movements and improve reservoir development plans. Some models are used to characterize and determine well and reservoir parameters to enhance the accuracy and reliability of the reservoir properties. Petro-physical analysis was done for Qishn Clastic formation by using Tech-log software to determine porosity, shale volume, water saturation and lithology distribution. Pressure Transient Analysis (PTA) was done for Qishn Clastic formation by using Excel and Ecrin Softwares to determine well and reservoir parameters such as permeability, skin factor, initial reservoir pressure and other parameters. In this study the pressure builds up test analysis Using Semi-log and derivative methods was done. The Semi-log method used Horner and MDH Plots, and the derivative method used infinite acting model, reservoir boundary model, single fault boundary model, and intersecting fault boundary model to determine well and reservoir parameters as well to make some scenarios then we selected the best match. Finally, our results show summary of Qishn clastic reservoir characterization and Sharyoof-2 well doesn't require a stimulation operations job because the low values of skin factor moreover a good match was observed from the models as well, we recognized and make sure there is no fault between Sharyoof-1 well and Sharyoof-2 well.

ACKNOWLEDGMENTS

At the beginning, we definitely confess our most genuine gratitude to Allah, who is the most omnipotent and the powerful for granting us such, a strength, endurance, patience, immutability, capability to accomplish this research.

We would also like to express our deep and sincere gratitude to our supervisor, Eng. Mohammed Abbas, for his valuable and constructive suggestions during the planning and development of this research work and his wide knowledge and his logical way of thinking that have been of great value for us. His willingness to give his time so generously has been very much appreciated. His feedback, support, encouraging, patience and personal guidance have provided a good basis for the present project.

Not to forget thanking Dr. Ibrahim Farea the head of the faculty of Oil and Gas Engineering for his great effort and time. Our special gratitude is due to all those who have helped in carrying out the research and contributed in any way for the success of this Project.

Finally, yet importantly, we would like to express our heartfelt thanks to our beloved family for their blessings, our friends/classmates for their help and wishes for the successful completion of this project.

THE CONTENTS

CHAPTER ONE	1
1. INTRODUCTION	2
1.1 OVERVIEW.....	2
1.2 AIMS AND OBJECTIVES.....	3
1.2.1 AIMS	3
1.2.2 OBJECTIVES	3
1.3 PROBLEM STATEMENT:	3
1.4 GEOLOGY OF YEMEN.....	5
1.4.1 STRATIGRAPHY OF YEMEN:	6
1.4.1.1 PALEOZOIC SEDIMENTS:	6
1.4.1.2 MESOZOIC SEDIMENTS:	7
1.4.1.3 CENOZOIC SEDIMENTS:	7
1.4.1.4 BASEMENT ROCKS.....	9
1.4.2 MASILA-SAY'UN BASIN.....	9
1.5 STUDY OF AREA	10
1.5.1 BLOCK (53)	10
1.5.2 SHARYOOF OILFIELD	12
CHAPTER TWO	16
2. LITERATURE REVIEW AND THEORETICAL BACKGROUND.....	17
2.1 PREVIOUS STUDY	17
2.1.1 CASE STUDY (1).....	17
2.1.1.1 GENERAL INFORMATION ABOUT CASE STUDY.....	17
2.1.1.2 THE METHOD OF THE CASE STUDY	17
2.1.1.3 RESULTS AND CONCLUSION	17
2.1.2 CASE STUDY (2).....	23
2.1.2.1 GENERAL INFORMATION ABOUT CASE STUDY	23
2.1.2.2 THE METHOD OF THE CASE STUDY	24
2.1.2.3 RESULTS AND CONCLUSION	26
2.2 WELL TESTING	30
2.2.1 ROLE OF OIL WELL TESTS AND INFORMATION IN PETROLEUM INDUSTRY	30
2.2.2 TYPES OF WELL TESTS:.....	31
2.2.2.1 PRESSURE DRAWDOWN TEST	31
2.2.2.2 PRESSURE BUILDUP TEST	34
2.2.2.3 DRILL STEM TEST	41
2.3 WELL TEST INTERPRETATION METHODS:.....	51
2.3.1 CONVENTIONAL METHODS:	52
2.3.1.1 SEMI-LOG APPROACH	52
2.3.1.2 MDH PLOT	53
2.3.1.3 HORNER PLOT.....	54
2.3.1.4 MBH METHOD	56
2.3.2 TYPE CURVES METHODS.....	58
2.3.3 THE PRESSURE DERIVATIVE METHOD.....	65
2.4 WELL TEST ANALYSIS MODELS:	67
2.4.1 WELLBORE MODELS.....	67

2.4.1.1 CONSTANT WELLBORE STORAGE MODEL.....	67
2.4.1.2 CHANGE WELLBORE STORAGE MODEL	68
2.4.2 WELL MODELS	70
2.4.2.1 VERTICAL FULLY PENETRATING WELL.....	70
2.4.2.2 FRACTURED WELLS	71
2.4.2.3 LIMITED ENTRY WELL	73
2.4.2.4 HORIZONTAL WELLS.....	75
2.4.3 RESERVOIR MODELS	77
2.4.3.1 HOMOGENEOUS RESERVIOR	77
2.4.3.2 HETEROGENEOUS:	79
2.4.3.2.1 DOUBLE POROSITY.....	79
2.4.3.2.2 DOUBLE PERMEABILITY.....	81
2.4.3.2.3 COMPOSITE RESERVOIRS	82
2.4.4 RESERVOIR BOUNDARIES MODELS	84
2.4.4.1 LINEAR BOUNDARIES	85
2.4.4.2 CIRCULAR BOUNDARIES.....	87
2.4.4.3 INTERSECTING FAULTS	89
2.4.4.4 PARALLEL FAULTS (CHANNEL).....	90
2.4.4.5 MIXED BOUNDARY RECTANGLE	91
CHAPTER THREE.....	93
3.METHODOLOGY	94
3.1. INTRODUCTION	94
3.2 DATA REQUIRED	94
3.3.2 KAPPA ECRIN:.....	95
3.3.3 TECHLOG 2015.3.....	95
3.4. STEPS OF STUDY.....	96
3.5. EXPECTED OUTCOME	96
CHAPTER FOUR.....	97
4. INTERPETATION AND RESULTS	98
4.1 INTRODUCTION.....	98
4.1.1 SHARYOOF-2 WELL SUMMARY OVERVIEW	98
4.1.1.1 DRILLING AND COMPLETION SUMMARY	98
4.1.1.2 PETROPHYSICAL ANALYSIS SUMMARY	100
4.2 DST OVERVIEW	102
4.2.1 WELL TEST INFORMATION	103
4.2.2 DATA VALIDATION.....	103
4.3 PRESSURE TRANSIENT ANALYSIS (PTA)	104
4.3.1 PRESSURE BUILDUP ANALYSIS USING SEMI-LOG METHOD.....	105
4.3.1.1 SEMI LOG ANALYSIS USING MS EXCEL 2016:	105
4.3.1.1.1 HORNER PLOT METHOD.....	105
4.3.1.1.2 MILLER-DYE-HUTCHINSON MDH PLOT METHOD	108
4.3.1.2 SEMI-LOG ANALYSIS USING ECRIN 4.20 SOFTWARE:	111
4.3.1.2.1 HORNER PLOT METHOD.....	111
4.3.1.2.2 MILLER-DYE-HUTCHINSON MDH PLOT METHOD	112
4.3.2 PRESSURE BUILDUP ANALYSIS USING DERIVATIVE METHOD	115

4.3.2.1 INFINITE ACTING MODEL:	115
4.3.2.2 RESERVOIR BOUNDARY MODELS:	118
4.3.2.2.1 SINGLE FAULT BOUNDARY MODEL:	118
4.3.2.2.2 INTERSECTING FAULT BOUNDARY MODEL	120
4.4 SUMMARY RESERVOIR CHARACTERIZATION AND WELL PERFORMANCE EVALUATION	122
CHAPTER FIVE	123
5. CONCLUSIONS AND RECOMMENDATIONS	124
5.1. INTRODUCTION	124
2.2 CONCLUSIONS	124
5.3 RECOMMENDATIONS	125
5.4 LIMITATIONS	125
REFERENCES	126

FIGURE CONTENT

FIGURE 1.1 SEISMIC SECTION	4
FIGURE 1.2 SEDIMENTARY BASINS OF YEMEN	6
FIGURE 1.3 STRATIGRAPHY AND PETROLEUM SYSTEMS OF SAB'ATAYN AND SAY'UN-MASILAH BASINS. (SOURCE: AS-SARURI & SORKHABI (2016)).	8
FIGURE 1.4 MASILA BASIN STRATIGRAPHIC SUMMARY.	11
FIGURE 1.5 (A) MAIN SEDIMENTARY BASINS IN REPUBLIC OF YEMEN (MODIFIED AFTER BEYDOUN ET AL. [12]) AND (B) LOCATION MAP OF SOME MASILA BASIN'S BLOCKS INCLUDING SHARYOOF OILFIELD (BLOCK 53), HADRAMAWT REGION OF THE REPUBLIC OF YEMEN.....	12
FIGURE 1.6 STRATIGRAPHIC COLUMN IN THE MASILA BASIN, INCLUDING SHARYOOF OILFIELD OF THE EASTERN YEMEN.	14
FIGURE 1.7 LOG CHARACTERISTICS OF GAMMA AND RESISTIVITY LOGS USED FOR LITHOLOGIC CHARACTERIZATION OF MAIN UNITS OF QISHN SANDSTONE RESERVOIR.	15
FIGURE 2.1. PRESSURE GAUGES SYNCHRONIZATION	21
FIGURE 2.2 RATE AND PRESSURE PROFILE OF UKOT WELL	21
FIGURE 2.3 LOG-LOG MODEL OF UKOT WELL.....	22
FIGURE 2.4 LOG-LOG PLOT OF AGBA 8.....	22
FIGURE 2.5 LOG-LOG OUTPUT RESULT OF AGBA 8	23
FIGURE 2.6 STRUCTURE CONTOUR MAP	25
FIGURE 2.7A PRESSURE TRANSIENT TEST OVERVIEW.....	27
FIGURE 2.7B PRESSURE TRANSIENT TEST OVERVIEW	28
FIGURE-2.8A RADIAL COMPOSITE CASE	28
FIGURE-2.8B RADIAL COMPOSITE CASE	29
FIGURE 2.9A SINGLE FAULT MODEL	29
FIGURE 2.9B SINGLE FAULT MODEL	30
FIGURE 2.10 IDEALIZED PRESSURE DRAWDOWN TEST.....	32
FIGURE 2.11 SEMILOG PLOT OF PRESSURE DRAWDOWN DATA	34
FIGURE 2.12 PRESSURE BUILDUP TEST AND MAIN FLOW PERIOD	35
FIGURE 2.13 IDEALIZED PRESSURE BUILDUP TEST	36
FIGURE 2.14 BEHAVIOR OF THE STATIC PRESSURE ON SHUT-IN OIL WELL	37
FIGURE 2.15 SEMILOG PLOT OF PRESSURE BUILDUP DATA.....	38
FIGURE 2.16 OPERATIONAL DST TOOL	44
FIGURE 2.17 DST PRESSURE RECORD	45

FIGURE 2.18 DST PRESSURE CHART FOR TWO-CYCLE TEST	45
FIGURE 2.19 FLOW RATE THREE-CYCLE DST	46
FIGURE 2.20 BOTTOM-HOLE PRESSURE THREE-CYCLE DST.....	46
FIGURE 2.21 MOST COMMON METHODS TO ANALYZE DST DATA AND THEIR LIMITATIONS.	48
FIGURE 2.22 PRE-FLOW PERIOD	49
FIGURE 2.23 INITIAL SHUT-IN	50
FIGURE 2.24 MAIN FLOW	50
FIGURE 2.25 FINAL SHUT-IN	51
FIGURE 2.26 WTI ESSENTIALS	51
FIGURE 2.27 SEMI-LOG APPROACH.....	52
FIGURE 2.28 MDH PLOT	53
FIGURE 2.29 HORNER PLOT	55
FIGURE 2.30 CURVES FOR SQUARE DRAINAGE AREA	57
FIGURE 2.31 CURVES FOR 2x1 RECTANGLE	57
FIGURE 2.32 CURVES FOR 4x1 RECTANGLE	58
FIGURE 2.33 DIMENSIONLESS PRESSURE FOR A SINGLE WELL IN AN INFINITE SYSTEM	59
FIGURE 2.34 TRACING PAPER.....	60
FIGURE 2.35A GRINGARTEN TYPE CURVE	61
FIGURE 2.35B GRINGARTEN TYPE CURVE	61
FIGURE 2.36 DERIVATIVE AND PRESSURE TYPE CURVES FOR A WELL WITH WELLBORE STORAGE AND SKIN IN INFINITE-ACTING HOMOGENEOUS RESERVOIR.3	66
FIGURE 2.37 WELLBORE STORAGE	67
FIGURE 2.38 WELLBORE STORAGE.....	68
FIGURE 2.39 PRODUCTION INCREASING STORAGE	69
FIGURE 2.40 BUILD-UP DECREASING STORAGE	69
FIGURE 2.41 LOGLOG PLOT, SKIN	70
FIGURE 2.42 SEMILOG PLOT, SKIN.....	71
FIGURE 2.43 INFINITE CONDUCTIVITY FRACTURE BEHAVIOR	73
FIGURE 2.44 LIMITED ENTRY	73
FIGURE 2.45 LIMITED ENTRY FLOW REGIMES	74
FIGURE 2.46 LIMITED ENTRY RESPONSE	74
FIGURE 2.47 HORIZONTAL WELL.....	75
FIGURE 2.48 HORIZONTAL WELL FLOW REGIMES	76
FIGURE 2.48 HORIZONTAL WELL RESPONSES	76
FIGURE 2.49 HORIZONTAL WELL RESPONSES	77
FIGURE 2.50 HOMOGENEOUS LOGLOG PLOTS.....	78
FIGURE 2.51 LINE SOURCE.....	78
FIGURE 2.52 HOMOGENEOUS SEMILOG PLOT	79
FIGURE 2.53 FISSURE SYSTEM PRODUCTION.....	80
FIGURE 2.54 TOTAL SYSTEM PRODUCTION	80
FIGURE 2.55 DOUBLE PERMEABILITY	81
FIGURE 2.56 DOUBLE PERMEABILITY TYPE-CURVE	82
FIGURE 2.57A RADIAL COMPOSITE RESERVOIR.....	83
FIGURE 2.57B LINEAR COMPOSITE RESERVOIR	83
FIGURE 2.58A BOUNDARY MODELING	84
FIGURE 2.58B BOUNDARY MODELING	84
FIGURE 2.58C BOUNDARY MODELING	84

FIGURE 2.59 LINEAR BOUNDARIES	85
FIGURE 2.60 LINEAR BOUNDARY RESPONSE	86
FIGURE 2.61 SEMI-LOG RESPONSE	86
FIGURE 2.62 CIRCULAR BOUNDARIES.....	87
FIGURE 2.63 CLOSED CIRCULAR BOUNDARY	88
FIGURE 2.64A CONSTANT PRESSURE CIRCLE.....	88
FIGURE 2.64B CONSTANT PRESSURE CIRCLE.....	89
FIGURE 2.64C CONSTANT PRESSURE CIRCLE	89
FIGURE. 2.65 INTERSECTING FAULTS	90
FIGURE 2.66A PARALLEL FAULTS	90
FIGURE 2.66B PARALLEL FAULTS.....	91
FIGURE 2.67A MIXED BOUNDARY RECTANGLE	91
FIGURE 2.67B MIXED BOUNDARY RECTANGLE	92
FIGURE 3.1 SHOWS THE DISPLAY WINDOW OF ECRIN SOFTWARE	95
FIGURE 3.2 SHOWS THE DISPLAY WINDOW OF TECHLOG 2015.3	96
FIGURE 4.1 SHARYOOF-2 COMPLETION SCHEMATIC.....	99
FIGURE 4.2 SHARYOOF-2 WELL CPI.....	101
FIGURE 4.3 DST_2 LOWER S1A HISTORY PLOT.....	102
FIGURE 4.4 PRESSURE GAUGE COMPARISON.....	103
FIGURE 4.5 HISTORY PLOT USING ECRIN 4.2	104
FIGURE 4.6 HISTORY PLOT USING EXCEL 2016	105
FIGURE 4.7 HORNER PLOT USING MS EXCEL2016.....	106
FIGURE 4.8 LOG-LOG PLOT	106
FIGURE 4.9 LOG-LOG PLOT	107
FIGURE 4.10 MDH PLOT METHOD.....	108
FIGURE 4.11 HORNER PLOT USING ECRIN 4.20.....	111
FIGURE 4.12 MDH PLOT USING ECRIN SOFTWARE	112
FIGURE 4.13 HORNER PLOT RESULTS USING ECRIN 4.20.....	114
FIGURE 4.14 INFINITE MODEL	116
FIGURE 4.15 INFINITE MODEL PLOT RESULTS USING ECRIN 4.20	117
FIGURE 4.16 SINGLE FAULT BOUNDARY MODEL.....	118
FIGURE 4.17 SINGLE FAULT BOUNDARY MODEL RESULTS USING ECRIN 4.20	119
FIGURE 4.18 INTERSECTING FAULT BOUNDARY MODEL.....	120
FIGURE 4.19 INTERSECTING FAULT BOUNDARY MODEL RESULTS USING ECRIN 4.20	121

TABLES CONTENT

TABLE 2.1 WELL AND RESERVOIR DATA OF UKOT AND AGBA 8WEL	18
TABLE 2.2 UKOT WELL RATE PROFILE.....	18
TABLE 2.3 SCHEDULE OF AGBA 8.....	18
TABLE 2.4 RESULT FROM SAPHIR (UKOT WELL).....	19
TABLE 2.5 RESULT FROM SAPHIR (WELL AGBA 8)	20
TABLE 2.6 THE GENERAL WELL DATA	24
TABLE 2.7 RESERVOIR FLUID PROPERTIES USED FOR BUILD-UP ANALYSIS.....	26
TABLE 2.8 COMPARISON OF THE RESULTS GENERATED BY BOTH THE MODELS	27
TABLE 3.1 DATA AVAILABLE FOR THE PROJECT.....	94
TABLE 4.1 WELL COMPLETION	98
TABLE 4.2 SUMMARIZE PETROPHYSICAL PROPERTIES USING WELL LOG ANALYSIS	102
TABLE 4.3 WELL AND TEST INFORMATION	103
TABLE 4.4 HORNER PLOT RESULT USING MS. EXCEL	107
TABLE 4.5 MDH PLOT RESULT USING MS. EXCEL	109
TABLE 4.6 COMPARATION AND SUMMARIZE OF THE DIFFERENCE VALUES ESTIMATED OF WELL TEST INTERPRETATION PARAMETERS OF LOWER QISHN CLASTIC S1A FOR SHARYOOF-2	110
TABLE 4.7 HORNER PLOT RESULT USING ECRIN SOFTWARE	111
TABLE 4.8 MDH PLOT RESULT USING ECRIN SOFTWARE	112
TABLE 4.9 IS COMPARISON SEMI LOG METHODS RESULTS FROM EXCEL AND ECRIN SOFTWARE	113
TABLE 4.10 S1A LOWER QISHN CLASTIC RESERVOIR CHARACTERIZATION	122
TABLE 4.11 SHARYOOF-2 WELL PERFORMANCE EVALUATION	122

LIST OF ABBREVIATIONS USED IN OUR GP

- **WT:** Well Test
- **DDT:** Drawdown Test
- **BUT:** Buildup Test
- **DST:** Drill Stem Test
- **PTA:** Pressure Transient Analysis
- **ETR:** Early Time Region
- **MTR:** Middle Time Region
- **LTR:** Late Time Region
- **WBS:** Wellbore Storage
- **m:** Cementation Factor
- **n:** Saturation Exponent
- **a:** Porosity Tortuosity Constant
- **R_w:** Formation Water Resistivity
- **Q_o:** Oil flow rate
- **Bo:** Oil formation volume factor
- **μ_o:** Oil viscosity factor
- **Co:** Oil compressibility factor
- **Ct:** Total compressibility factor
- **h:** Net pay
- **Ø:** Porosity
- **Sw:** Water Saturation
- **r_w:** Wellbore radius
- **P_{wf}:** Bottom hole flowing pressure
- **P_{ws}:** Shut-in bottom hole pressure
- **P_i:** Initial or Intercept Pressure
- **P_{1hr}:** Pressure at one hour
- **m:** Slope
- **K:** Effective Permeability
- **Kh:** Formation Transmissibility
- **S:** Skin Factor
- **DP_{skin}:** Pressure Drop due to skin factor
- **FE:** Flow Efficiency
- **DR:** Damage Ratio
- **R_{inv}:** Radius of investigation
- **PI:** Productivity Index
- **Cs:** Wellbore Storage
- **Twbs:** End of the wellbore storage distortion



CHAPTER ONE





1. Introduction

1.1 Overview

Reservoir characterization is a process of describing variations in rock and fluid properties related to the reservoir. Well testing may provide important information related to reservoir pressure, reservoir size, distance from well to boundaries, type of boundaries (permeable/impermeable), heterogeneities in reservoir, flow rates, formation condition, productivity index. Well tests are good for geological modeling through analyzing pressure transient tests to identify reservoir characteristics and boundaries. Reservoir parameters found from pressure transient analysis (PTA) is then used to update geological models and to see if it is consistent with already known data.

Well Test Analysis is an area of reservoir engineering that deals with understanding reservoir characteristics with principles of fluid flow in porous rock using different techniques. There are several formulas used in well test analysis in determination of important parameters including but not limited to permeability, thickness, skin, extent, pressure of the reservoir. Also, in this project the data which is interpreted using Ms Excel and Ecrin Software were from one well DST. The buildup test result is interpreted using analytical models and a Horner and MDH plots in order to evaluate the reservoir. Pressure transient test is designed to create pressure disturbance in reservoir by controlled flow periods known as drawdown and buildup tests. These two periods are a result of production from reservoir as rate changes, constant rate (well shut) for buildup and variable rates (producing reservoir effluent) for drawdowns. Presence of wellbore storage, skin effects, production history (if any) and rate changes will distort important features in pressure and rate responses. In Sharyoof field a re-interpretation of performed well test are conducted. Analytical models are used to identify new possible flow patterns and test leakage through faults (if present). Using existing pressure/rate data from historical production and a geological map to outline faults and fractures analytical model is created.

The importance of well test analysis in reservoir characterization will keep increasing together with the understanding of geology, new interpretation techniques and development of improved downhole gauges and flowmeters. However, for wider testing and identification of bigger fracture networks a well test (drill stem test) is needed.

Since a well test and subsequent pressure transient analysis is the most powerful tool available to the reservoir engineer for determining reservoir characteristics, the subject of well test analysis has attracted considerable attention. A well test is the only method available to the reservoir engineer for examining the dynamic response in the reservoir and considerable information can be gained from a well test.

1.2 Aims and objectives

1.2.1 Aims

The aim of this graduation project is conducted to determination of key well and reservoir parameters to enhance the accuracy and reliability of reservoir characterization to make sure it is consistent with already known data.

1.2.2 Objectives

To achieve the aim of the project, the following objectives are defined:

1. Conduct pressure transient analysis on existing data in Sharyoof-2 using conventional and analytical approach together with geological information
2. Utilizing Ecrin software to implement different scenarios of for analytical models and selecting the most suitable approach that give the best match
3. Understand analytical modeling and how it may be used to increase knowledge on reservoir formation in Sharyoof field and identify possible compartments and boundaries around the well tested
4. Provide recommendations, based on the study results, as to the best way to develop and manage field strategies.
5. Come out with conclusion and recommendations points that add positive value to the study.

1.3 Problem statement:

Initial seismic mapping (Fig.1.1) suggested the possibility of a fault close to S-2 and between the Sharyoof-1 and Sharyoof-2 wells but the response Sharyoof-1 indicated it seems there is no fault exist so well test response needed to enhance the accuracy and reliability of reservoir characterization .Run well test interpretation by using Ecrin software, the results will help to properly characterize the reservoir if it is recognized possibility of fault near Sharyoof-2 and a lot of valuable information is obtained, such as formation permeability, formation damage around the wellbore due to drilling and complexity, reservoir pressure and reservoir boundaries. This experiment will be analyzed by using Pressure Build Up test and will also analyses curve derivative type. In this analysis the Horner plot, MDH plot and Derivative plot are used to determine the reservoir characteristics of Sh-2 well, moreover to find the reservoir model and the indication of formation damage due to skin.

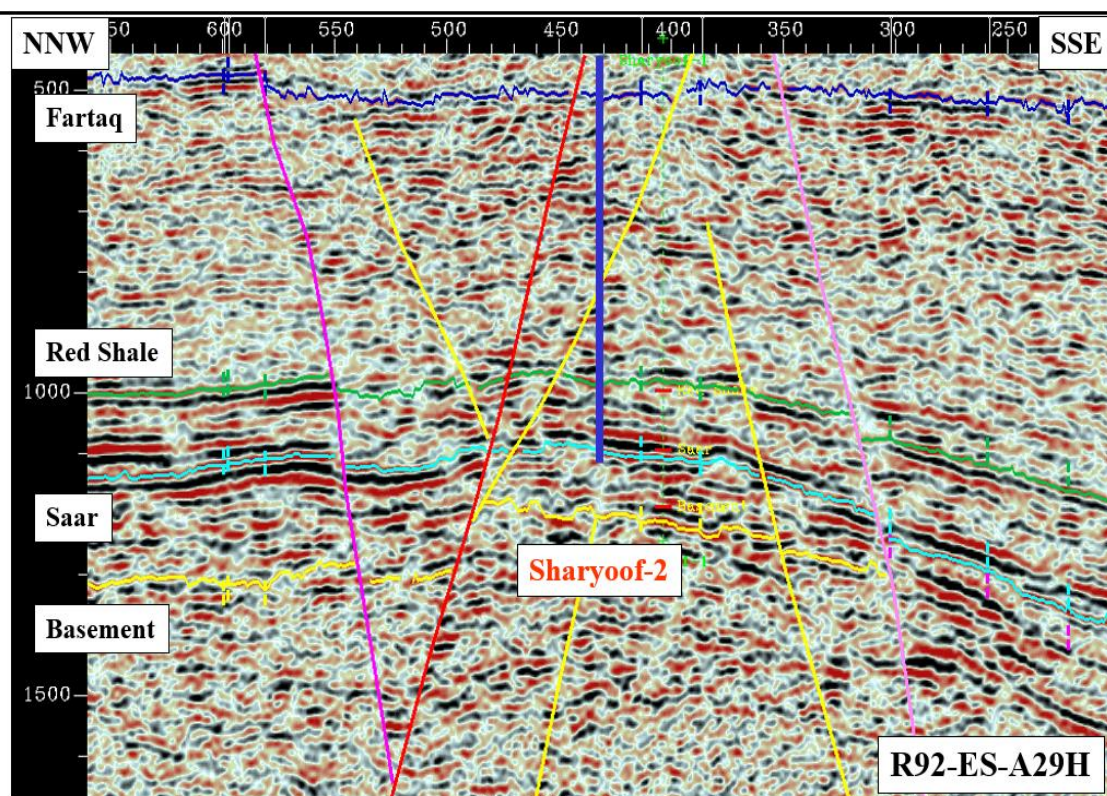
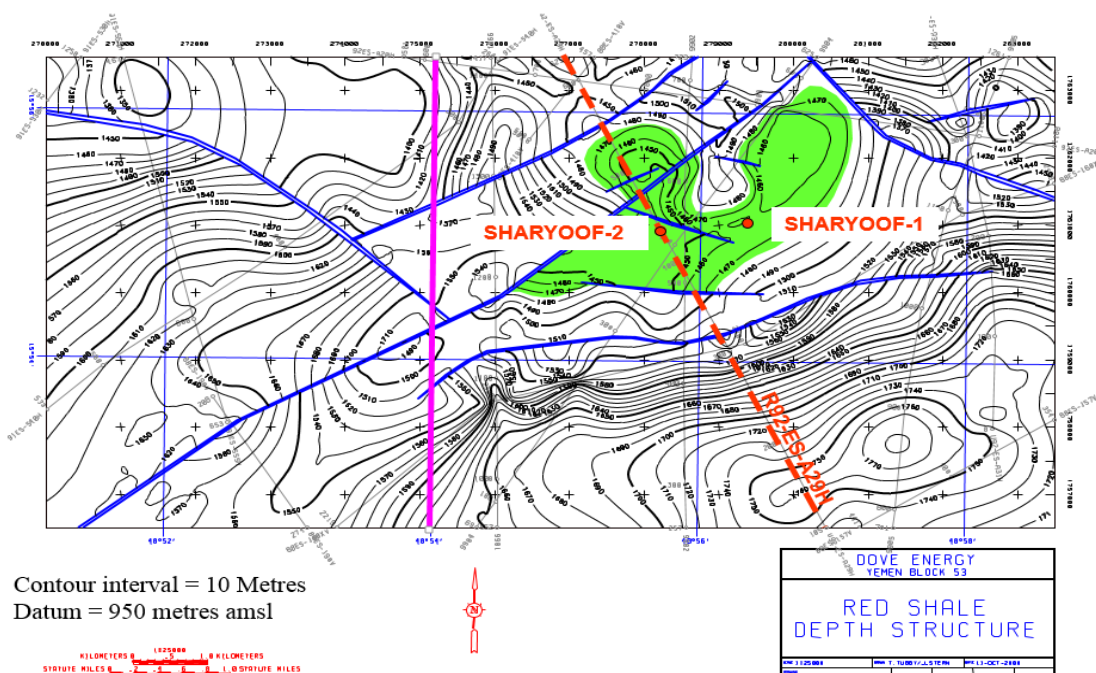


Figure 1.1 seismic section

1.4 Geology of Yemen

Republic of Yemen, is an Arab country in Western Asia, occupying South Arabia, the southern end of the Arabian Peninsula. Yemen is the second-largest country in the peninsula, occupying 555,000 km². The coastline stretches for about 2,200 km. It is bordered by Saudi Arabia to the north, the Red Sea to the west, the Gulf of Aden and Arabian Sea to the south, and Oman to the east-northeast. Yemen is in the Asia continent and the latitude and longitude for the country are 12° - 18° N, 42° - 53° E.

Yemen is covered with rocks whose ages date back to an era prior to the Cambrian era, about 3 billion years ago. Geologically speaking, Yemen composes part of the Arabian Shield within the larger framework of the Arabian-Nubian Shield. It has twelve onshore and offshore sedimentary basins have been identified in Yemen, categorized into three groups based on the geological era in which they originated: Paleozoic, Mesozoic and Cenozoic. (Fig 1.2).

Paleozoic basins:

- Rub' Al-Khali (the southern flank of a much larger basin extending into Saudi Arabia).
- Sana'a.
- Suqatra (an island in the Gulf of Aden).

Mesozoic basins:

- Siham-Ad-Dali.
- Sab'atayn.
- Say'un-Masilah.
- Balhaf.
- Jiza'-Qamar.

Cenozoic basins:

- Mukalla-Sayhut.
- Hawrah-Ahwar.
- Aden-Abyan.
- Tihamah.

Only Two, Sab'atayn and Say'un-Masilah basins, are well explored and produced hydrocarbon.

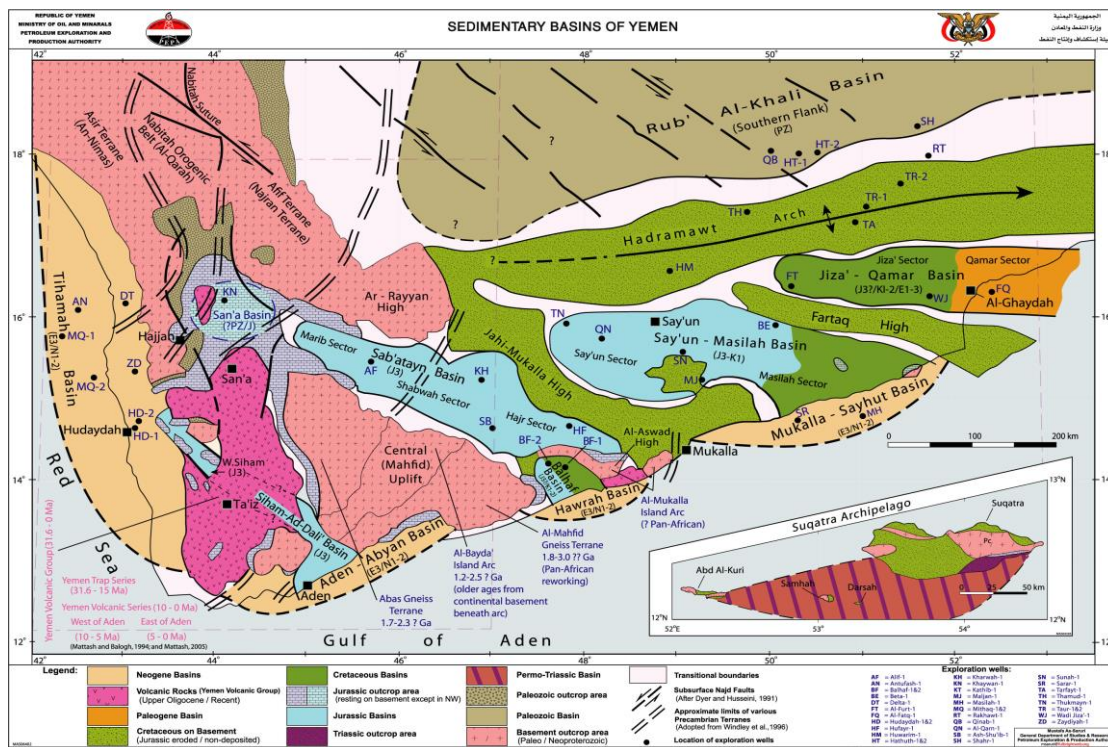


Figure 1.2 Sedimentary basins of Yemen

1.4.1 Stratigraphy of Yemen:

The stratigraphic manners in which The Sedimentological characters of sedimentary rocks i.e. environment, sediment transport agencies and the nature of the syn to post depositional tectonic activities modify the stratigraphic order of deposition are significant in terms of their depositional environment, the thickness of the formations and primary structures. Since the tectonics related to stratigraphy are manifested in the distribution of sediments in Yemen, as illustrated in the geological column (Fig1.3).

1.4.1.1 Paleozoic Sediments:

- Ghabar Group (Infra-Cambrian-Earliest Paleozoic): Sandstone limestone, silt, gypsum.
- Qina Group (Infra Cambrian-Lowest Cambrian): Volcano-sedimentary succession consisting of dolerite, sandstone, silty shale and tuff.
- consisting of dolerite, sandstone, silty shale and tuff.
- Wajid Formation (Cambrian - Carboniferous): Quartz sandstone.
- Akbarah formation (Late Carboniferous-Permian): Tillite (pebbles & boulders of basement rocks), shales, mudstones, sandstones and siltstones.



1.4.1.2 Mesozoic Sediments:

- Kuhlan Formation (Lower-Middle Jurassic): Sandstones, thin claystone and siltstone interbeds.
- Amran Group (Middle Jurassic-Lower Cretaceous): Carbonate marl/shale with evaporitic succession.
- Tawilah Group (Cretaceous): Sandstone with siltstone, marl, and shale, often interbedded with sandstone and also forming distinct marl or shale intervals and with generally persistent limestone-marl clasts.
- Mahra Group (Cretaceous): Limestone, marl, and shale, often interbedded with sandstone.

1.4.1.3 Cenozoic Sediments:

- Hadramawt Group (Paleocene-Middle Eocene): Dolomite, shale, limestone with chalk and dolomite, marl, papery shale, bedded gypsum, and alternating sandstone and claystone.
- Majzir Formation (Paleocene-Lower Eocene): A shallow marine-littoral sandstone succession.
- Shihr Group (Oligocene-Pliocene): Conglomerate, sandstone, silt, lime tone and Gypsum.

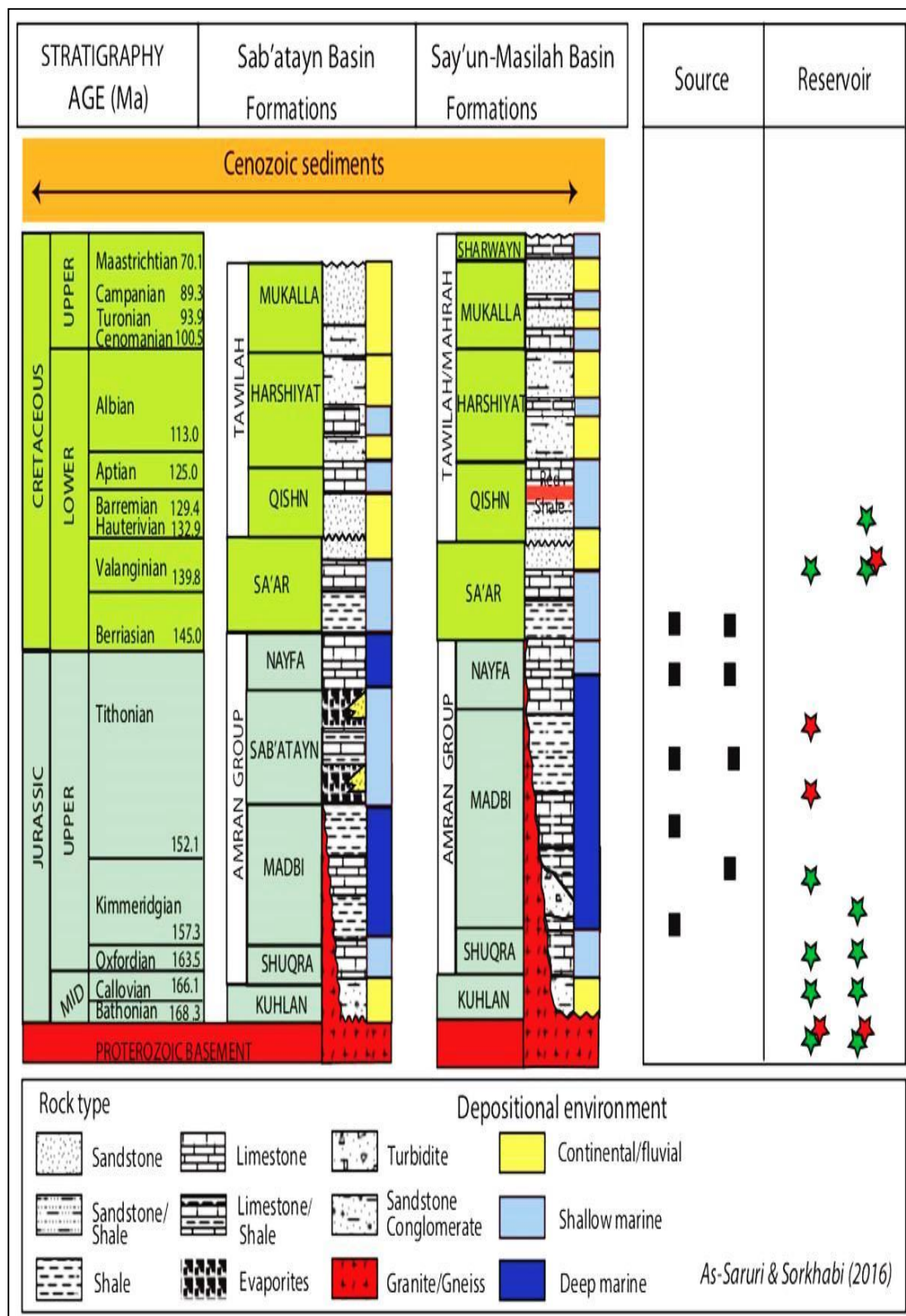


Figure 1.3 Stratigraphy and petroleum systems of Sab'atayn and Say'un-Masilah Basins. (Source: As-Saruri & Sorkhabi (2016)).

1.4.1.4 Basement rocks


The basement rocks of Yemen are considered a part of the Arabian shield which can be divided into five terranes. Asir terrane, Abbas terrane, Al Bayda terrane, Al Mah-fid terrane and Al Mukalla terrane. They arrange in manner that reflect the magnitude of tectonic process in time and space. Two of them represent island arcs which are abducted to continental crust, the Al Bayda terrane, and Al Mukalla terrane. The remaining three others from Archean to Proterozoic gneissic terranes, the Abbas terrane, Asir terrane and the Al Mahfid terrane. The Precambrian basement of Yemen covers a key location in the Pan-African orogeny of Gondwana.

1.4.2 Masila-Say'un basin

Masila Basin is one of the most productive basins in Republic of Yemen. In 1991, significant oil discoveries followed by more findings, were made on Sounah Field at Masila block (Block-14) by Canadian Oxy Company (now PetroMasila). Then, the block was developed by building its plants and construction of the oil pipeline to Al-Dhabah (Ash Shihr) area, Hadhramout governorate, on the Arab Sea. In 1998, Total E&P Yemen (Total Fina Alf) made a number of oil discoveries in the fields of Kharir, Atouf, and Wadi Taribah, (East Shabwah block-10). Production was linked with Masila block-14. On December 18, 1999, DNO, a Norwegian company as operator of Hwarim block-32 announced the discovery of oil and started production and exporting oil through Masila pipeline by November 2001(PEPA, 2014).

Masila Basin is Mesozoic sedimentary basins of Yemen (Fig. 1.4) and was formed as a rift-basin linked to the Mesozoic breakup of Gondwanaland and the evolution of the Indian Ocean during the Jurassic and Cretaceous (Beydoun et al. 1998; Redfern and Jones 1995; Csato et al. 2001). Mesozoic and Cenozoic units are widely exposed in the sedimentary basins of Yemen. The stratigraphic section of the Masila Basin including studied Sharyoof oilfield in age from Precambrian to Tertiary. Basement complex rocks of Precambrian age underlie the Jurassic rocks at a sharp unconformity surface. They consist of granite, diorite, and metamorphic rocks. The Jurassic units comprise clastic, carbonate, and argillaceous sediments. The lower part of the Jurassic is composed of sandstone and limestone (Kuhlan and Shuqra Formations). Here, the Kuhlan and Shuqra are regarded as a discrete pre-rift package (Eills et al. 1996). The Kuhlan Formation is predominantly clastic with local basement topography commonly providing the provenance of sediment. The Shuqra Formation conformably overlies the Kuhlan Formation with a gradational contact. This conformable relationship reflects the gradual transgression and a slight deepening of marine conditions.

It conformably underlies the Madbi Formation. During the late Jurassic commencing in the Kimmeridgian, syn-rift sediments of the Madbi Formation were deposited. The lithofacies of this unit divided into two members. The lower member, Madbi limestone, and the upper member is called Madbi shale. During latest Jurassic to early Cretaceous time, the rifting system of the Masila Basin continued but the subsidence became slower. It was accompanied by the accumulation of carbonates in shallow-marine shelf deposits (Naifa Formation). The Naifa Formation consists mainly of silty and dolomitic limestone and lime mudstone with wackestone. The Cretaceous units comprise the Saar, Qishn, Harshiyat, Fartaq, Mukalla, and Sharwayn formations (Mahara Group).




The Saar Formation is conformably overlies the Naifa Formation and unconformably underlies the Qishn Formation. The Qishn Formation consists mainly of sandstones, with shale and minor carbonate interbeds, deposited in braided river channels, shoreface and shallow-marine settings as predominantly post-rift sediments. The Lower Cretaceous Qishn Formation in the Masila Basin has a variety of usage by the various operating oil companies and authors (e.g., Redfern and Jones 1995; Putnam et al.) interpreted the Qishn clastics as being age-equivalent of the Biyadh Sandstone of Saudi Arabia. They also identified a clear overall transgressive signature through the Qishn clastics and noted that the upper part of the formation typically consists of carbonates. A down-systems-tract facies change from coarse grained clastic deltas in the west to shale and limestone dominated successions farther east was recognized by Redfern and Jones (1995), Holden and Kerr (1997) and Brannan et al. (1999). The Qishn clastic underling the Qishn Carbonates, which comprises carbonate rocks with red shale beds at the base and represented the proven seal rock in the Masila Basin (Fig.1.4). The Qishn Carbonates sediments were deposited in deep water under alternating open and closed marine conditions.

1.5 Study of Area

1.5.1 Block (53)

Block (53) is located at northeastern portion of the Masila Basin, towards the east of Hadhramout Province, adjacent to three prolific Blocks which are, Block-14 (contains 16 producing fields) that operated by Nexen Petroleum Yemen Ltd (Dove, 2000)., Block (32) (contains 3 producing fields) that operated by DNO from East side and Block (10) that operated by Total (Now PetroMasila) from west side. It was awarded to Dove in 1998 in relinquished acreage.

Block-53 hold three discoveries Sharyoof, Bayoot and Hekma. The main reservoir in the block are Qishn sandstone and Basement. Now it is operated by PetroMasila.



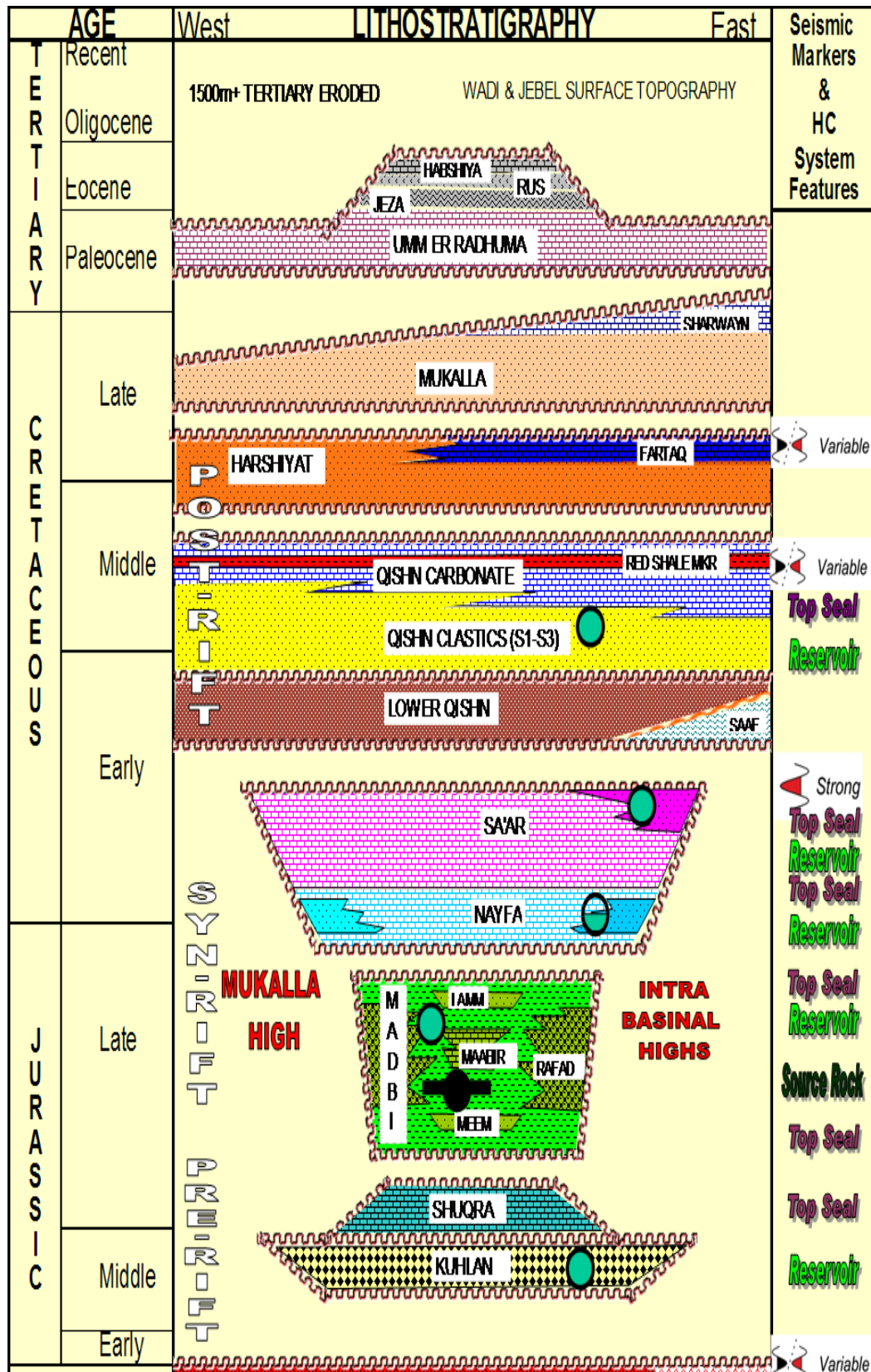


Figure 1.4 Masila Basin Stratigraphic Summary.

The Sharyoof oilfield is one of the most productive oilfields in the onshore of Block-53 in the Masila Basin, located in the N/W sector of the Masila Basin, 550 km east of Sana'a city, with area of 474 km² (Fig.1.5). Sharyoof oilfield is also located between several successful producing oil fields: the Sunah oilfield to the southeast, the Kharir oilfield to the west, and the Tasour field to the east. Sharyoof field was discovered by Dove Energy in June 2000 by Dove energy Company, Sharyoof-1 (TD 1765 m) and second well Sharyoof-2 (TD 1630 m) drilled which targeted the Cretaceous units. The field was put on development in December 2001. On December 17, 2003, Nexen announced the first oil commercial discovery. It started production and exporting oil through Masila pipeline in November 9, 2005 (PEPA, 2014). Successful exploration and appraisal drilling through 2007 and 2008 has provided 4 wells already completed for production from block-53. In 2008 well production capacity is more than 5,000 B/D. Oil samples were recovered from both Qishn sandstone and Kholan sandstone. Water was first injected in 2004 and infill drilling has been continued since then. The field is now at the late Stage of Water injection (secondary recovery) with water-cut of more than 90% in most of the producing wells.



The structure types in the Sharyoof oilfield are characterized by horst, tilted fault blocks. These structures were formed during late Jurassic-early Cretaceous and developed during Oligocene–Middle Miocene time as a result of opening of the Red Sea and the Gulf of Aden during the Tertiary rifting tectonic event (Haitham and Nani 1990; Bott et al. 1992; Crossley et al. 1992; Huchon et al. 1991; Redfern and Jones 1995). The Sharyoof oilfield contains sedimentary rocks ranging from Jurassic to Tertiary in age, including Saar Formation (Fig.1.6). The early Cretaceous Qishn Formation Sandstone is an important hydrocarbon (oil) main reservoir in the Sharyoof oilfield.

Qishn sandstone reservoir is divided into three main units named S1, S2, and S3. S1 is main hydrocarbon-bearing unit which is further subdivided into three sub-units, i.e. S1A, S1B and S1C. S1A and S1C subunits attain the best hydrocarbon saturations and in same time S1A zone is the best petrophysical and reservoir quality properties and higher hydrocarbon content. The 100% water-bearing nature of the S1B subunit. The hydrocarbon content of S2 unit is lower than that of the S1A-and-S1C subunits as you can see in (Fig.1.7).

Based on operating oil companies' unpublished data the productivity varies significantly within the Pre Cambrian/Archean granitic basement, lower Cretaceous Saar Formation carbonates, and middle Cretaceous Qishn Formation clastic deposits. The produced oil at Sharyoof oilfield is intermediate oil and has a specific gravity between 28 and 32 API. The source rock is Upper Jurassic Madbi Formation (Hakimi et al. 2010a), which began to generate oil began during Late Cretaceous (99–66 Ma), and reached a maximum during the Paleocene (<66 Ma) (Hakimi et al. 2010b). However, the lower Cretaceous Saar Formation carbonates are represents as secondary reservoir rocks in the Sharyoof oilfield (DNO Oil Company, 1999 personal communication).

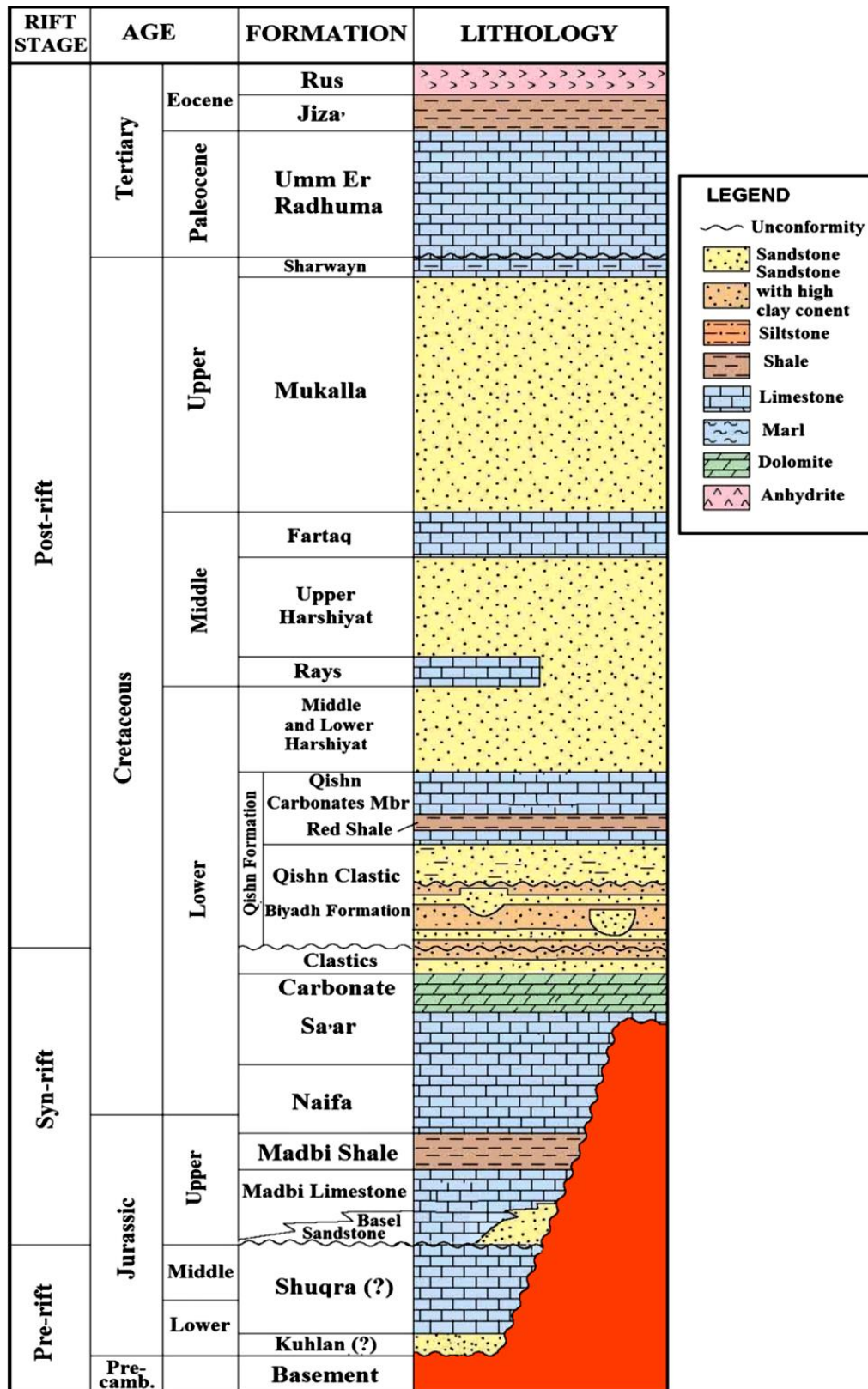


Figure 1.6 Stratigraphic column in the Masila Basin, including Sharyoof oilfield of the eastern Yemen.

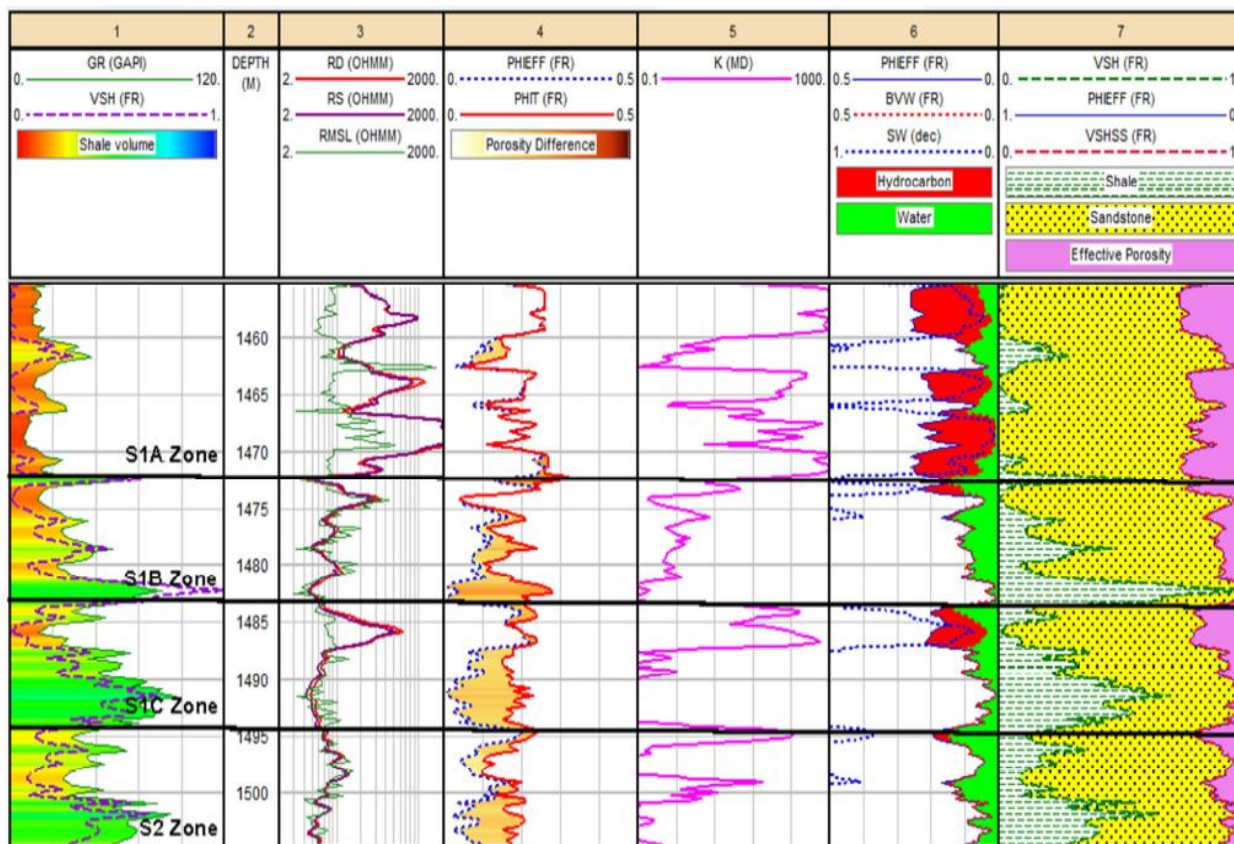


Figure 1.7 Log characteristics of gamma and resistivity logs used for lithologic characterization of main units of Qishn sandstone reservoir.

CHAPTER TWO

2. Literature Review and Theoretical Background

2.1 Previous study

2.1.1 Case study (1)

2.1.1.1 General information about case study

Well Test and PTA for Reservoir Characterization of Key Properties, Agba 8 and Ukot wells in the Niger Delta region of Nigeria.

2.1.1.2 The Method of the case study

This study is basically carried out on Ukot and Agba 8 wells to determine key well and reservoir parameters such as permeability and skin to know if the wells are damaged or ascertain the success of stimulation jobs with the use of well test analysis software “saphir”. The results will help to properly characterize the reservoir for an effective reservoir management, candidate well selection for stimulation, an input data for reservoir simulation and also for production surveillance.

2.1.1.3 Results and Conclusion

Result of Ukot Well and Agba 8 Well Ukot well was analyzed as oil well and the data are given in Table 2.1-2.3. The test was conducted for 2 days and ukot well on 2/16/2001 at 19:00:00 time of the day was producing with a rate of 1650STB/D for 16 h before the rate was increased to 2300 for another 10.11 h before it was shut-in at 21:07:10 the next day for pressure build. 9.61 h on that same day, the well was open for production with a rate of 1650STB/D, 3 h later rate was reduced to 720ST/D before it was shut-in. Four pressure gauges were used during the test period to test for consistency in result of pressure values and (Fig. 2.1) shows that these gauges are consistent in reading from the pressure difference plot. The rate and pressure profile of Ukot well (Fig. 2.2) indicates two build period and multi-rate draw down prior to shut-in in the first build from the test result. Though the second build did not take longer time and thus, analysis was made using the first build up period. The result generated using well test analysis software, Saphir is given (Fig. 2.3). Several reservoir and boundary models were selected to actually match the field data and in the end, a homogenous reservoir model with leaky fault boundary was preferred which fits the field data.

The skin shows that the well is not damaged and it is not recommended for stimulation (Table 2.4). From the pressure transient analysis to determine the Agba 8 skin and permeability using saphir as shown in (Fig. 2.4 and 2.5).

This data is actually a buildup test, which implies that the well must have been flowing for a long time before it was shut-in for the buildup test. Result obtained when these data were inputted into the well test analysis software shows that the wellbore storage constant is 0.0175 bbl/psi, skin is 22.4; permeability of 872 mD, the capacity is 39200 mD-ft and initial pressure of 5980.62 psia. This is an indication of damage as a result of the positive skin. Hence requires a stimulation job to remove the damage (Table 2.5).

Parameter	Value	
	Ukot well	Agba 8 well
Porosity	0.33	0.12
Ct, psi-1	10–5	3E-6 psi-1
Reservoir thickness, ft	45	34 ft
Wellbore radius, rw, ft	0.265	0.29 ft
Formation volume factor	1.078	1.25 B/STB
Oil viscosity, cp	0.31	0.58 cp
Perforations, ft, (MD)	3771-4599	
Total perforated length, ft	1531	
Pump depth, ft, (MD)/TVD (SS)	1965/1817	
Gauge depth, ft, (MD)/TVD (SS)	3771/2583	
Bottom hole temperature °F	155	
Rate, bbl/d	1500	
API gravity	18.5	
Shut in time	310 h	

Table 2.1 Well and reservoir data of Ukot and Agba 8wel

Date	ToD	Liquid rate STB/D	Duration hr
2/16/2001	19:00:00	1650	16.0056
2/17/2001	11:00:20	2300	10.1139
2/17/2001	21:07:10	0	10.7361
2/18/2001	7:51:20	1650	9.61389
2/18/2001	17:28:10	720	3.03889
2/18/2001	20:30:30	0	2.5

Table 2.2 Ukot well rate profile

First shut-in period	5.47 h	Stimulating well
First pumping period	5 min	Using submersible pump
Second shut-in period	9.25 h	Take out plug at 19163 (MD) and BHP guage to 2182 (MD)
Second pumping period	8.08 h	Using submersible pump
First shut-in period	12.08 h	Build up test

Table 2.3 Schedule of Agba 8

Gauge 1 build-up #1	Model parameters	Well and wellbore parameters (Moliere 1)	
Rate	0 STB/D	C	0.00299 bbl/psia
Rate change	2300 STB/D	Skin	-3.73
P@dt=0	3086.62 psia	Reservoir and boundary parameters	
Pi	3597.35 psia	Pi	3597.35 psia
Smoothing	0.1	k.h	2520 md.ft
Select model	K	74 md	
Model option	Standard Model	L	287 ft
Well	vertical	Leakage	0.507397
Reservoir	homogeneous	Derived and secondary parameters	
Boundary	Leaky fault	Delta P (Total skin)	-348.959 psi
Main model parameters	Delta P Ratio (Total Skin)	-0.762749	
TMatch	428 [h]-1		
PMatch	0.0107 [psia]-1		
C	0.00299 bbl/psia		
Total skin	-3.73		
k.h, total	2520 md.ft		
K, average	74 md		
Pi	3597.35 psia		

Table 2.4 Result from saphir (Ukot Well)

Gauge 1 build-up #1	Model parameters	Well and wellbore parameters (Tested well)	
Rate	0 STB/D	C	0.0175 bbl/psia
Rate change	1500 STB/D	Skin	22.4
P@dt=0	5859.08 psia	Reservoir and boundary parameters	
Pi	5980.62 psia	Pi	5980.62 psia
Smoothing	0.1	k.h	39200 md.ft
Select model	K	872 md	
Model option	Standard model	Omega	6.45E-4
Well	vertical	Lamda	4.33E-6
Reservoir	Two porosity sphere	Derived and secondary parameters	
Boundary	Infinite	Delta P (total skin)	79.8925 psi
Main model parameters	Delta P ratio (total skin)	0.699157	
TMatch	1180 [hr] ⁻¹		
PMatch	0.28 [psia] ⁻¹		
C	0.0175 bbl/psia		
Total skin	22.4		
k.h, total	39200 md.ft		
K, average	872 md		
Pi	5980.62 psia		

Table 2.5 Result from saphir (Well Agba 8)

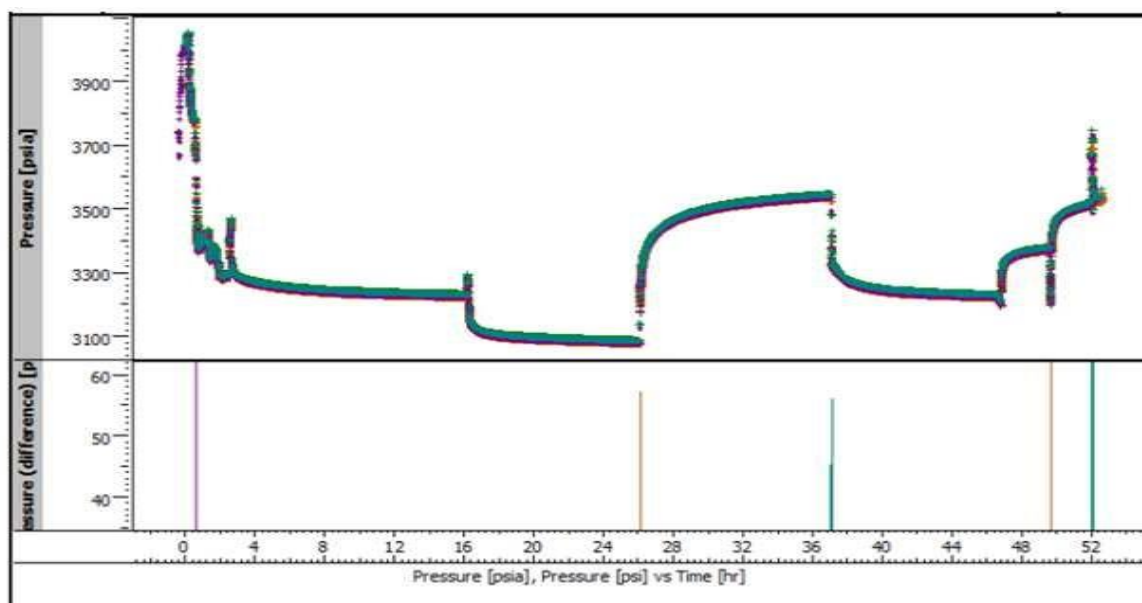


Figure 2.1. Pressure gauges synchronization

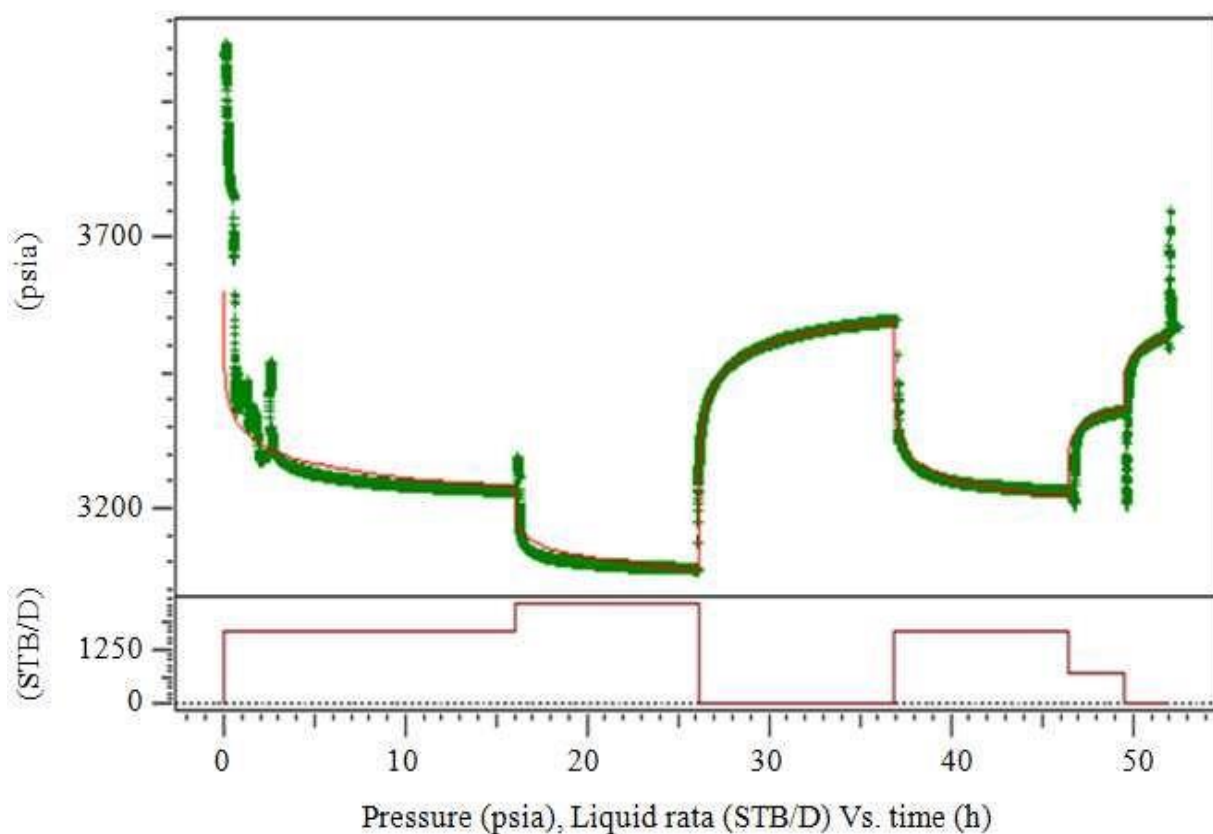


Figure 2.2 Rate and pressure profile of Ukot well

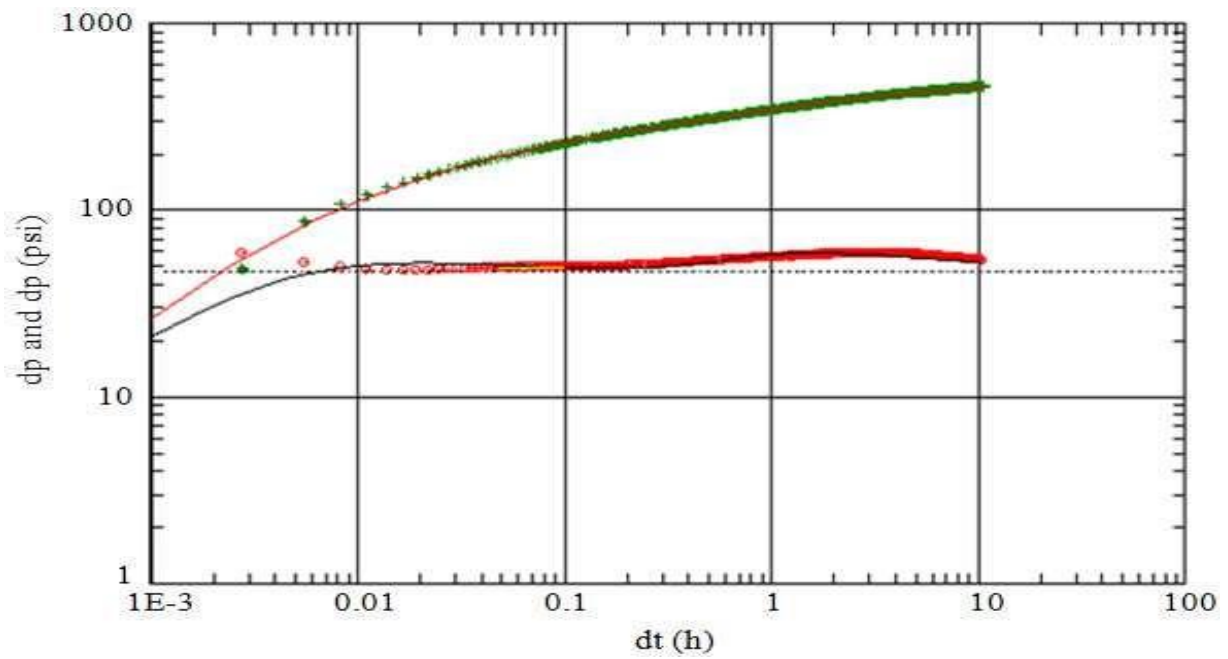


Figure 2.3 Log-log model of Ukot well

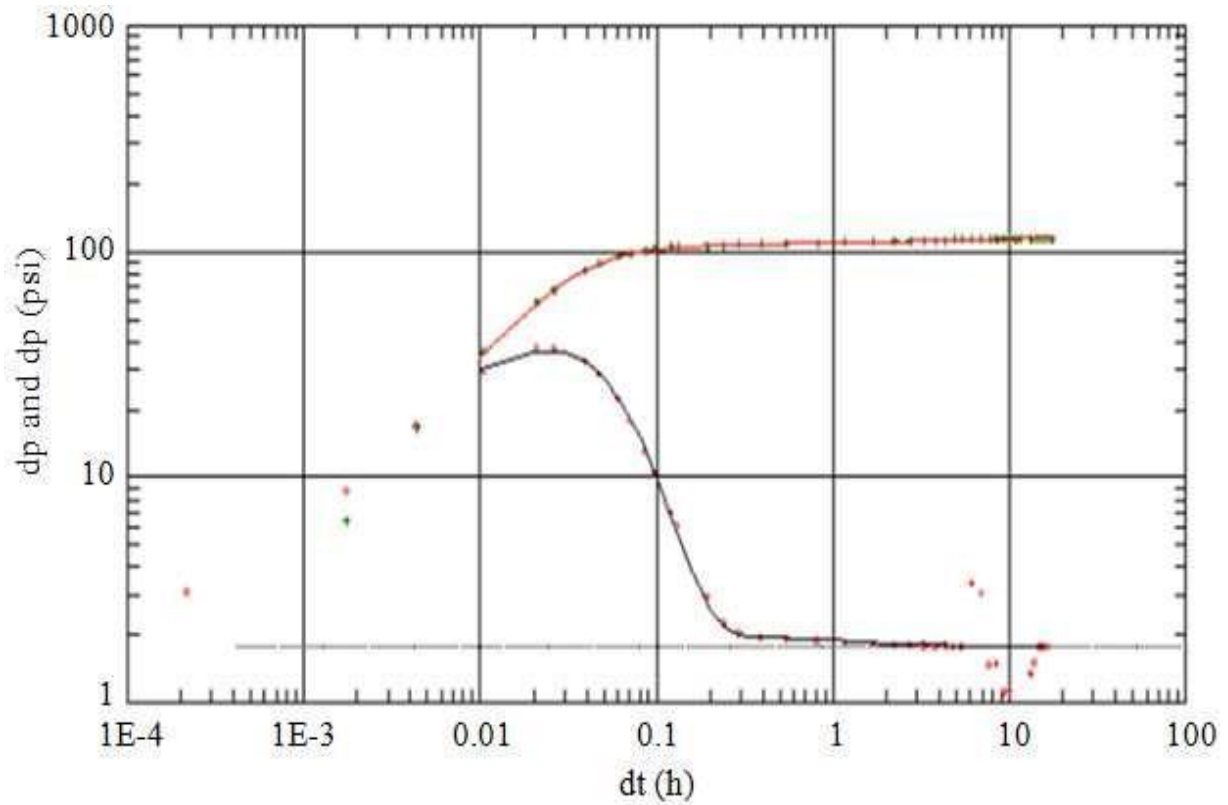


Figure 2.4 log-log plot of Agba 8

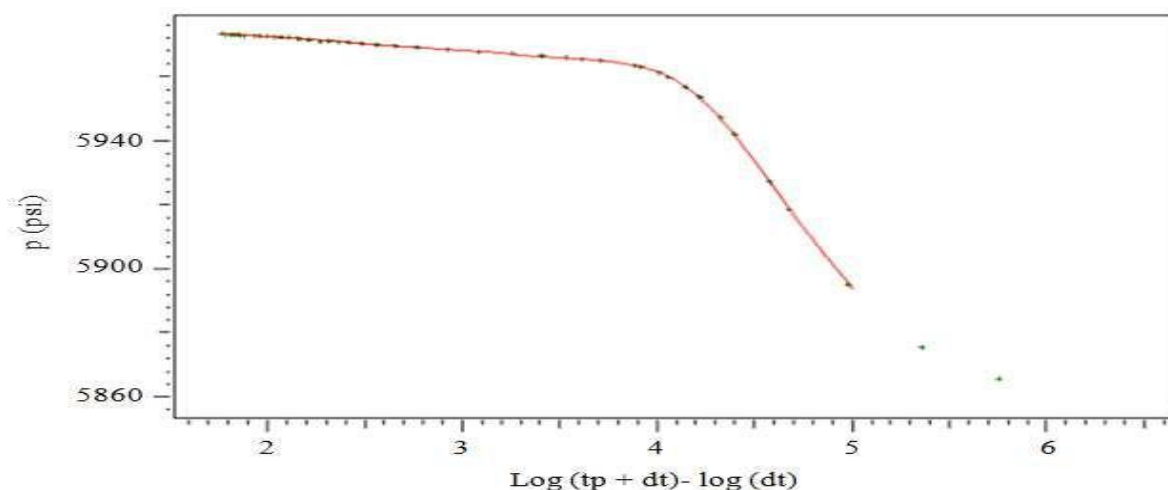


Figure 2.5 Log-log output result of Agba 8

Well test analysis has come a long way since the 1950s when the interpretation methods on the basis of straight lines gave unreliable results.

The derivative approach improves the definition of the analysis plots and therefore the quality of the interpretation. The differentiation of actual data has to be conducted with care to remove noise without affecting the signal. The derivatives approach does not produce errors or noise but only reveals them. The interpretation of pressure derivative is a single-plot procedure. If enough data are available, pressure and time matches are fixed, so analysis is faster. This is important for real-time interpretation during well-test monitoring.

The well interpretation of all the three wells had been presented in the previous and result show that well Ukot and J5 wells are not damaged and do not require stimulation job since they gave negative skin value. Agba 8 is a candidate well for stimulation with a high positive skin value. Thus, characterization of a reservoir is very important for field development study.

2.1.2 case study (2)

2.1.2.1 General information about case study

Anklav field is located on the rising flank of CambayTarapur block between Kathana and Padra field. Nine wells have been drilled in this area, out of which the Anklav#7 & Anklav#3 is hydrocarbon bearing. In Anklav#7 Block, EP-1 is the main producer sand and the structure contour map on top of EP-1 sand shows that the Anklav#7 Block is a fault closure which trends N-S in direction and dip towards east (Fig 2.6)

The structure is broad in South side relatively narrow to the North side. Based on the encouraging results of exploratory well Anklav#7, which is situated structurally in the downdip position and has encountered EP-1 sand top at 1068 m at MSL, which is structurally down by around 40 m w.r.t. Anklav#2 and shallow by 88m w.r.t. Siswa#8. Anklav#7 has produced oil @ 35 M3 /D and oil shale contact has been seen at 1072.5 m at MSL. The performance of the Anklav#7 and effective thickness of 6m sand body has resulted in release of Anklav#9 development well

2.1.2.2 The Method of the case study

A comprehensive reservoir studies plan was made with a view to get a clearer picture of the Reservoir characteristics. Identifying and mapping fractures/faults networks would help in understanding the reservoir fluid movements and improve reservoir development plans, the general well data is given in (Table 2.6). The pressure transient analysis was done through the well test software PAN System: Version2011. The test overview is given in (Fig 2.7A-2.7B).The formation and reservoir fluid properties used for build-up analysis are given in (Table 2.7). During the present analysis two different models were used for interpreting the data generated from the 94 hours Pressure Buildup Study. The two models selected for interpretation of data are: Radial composite-infinitely acting (Fig 2.8A-2.8B) and Single fault model (Fig 2.9A-2.9B).

Well number	Anklav#09
Name of the field	Anklav
Tectonic block	Cambay-Tarapur
Well category	B
Well type	Development
Drilled depth	1265m (MD), 1134m (TVD)
Status of well	Oil producer from EP-I b Sand

Table 2.6 The general well data

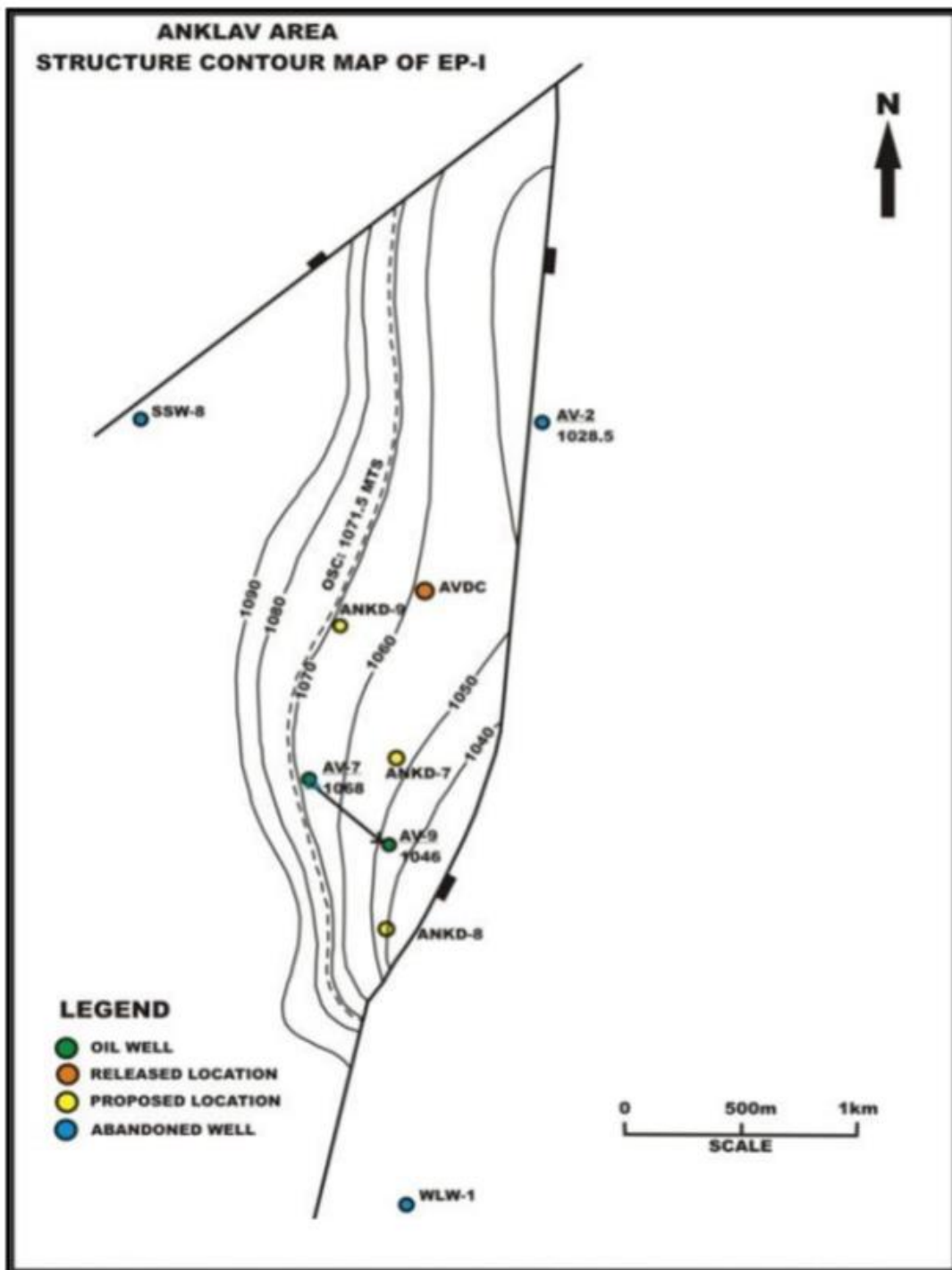


Figure 2.6 Structure Contour Map

2.1.2.3 Results and Conclusion

It is observed that there is an increasing trend in derivative plot. reservoir is having a radial homogenous, single phase flow, constant compressibility with a single fault effect at a distance of 1789 ft... The log-log plot revealed the transition phase from radial flow which can be considered as a presence of boundary effect. This is also in conformity with the geological and structural set up of the study area. The results obtained from straight line analysis for Radial Composite Model are as $K=451.68$ md, $S=9.03$, Distance to anomaly=540 m and for Single nonsealing fault model are $K=450.44$ md, $S=9.01$, Distance to anomaly=1789 ft respectively. A comparison of the results generated by both the models is given in (Table 2.8). The comparison study reveals that there is not much difference in parameters like the Permeability (k), Skin factor (S), and estimated reservoir pressure. But, considering the Geological and structural set up of the study area along with the subsurface position of the well presumes the Single non-sealing fault model to be best fit. Interpretation of Pressure Transient contributes to the improvement of the Geological understanding and model. Identifying and mapping faults networks would help in understanding the reservoir fluid movements and improve reservoir development plans. Fault could be a leaky fault as the derivative does not completely stabilize at $\frac{1}{2}$ unit slope (Fig 2.9A-2.9B). We could have got a better picture of the boundary condition, if the well been shut for more than 100 Hrs.

DERPTH OF MEASUREMENT (m)	1175 m
PAY THICKNESS,h(m)	4 m
WELL BORE RADIOUS (inch)	8 1/2
PRODUCTION RATE (m3/d)	50 (6 mm)
PESUDO PRODUCTION PERIOD, (hrs.)	288 (HRS)
AVERAGE POROSITY (%)	15
OIL VISCOSITY AT RESERVOIR TEMP. (cp)	1.0448
OIL FORMATION VOL. FACTOR (B_o)	1.2116
COMPRESSIBILITY (C_t)	17.1207×10^{-5}
RESERVOIR TEMPERATURE (C)	81.15
BUBBLE POINT (P_b) (kg/cm2)	42
API GRAVITY	30.7

Table 2.7 reservoir fluid properties used for build-up analysis

Resulted Parameters	Radial composite Infinitely acting model	Single nonsealing fault model
Estimated Permeability (k)	451.688 md	450.443
Capacity (kh)	5927.4695 md.ft	5927.4695 md.ft
Skin Factor (S)	9.03	9.01
Estimated Initial Reservoir Pressure (Psia)	1533.1614 Psia at 1175 m depth	1534.5781 Psia at 1175 m depth
Radius of Investigation (Ri)	540 m	
Pressure drop due to skin factor (dpS)	86.1732 Psia	86.00256 Psia
Mobility Ratio (M)	0.6	
Pseudo-radial skin factor (Spr)	2.0165	
Distance to boundary (L)	-	1789 ft

Table 2.8 comparison of the results generated by both the models

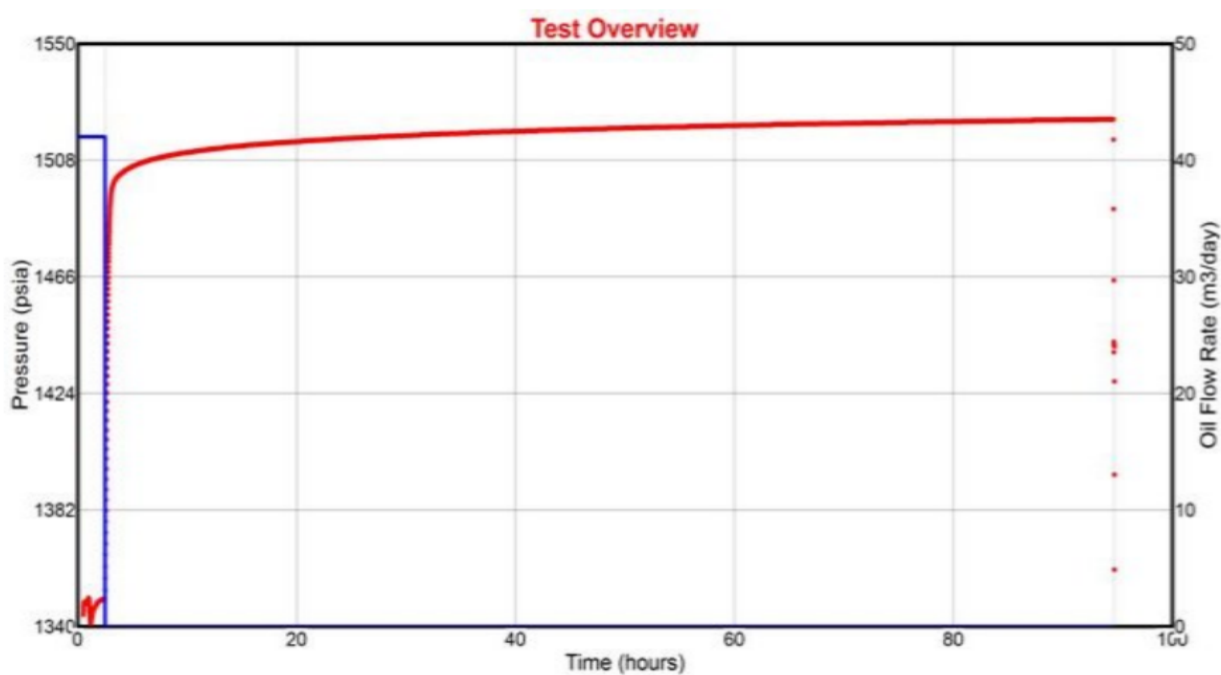


Figure 2.7A Pressure Transient Test Overview

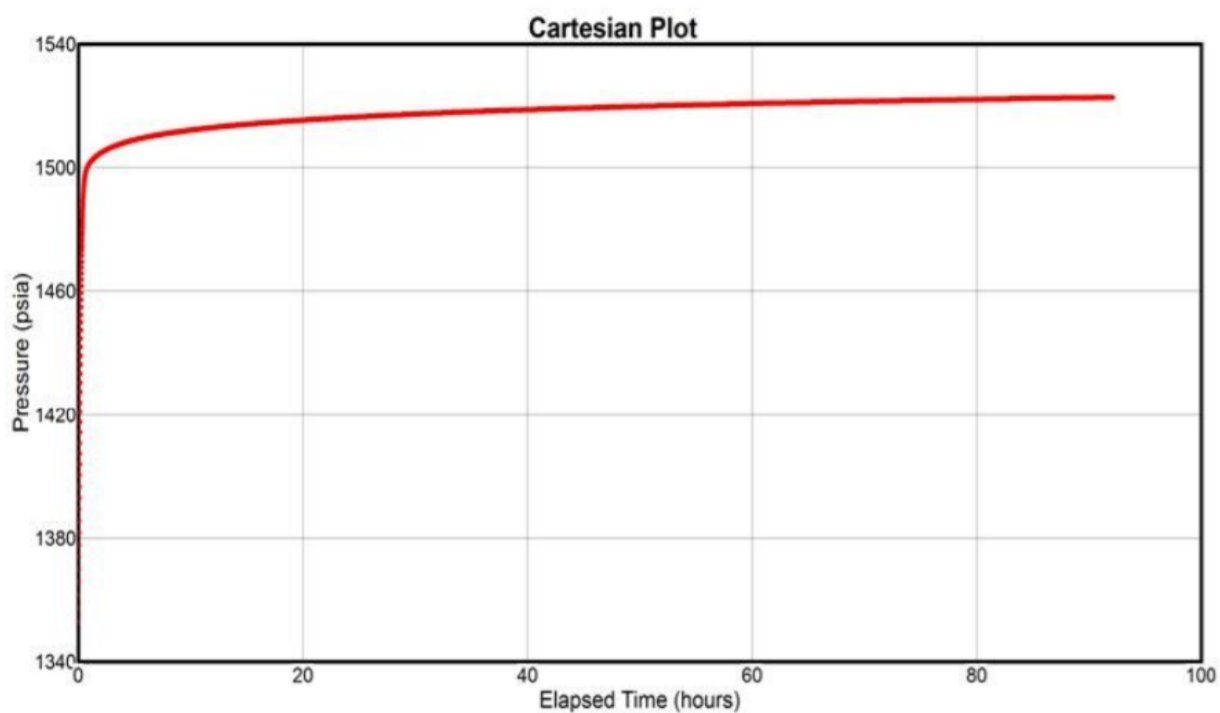


Figure 2.7B Pressure Transient Test Overview

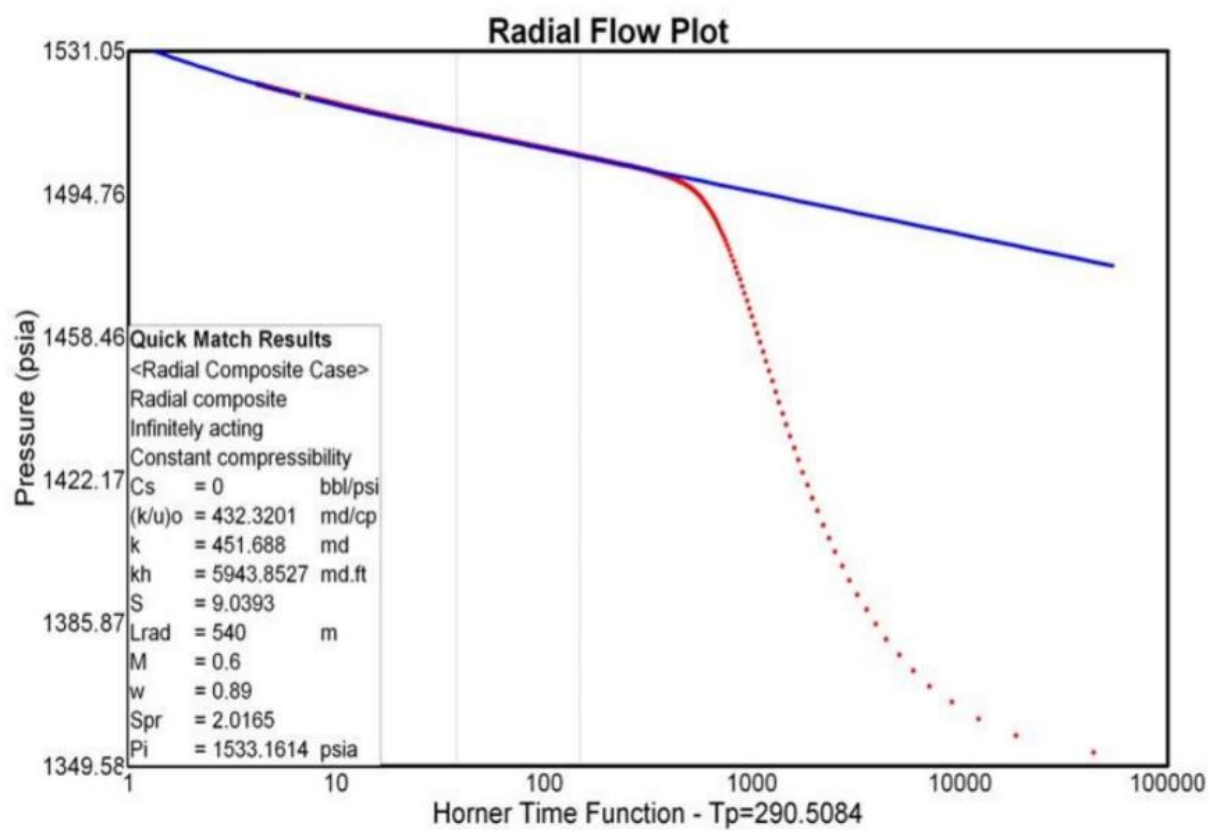


Figure-2.8A Radial Composite Case

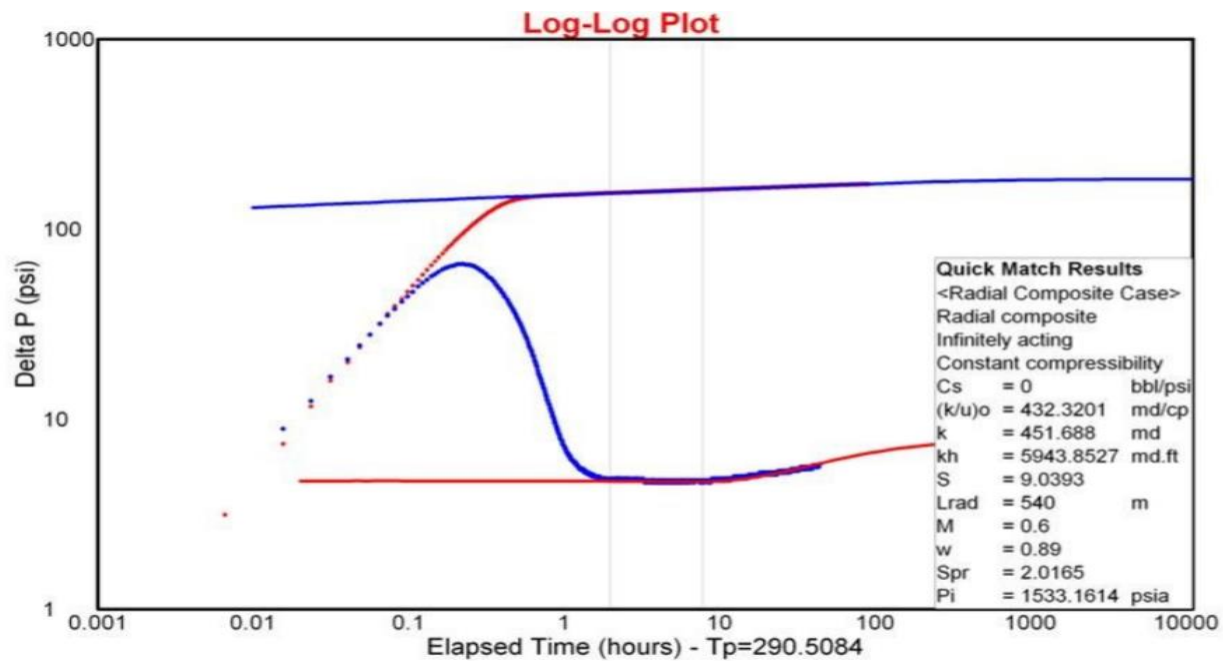


Figure-2.8B Radial Composite Case

SINGLE FAULT CASE

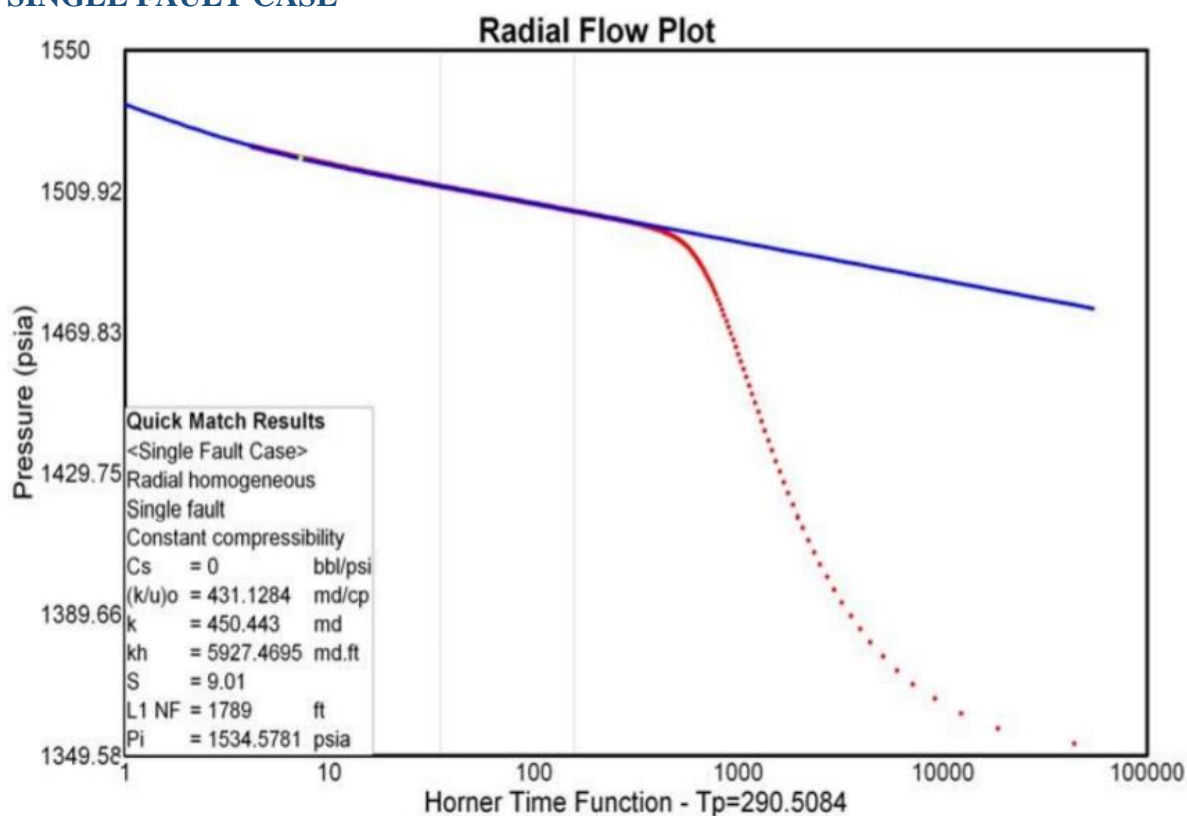


Figure 2.9A Single Fault Model

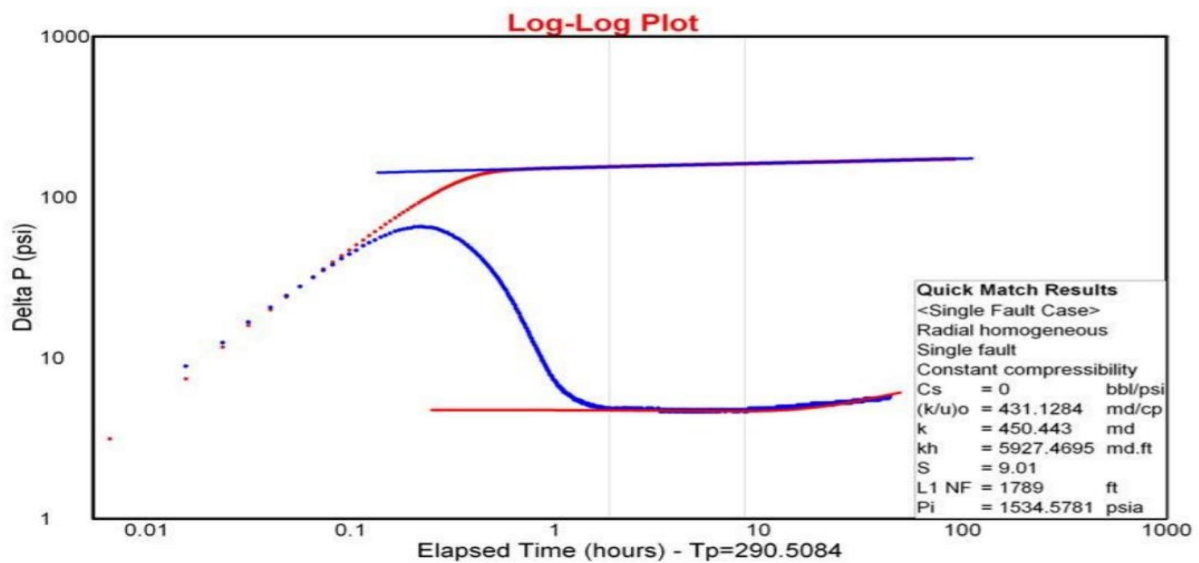


Figure 2.9B Single Fault Model

Interpretation of Pressure Transient contributes to the improvement of the Geological understanding and model. Identifying and mapping faults networks would help in understanding the reservoir fluid movements and improve reservoir development plans. Fault could be a leaky fault as the derivative does not completely stabilize at $\frac{1}{2}$ unit slope (Fig2.9A-2.9B). We could have got a better picture of the boundary condition, if the well been shut for more than 100 Hrs.

2.2 Well Testing

2.2.1 Role of Oil Well Tests and Information in Petroleum Industry

Oil well test analysis is a branch of reservoir engineering. Information obtained from flow and pressure transient tests about in situ reservoir conditions are important to determining the productive capacity of a reservoir. Pressure transient analysis also yields estimates of the average reservoir pressure. The reservoir engineer must have sufficient information about the condition and characteristics of reservoir/well to adequately analyze reservoir performance and to forecast future production under various modes of operation. The production engineer must know the condition of production and injection wells to persuade the best possible performance from the reservoir. Pressures are the most valuable and useful data in reservoir engineering directly or indirectly, they enter into all phases of reservoir engineering calculations. Therefore, accurate determination of reservoir parameters is very important. In general, oil well test analysis is conducted to meet the following objectives:

- To evaluate well condition and reservoir characterization;
- To obtain reservoir parameters for reservoir description;
- To determine whether all the drilled length of oil well is also a producing zone;
- To estimate skin factor or drilling- and completion-related damage to an oil well. Based upon the magnitude of the damage, a decision regarding well stimulation can be made.

2.2.2 Types of well tests:

Various types of pressure transient test carried out in oil, gas and water injection wells are as follows:

Drawdown, build-up, and interference tests are the three main well tests. Additionally, there are tests for injection and falloff, which are comparable to the drawdown and build-up tests for injectors. In exploratory wells and newly drilled wells, a unique drawdown and build up test called the Drill Stem Test (DST) is usually conducted.

❖ PTA: Single-Well Tests:

One well in which the pressure response is measured following a rate change.

- pressure buildup test
- drawdown or flow test
- pressure falloff test
- injectivity test

❖ PTA: Multiwell Tests

Interference tests

The active well is produced at a measured, constant rate throughout the test (Other wells in the field must be shut in so that any observed pressure response can be attributed to the active well only.)

Pulse tests

The active well produces and then, is shut in, returned to production and shut in again Repeated but with production or shut-in periods rarely exceeding more than a few hours Produces a pressure response in the observation wells which usually can be interpreted unambiguously (even when other wells in the field continue to produce)

❖ Deliverability tests (DT)

- Flow-After-Flow Tests
- Isochronal Tests

❖ Combination of two or more test types:

Drillstem test Below the most important well tests will discussed:

2.2.2.1 Pressure Drawdown Test

classified into three periods for analysis:

- Transient or early flow period is usually used to analyze flow characteristics;
- Late transient period is more completed; and
- Semi-steady-state flow period is used in reservoir limit tests.

The pressure Drawdown test (DDT) is just a sequence of bottom-hole pressure observations because of the constant producing rate. Usually, before the constant flowing rate, the well is closed for enough time to make the pressure widespread in the reservoir reach static reservoir pressure. The diagram showing this phenomenon is in (Fig. 2.10).

The reservoir is initially kept at a constant pressure during the drawdown tests, and the well is originally closed off. The well is starting to flow, and the variations in the pressure response are being recorded over time. Normally, it is difficult to maintain a flow rate that is absolutely constant, and even little variations in flow rate during the test may significantly change the pressure response's trend. Rate normalization is a technique that may be used to account for changing flow rates when the rate is gradually changing and the reservoir is infinite-acting at all relevant times.

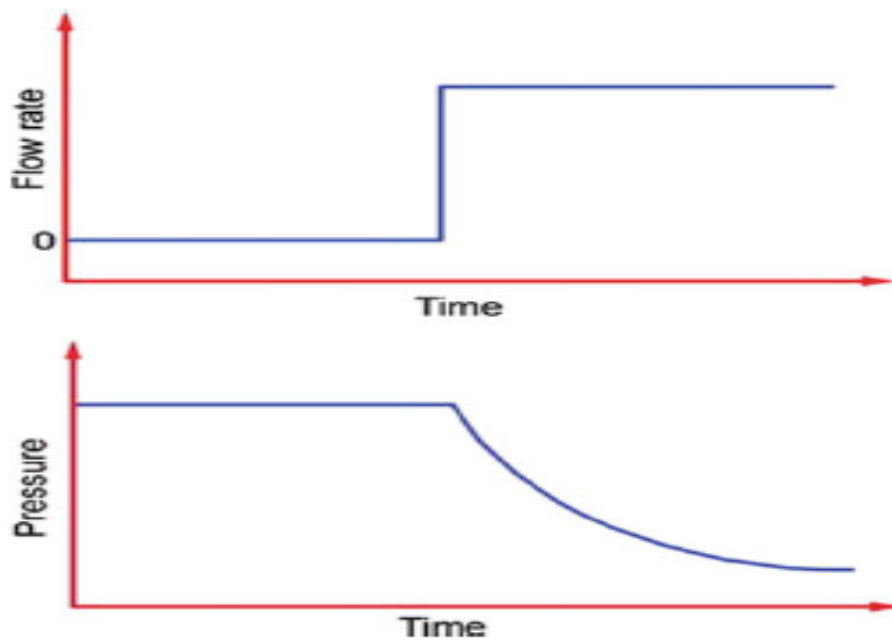


Figure 2.10 Idealized Pressure Drawdown Test

A pressure drawdown test is simply a series of bottom-hole pressure measurements made during a period of flow at constant production rate. Usually the well is closed prior to the flow test for a period of time sufficient to allow the pressure to stabilize throughout the formation, i.e., to reach static pressure.

As discussed by Odeh and Nabor, 1 transient flow condition prevails to a value of real time approximately equal to.

$$t \approx \frac{\phi \mu_o r_e^2}{0.00264k} \quad (1)$$

Semi-steady-state conditions are established at a time value of

$$t \approx \frac{\phi \mu_o c r_e^2}{0.00088k} \quad (2)$$

In this chapter, we will discuss drawdown tests in infinite-acting reservoir tests. An analysis technique applicable to pressure drawdown tests during each of these periods including other types of tests.

Pressure-Time History for Constant-Rate Drawdown Test

The flow history of an oil well can be

Transient Analysis - Infinite-Acting Reservoirs

An ideal constant-rate drawdown test in an infinite-acting reservoir is modeled by the logarithmic approximation to the Ei function solution:

$$P_{wf} = P_i - 141.2 \frac{q_o \mu_o \beta_o}{kh} [P_D(t_D) + s] \quad (3)$$

Assuming initially the reservoir at initial pressure, P_i the dimensionless pressure at the well ($r_D = 1$) is given as

$$P_D = 0.5[\ln(t_D) + 0.80907] \quad (4)$$

After the wellbore storage effects have diminished and $tD/r_2D > 100$, dimensionless time is given by

$$t_D = \frac{0.000263kt}{\phi\mu_o C_t r_w^2} \quad (5)$$

Combining and rearranging Eqs.3 through 5, we get a familiar form of the pressure drawdown equation. As an infinite-acting reservoir, the equation for pressure response at a constant rate may be written as:

$$P_{wf} = P_i - \frac{162.6q\mu\beta}{kh} \left[\log t + \log \left(\frac{k}{\phi\mu C_t r_w^2} \right) - 3.23 + 0.869s \right] \quad (6)$$

The relation of $p_{wf}(t)$ versus $\log(t)$ will yield a linear trend with the downward direction line (Fig.2.11) with slope m which can be expressed as:

$$m = - \frac{162.6q\mu\beta}{kh} \quad (7)$$

Then determine the permeability:

$$k = \frac{162.6q\mu\beta}{mh} \quad (8)$$

The intercept of the Y-axis, bottom-hole pressure, corresponds when $\ln t$ equals zero when $t = 1h$. The corresponding pressure value is often written as $P_{t=1}$. Therefore, considering these procedures, the equation is simplified as:

$$y = P_{t=1h} = mx + b \quad (9)$$

The intercept of this line with the Y-axis related to the value of pressure when t equals to 1h is:

$$P_{t=1h} = P_i - \frac{162.6q\mu\beta}{kh} \left[\log \left(\frac{k}{\phi\mu C_t r_w^2} \right) - 3.23 + 0.869s \right] \quad (10)$$

To adequately estimate skin factor, Eq. (11) can be re-written as follows:

$$s = 1.151 \left[\frac{P_i - P_{1h}}{m} - \log \left(\frac{k}{\phi\mu C_t r_w^2} \right) + 3.23 \right] \quad (11)$$

So, from the semi-log plot, the permeability can be obtained from the slope m of the straight line and the skin factor can be determined to form the intercept at p_{1h} .

The additional pressure drop due to the skin effects can be expressed as:

$$\Delta P_{skin} = 141.2 \left(\frac{q\beta\mu}{kh} \right) s = 141.2|m|s \quad (12)$$

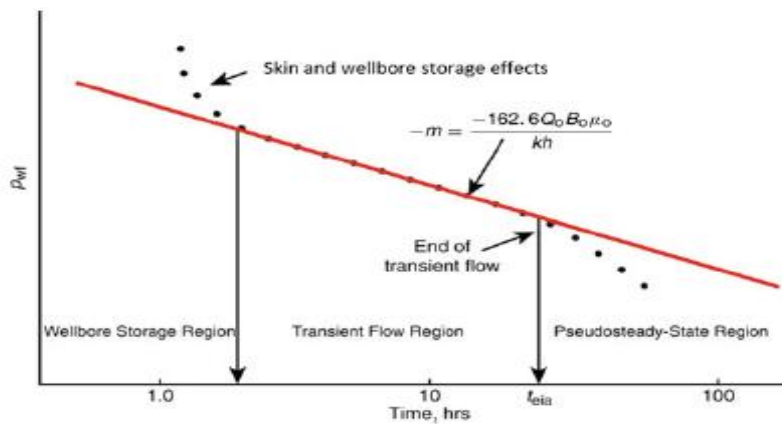


Figure 2.11 Semilog Plot of Pressure Drawdown data

2.2.2.2 Pressure Buildup Test

The buildup test is the method of transient well testing that is most often performed. Closing the well and measuring the bottom-hole pressure are two steps in the analysis of pressure buildup. However, before closing the well, a steady flow rate must be achieved. This can be obtained from the well either at the beginning of production or during a time of continuous production to provide a steady pressure variation (Streltsova and McKinle 1984). In case the objective also determines the skin factor, then recording the pressure measurement before the shut-in of the well becomes necessary.

(Fig 2.12) show the well test in the appraisal well starting with a well clean-up period followed by two pressure BU tests and a main flow period. (Fig 2.12) show the well test is performed when the well has a stable flow and is then quickly

slam shut with the wing valve for a period. Pressure will build-up (PBU) in the well and PBU test will be available (Fig. 2.12).

The production rate and bottom-hole pressure time relevant to the buildup test are shown in (Fig 2.13). Where t_p denotes the production time and t represents the time since the shut-in. Before shutting in the well, the pressure is measured; there-after, the wellbore pressure is quantitatively recognized to determine the reservoir parameter values and the wellbore condition. Before starting the well test interpretation, much important information must be available and measured accurately such as, choke size variation, tubing size, casing sizes, and tested interval depth. This information has a significant impact on the interpretation process (Tarek 2001). Well stabilization at a constant rate is also crucial, otherwise applying conventional methods to interpret the test results can lead to widely erroneous results.

Many methods are offered for the interpretation of the BU test, such as the Horner plot and MDH plot method, but the Horner plot is the commonly used method.

Pressure buildup testing is the most familiar transient well-testing technique, which has been used extensively in the petroleum industry. Basically, the test is conducted by producing a well at constant rate for some time, shutting the well in (usually at the surface), allowing the pressure to build up in the wellbore, and recording the down-hole pressure in the wellbore as a function of time. From these data, it is possible to estimate the formation

permeability and current drainage area pressure, and to characterize damage or stimulation and reservoir heterogeneity or boundaries frequently. Knowledge of surface and subsurface mechanical conditions is important in buildup test data interpretation. Therefore, it is recommended that testing and casing sizes, well depth, packer condition, etc., be determined before data interpretation starts. Usually, short-time pressure observations are necessary for the complete delineation of wellbore storage effects. Data may be needed at intervals as short as 15 seconds for the first few minutes of some buildup tests. As the test progresses, the data collection interval can be expanded. In this chapter we will discuss ideal, actual buildup tests, buildup tests in infinite-acting reservoirs.

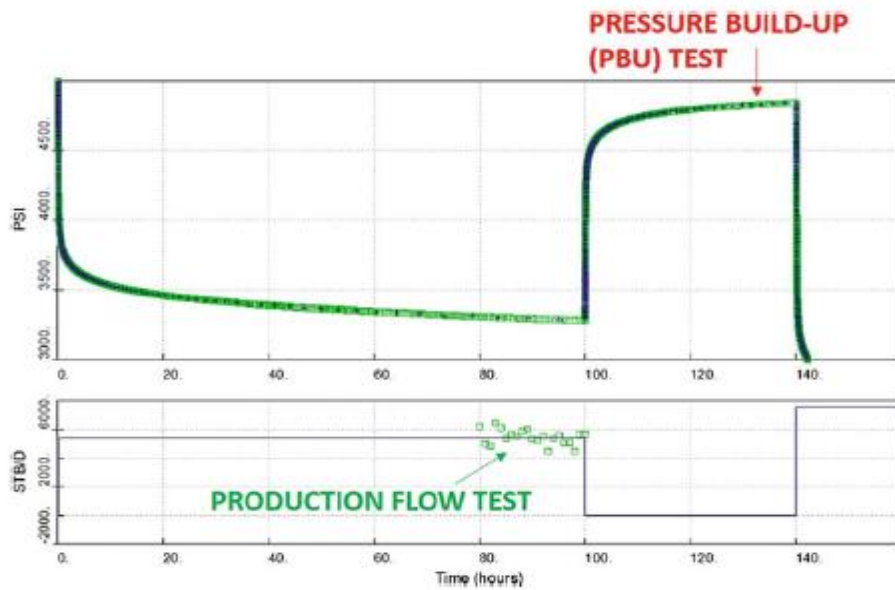


Figure 2.12 Pressure Buildup Test and Main Flow Period

Ideal Pressure Buildup Test

In an ideal situation, we assume that the test is conducted in an infinite acting reservoir in which no boundary effects are felt during the entire flow and later shut-in period. The reservoir is homogeneous and containing in as lightly compressible, single-phase fluid with uniform properties so that the E_i function and its logarithmic approximation apply. Horner's approximation is applicable. Wellbore damage and stimulation is concentrated in a skin of zero thickness at the wellbore. Flow into the wellbore ceases immediately at shut-in. If a well is shut-in after it has produced at rate q for time t_p and the bottom-hole pressure P_{ws} is recorded at time Δt , then a plot of P_{ws} versus $\log(t_p + \Delta t)$ will give a straight line, which is represented by the following equation:

$$P_{ws} = \frac{162.6q_o\mu_o\beta_o}{kh} \log\left(\frac{t_p + \Delta t}{\Delta t}\right) \quad (1)$$

Where the slope m is $162.6q_o\mu_o\beta_o/kh$ and P_i (initial reservoir pressure) is the intercept at $\left(\frac{t_p + \Delta t}{\Delta t}\right) = 1.0$. The absolute value of the slope m is used in analyzing the test result. The formation permeability k can be calculated from the slope and given by

$$k = \frac{162.6q_o\mu_o\beta_o}{mh} \quad (2)$$

and the skin factor is

$$s = 1.151 \left[\frac{P_{1hr} - P_{ws}(\Delta t=0)}{m} - \log \left(\frac{k}{\phi \mu_o c_t r_w^2} \right) + 3.23 \right] \quad (3)$$

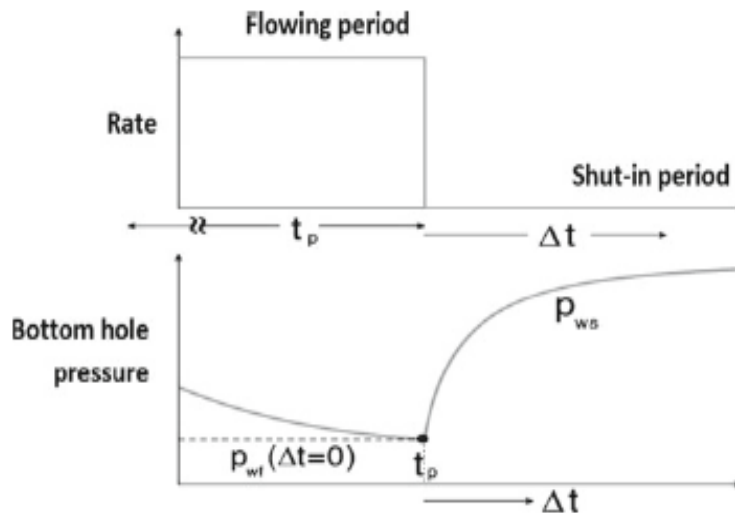


Figure 2.13 Idealized Pressure Buildup Test

Actual Buildup Tests - Infinite Reservoir

Instead of a single straight line for all times, we obtain a curve with a complicated shape, which indicates the effect of after flow, we can logically divide a buildup curve into three regions see (Fig2.14): Early-time region (ETR). In this region, a pressure transient is moving through the formation nearest the wellbore. Middle-time region (MTR). In this region, the pressure transient has moved away from the wellbore into the bulk formation. Late-time region (LTR). In this region, the pressure transient has reached the drainage boundaries well. MTR is a straight line. This is the portion of the buildup curve that we must identify and analyze. Analysis of this portion only will provide reliable reservoir properties of the tested well. The reasons for the distortion of the straight line in the ETR and LTR are as follow: In the ETR, the curve is affected by:

- Altered permeability near the wellbore;
- Wellbore storage.

Using a packer in the hole and shutting-in the well at the packer can minimize this effect. In the LTP, the pressure behavior is influenced by boundary configuration, interferences from nearby wells, reservoir heterogeneities, and fluid/fluid contacts.

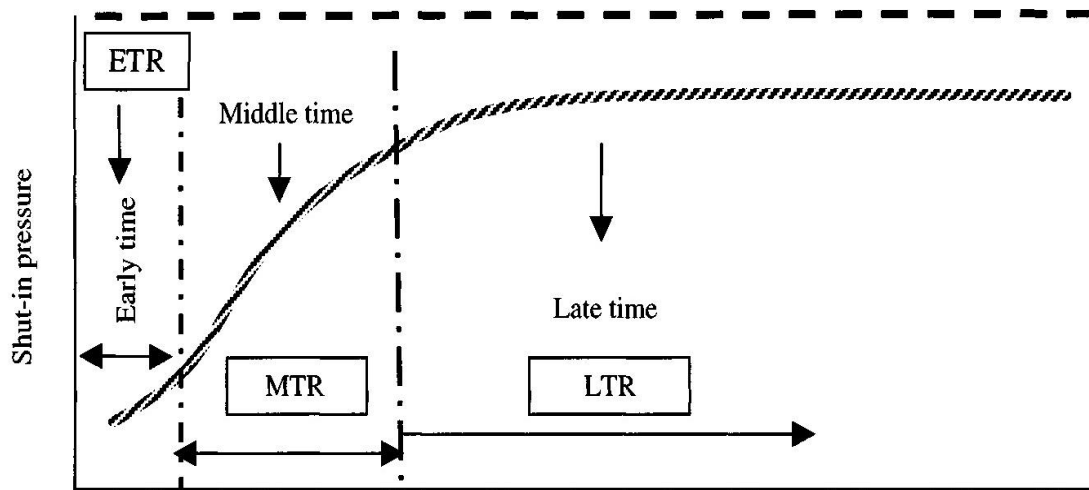


Figure 2.14 Behavior of the static pressure on shut-in oil well

Analyzing a pressure buildup in an infinite-acting reservoir using Horner's technique involves the following steps:

- Find t_p , the cumulative production since completion divided by the rate, immediately before shut-in (when rate varies). As a matter of general practice to approximate, t_p using cumulative production since last pressure equalization:

$$t_p = \frac{24V_p}{q_o} \quad (4)$$

- Plot P_{ws} versus $\log(t_p + \Delta t)/\Delta t$ on semilog graph paper.
- Plot $\Delta P_{ms} = (P_{ms} - P_{wf}(\Delta t=0))$ versus Δt on log-log graph paper to identify wellbore effects, i.e., identify ETR and beginning of MTR which can be found using type curves. The MTR ends when the radius of investigation begins to detect the drainage boundaries of the tested well; at this time the buildup curve starts to deviate from the straight line.
- Find slope m of the straight-line portion of the Horner plot (MTR) and extrapolate the line to infinite time at $\log((t_p + \Delta t)/\Delta t) = 1$ to find p^* . Once the MTR is identified, determine the slope and intercept.
- On straight-line portion of the curve or the extrapolated portion read P_{ws} at $\Delta t = 1$ hour, referred to as P_{1hr} .
- Calculate the reservoir properties by using the equation in the following section.

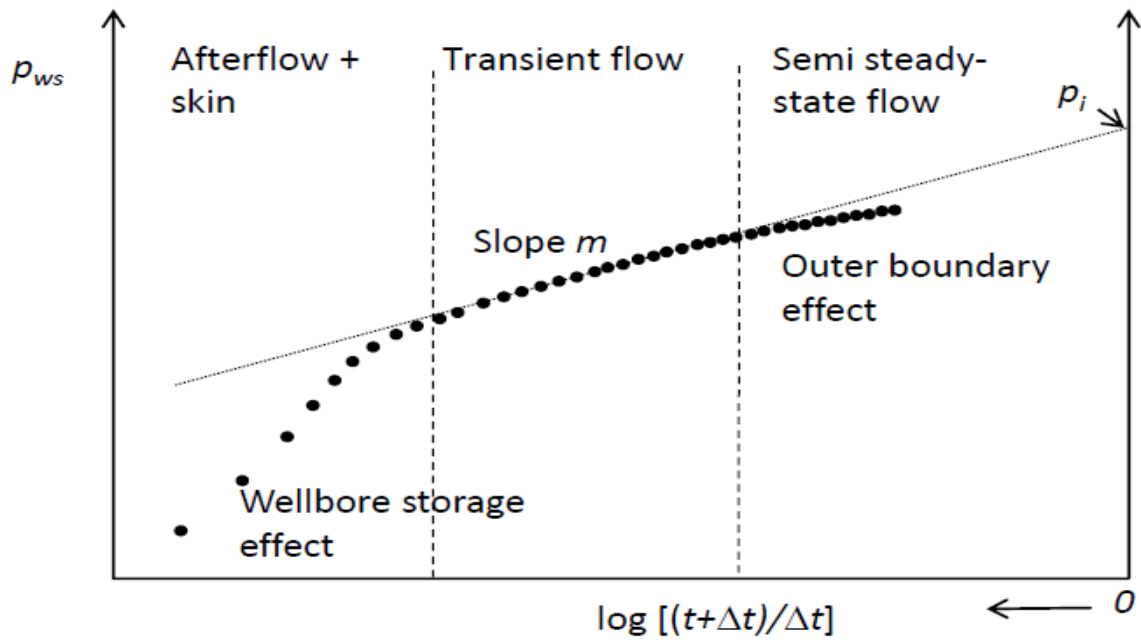


Figure 2.15 Semilog Plot of Pressure Buildup data

Pressure Buildup Test Analysis in Infinite-Acting Reservoir

For any pressure buildup testing situation, the bottom-hole shut-in pressure, P_{ws} , in the test well may be expressed using the principle of superposition for a well producing at rate q_o until time t_p , and at zero rate thereafter. At any time after shut-in

$$P_{ws} = P_i - \frac{141.2q_o\mu_o\beta_o}{kh} [P_D(t_p + \Delta t)_D - P_D(\Delta t_D)] \quad (5)$$

where P_D is the dimensionless pressure function and t_D the dimensionless time and is defined by the following equation:

$$t_D = \frac{0.000264kt}{\phi\mu_o c_t r_w^2} \quad (6)$$

During the infinite-acting time period, after wellbore storage effects have diminished and assuming there are no major indeed fractures, P_D in Eq. 5 may be replaced by the logarithmic approximation to the exponential integral:

$$P_D = 0.5(\ln t_D + 0.80907) \quad (7)$$

$$P_{ws}(\Delta t) = P_i - \frac{162.6q_o B\mu}{kh} \log \left(\frac{t_p + \Delta t}{\Delta t} \right) \quad (8)$$

Eq. 8 gives the pressure response during shut-in BHP, p_{ws} . This equation indicates that plotting p_{ws} versus $(t_p + \Delta t)/\Delta t$ on semilog coordinates will exhibit a semilog straight line of slope m , where

$$m = \frac{162.6q_o\mu_o\beta_o}{kh} \quad (9)$$

Effects and Duration of Afterflow

To recognize the MTR is essential for the successful buildup curve analysis based on the Horner plotting method, because the line must be identified to estimate the reservoir

properties. The following methods can be used to determine when (if ever) afterflow ceased.

log—log Curve Matching Procedures

The following steps should be used to estimate the beginning of MTR:

Plot P_{ws} versus $\log(t_p + \Delta t)/\Delta t$ on semilog graph paper.

Plot $(P_{ws} - P_{wf})$ versus A_{te} on log-log graph paper, where

$$\Delta t_e = \frac{\Delta t}{1 + \Delta t/t_p} \quad (10)$$

From the graph, find approximately at what shut-in time (Δt) does afterflow cease and boundary effects appear.

Find a uniform slope region (45° line at earliest time), choose any point on the unit slope line and calculate the wellbore storage constant, C_s :

$$C_s = \frac{q_o \beta_o}{24} \left(\frac{\Delta t}{\Delta p} \right) \quad (11)$$

where Δt and Δp are the values read from a point on the unit-slope line.

Using actual mechanical properties of the well, we can also establish

$$C_s = 25.65 \frac{A_{wb}}{\rho_{wb}} \quad (12)$$

for a well with a rising liquid/gas interface, where A_{wb} - wellbore area (ft^2) and ρ_{wb} = density. Also $C_s = C_{wb} V_{wb}$ for a wellbore containing only single-phase fluid (liquid only), where C_{wb} is the compressibility of the liquid in wellbore (psi^{-1}) and V_{wb} the wellbore volume (bbl).

- Establish dimensionless wellbore storage constant C_{SD} that characteristic the actual test from curve match or using the following equation:

$$C_{SD} = \frac{0.894 C_s}{\phi C_t h r_w^2} \quad (13)$$

- Determine k and the skin factor s .
- Find the end of wellbore storage effects, t_{wbs} (h), after selecting the proper Ramey's curve.
- Verify the time, t_{wbs} , marking the end of wellbore storage distortion using empirical relationships:

$$t_{wbs} \cong 50 C_s \exp(0.14s) \quad (14)$$

Or

$$t_{wbs} \cong \frac{170000 C_s \exp(0.14s)}{\frac{kh}{s}} \quad (15)$$

Calculation of Flow Capacity and Formation Permeability

The formation permeability k can be obtained as

$$k = \frac{162.6 q_o \mu_o \beta_o}{mh} \quad (16)$$

and Kh is the flow capacity (mDft). Both Theis and Horner proposed the estimating permeability in this manner. The P_{ws} versus $\log [(tp + \Delta t)/\Delta t]$ plot is commonly called the Horner plot (graph method) in the petroleum industry. Extrapolation of the straight-line section to an infinite shut-in time $[(tp + \Delta t)/\Delta t] = 1$ gives a pressure and we will denote this as p^* throughout. In this case $p^* = p_i$ the initial pressure. However, the extrapolated pressure value is useful for estimating the average reservoir pressure.

Estimation of Skin Factor

The skin factor does affect the shape of the pressure buildup data. In fact, an early-time deviation from the straight line can be caused by skin factor as well as by wellbore storage. Positive skin factor indicates a flow restriction, i.e., wellbore damage. A negative skin factor indicates stimulation. To calculate skin factor, s from the data available in the idealized pressure buildup test. At the instant a well is shut-in, the flowing BHP, P_{wf} , is

$$P_{wf} = P_i + m \left[\log \left(\frac{16.88 \phi \mu_o C_t r_w^2}{k t_p} \right) - 0.869s \right] \quad (17)$$

At shut-in time Δt at in the buildup test

$$P_{wf} = P_i + m \left[\log \left(\frac{t_p + \Delta t}{\Delta t} \right) \right] \quad (18)$$

Combining Eqs. 17 and 18 and solving for the skin factor s , we have

$$s = 1.151 \left(\frac{P_{ws} - P_{wf}}{m} \right) + 1.151 \log \left(\frac{16.88 \phi \mu_o C_t r_w^2}{k \Delta t} \right) + 1.151 \log \left(\frac{t_p + \Delta t}{\Delta t} \right) \quad (19)$$

It is a convenient practice in the petroleum industry to choose a fixed shutin time Δt of 1 hour and the corresponding shut-in pressure, P_{1hr} to use in this equation. The pressure, P_{1hr} , must be on the straight line on its extrapolation.

Assuming further that $\log [(tp + \Delta t)/\Delta t]$ is negligible. P_{wf} is the pressure measured before shut-in at $\Delta t = 0$, With these simplifications, the skin factor is:

$$s = 1.151 \left[\frac{P_{1hr} - P_{wf}(\Delta t=0)}{m} - \log \left(\frac{k}{\phi \mu_o C_t r_w^2} \right) + 3.23 \right] \quad (20)$$

Pressure Drop Due to Skin

Pressure drop due to skin is also called an additional pressure drop $(\Delta P)_{skin}$ across the altered zone near the wellbore. Calculation of this pressure drop due to skin is meaningful in describing the effect of skin on actual production. In terms of the skin factor s and the slope m of the middle-time line

$$(\Delta P)_{skin} = 0.869ms \quad (21)$$

Determination of Effective Wellbore Radius

The effective wellbore radius r_{wa} is defined as

$$r_{wa} = r_w e^{-s} \quad (22)$$

If s is positive, the effective wellbore radius r_{wa} is smaller than r_w , then fluid must theoretically travel through additional formation to give the required pressure drop. If s is negative, the effective wellbore radius is larger than r_w .

Flow Efficiency and Damage Ratio

The flow efficiency is defined as the ratio of the actual productivity index of a well to its productivity index if there were no skin ($s=0$):

$$\text{Flow efficiency} = FE = \frac{J_{actual}}{J_{ideal}} \quad (23)$$

Since

$$J_{actual} = \frac{q_o}{P^- - P_{wf}} \quad (24)$$

and

$$J_{ideal} = \frac{q_o}{P^- - P_{wf} - (\Delta P)_{skin}} \quad (25)$$

Therefore

$$FE = \frac{P^- - P_{wf} - (\Delta P)_{skin}}{P^- - P_{wf}} \quad (26)$$

The quantity $(\Delta P)_{skin}$ is obtained from Eq. 21. The flow efficiency is also known as productivity ratio, condition ratio, and/or completion factor (1). When subtracted from unity it gives the damage factor (2) which is also a relative indicator of the wellbore condition and is the inverse of the flow efficiency.

2.2.2.3 Drill stem test

One of the most important testing scenarios is the exploration well drillstem test (DST). While the term DST originated in the practice of using the drillstring for production from a temporary completion, most DSTs today are conducted through tubing. In areas where the reservoir pressure and fluid type are not known, drillpipe may be used only if the well will be shut in downhole so that no reservoir fluid is allowed to flow to surface (McAleese 2000).

Objectives.

The three primary objectives for exploration and appraisal well DSTs are to collect fluid samples, to estimate reservoir pressure, and to estimate in-situ permeability. Because a DST is conducted with a temporary completion, the skin factor obtained from a DST has limited relevance to predicting well performance following a permanent completion. High rig costs make it impractical to run DSTs long enough to confirm minimum economic reservoir size. As a result, exploration well testing does not usually include extended testing to estimate reserves (Barnum and Vela 1984).

Data acquired during drillstem testing will be used to make decisions about whether to abandon the zone or to set casing, to conduct an extended well test, or to drill additional wells. Data Available. Data availability is limited for an exploration well. Much of the

design and planning for a testing program in an exploration well is based on geology, geophysics, and economic targets. Additional data become available as the well is drilled and logged. However, by the time this data have been acquired and interpreted, time constraints prevent extensive revision to the test design. Thus, the preliminary design phase is likely to be based on the minimum economic case. During the preplanning phase, the data available are essentially the same data supporting the decision to drill (i.e., regional geology, 3D seismic interpretation, and economic potential). Seismic interpretation provides an estimate of gross thickness and depth of the candidate zone. Regional geology may provide estimates of expected

pore pressure and temperature gradients. Burial history and temperature give a good idea of the type of fluid likely to be present. Additional data available after the well is drilled and logged may include mud weight, drill cuttings, cores, logging-while-drilling data, conventional wireline logs, and Wireline formation tests (WFTs) data. Logs may be used to identify specific zones of interest to be tested within the gross candidate interval. WFT data may be used to select target zones for and improve design of conventional DSTs (Kumar et al. 2010). Although the test objectives, design, and cost are likely to be similar for an appraisal well, there is much more data available. Interpreted logs, lab tests of fluid samples and cores, and test results from the discovery well should all be available by the time the test design for an appraisal well is to be finalized. Other Considerations. Because of the high cost of testing exploration wells, downhole shut-in is frequently used to reduce the time required to reach infinite-acting radial flow and to reduce the likelihood and severity of wellbore effects such as phase segregation. The high cost also justifies the widespread use of surface readout to allow tests to be terminated early if the objectives of the test are met (or if the zone proves to be uneconomic).

Even with surface readout, tests may be terminated prematurely if appropriate criteria for early termination are not clearly understood and specified.

To avoid having to repeat a test in the event of gauge failure, multiple gauges are virtually always used to provide redundancy, with some operators reportedly using as many as 18 gauges in a single test string. At least one vendor offers gauges that store identical copies of the data in four separate, nonvolatile memory banks to ensure data integrity (Metrolog 2012).

❖ **Testing a pumping well with memory gauges would require the following time-consuming process:**

- Shut the well in to pull the pump.
- Hang the gauge carrier below the pump.
- Re-install the pump.
- Resume pumping to reach stabilized flow
- Shut-in well for buildup.
- Pull the pump and remove the gauge carrier.
- Rerun the pump and resume production.
- Important well test objectives include
 - To obtain fluid samples for laboratory analysis
 - To estimate in-situ permeability
 - To quantify damage or stimulation
 - To estimate distances to boundaries
 - To estimate hydrocarbons in place or drainage area

- To estimate initial or average drainage area pressure
- To evaluate reservoir connectivity
- To obtain a flowing or static gradient survey
- To satisfy regulatory obligations

Drill-stem testing provides a method of temporarily completing a well to determine the productive characteristics of a specific zone. As originally conceived, a drill-stem test provided primarily an indication of formation content. The pressure chart was available, but served mainly to evaluate tool operation. Currently, analysis of pressure data in a properly planned and executed DST can provide, at reasonable cost, good data to help evaluate the productivity of the zone, the completion practices, the extent of formation damage and perhaps the need for stimulation. A drill-stem test provides an estimate of formation properties and wellbore damage. These data may be used to determine the well's flow potential with a regular completion that uses stimulation techniques to remove damage and increase effective wellbore size.

Important well test objectives

Reservoir characteristics that may be estimated from DST analysis include:

- Average effective permeability. This may be better than core permeability since much greater volume is averaged. Also, effective permeability rather than absolute permeability is obtained.
- Reservoir pressure: Measured, if shut-in time is sufficient, or calculated, if not.
- Wellbore damage: Damage ratio method permits the estimation of what the well should make without damage.
- Barriers, permeability changes, and fluid contacts: These reservoir anomalies affect the slope of the pressure buildup plot. They usually require substantiating data to differentiate one from the other.
- Radius of investigation: An estimate of how far away from the wellbore the DST can "see".
- Depletion: Can be detected if the reservoir is small and the test is properly run.

DST Equipment and Operational Procedures

The DST is performed in following steps

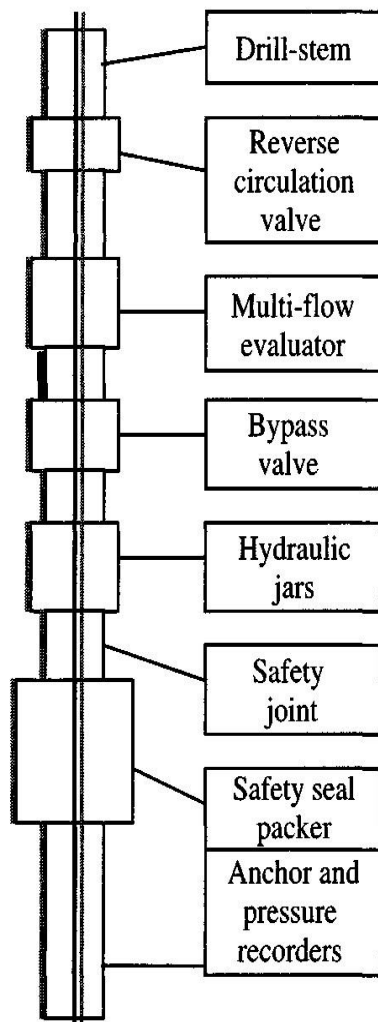
- The tool is lowered on the drill string to the zone to be tested.
- The packer or packers are set to isolate the zone from the drilling fluid column.
- The valves or ports are then opened to allow for formation flow while the recorders chart static pressures.
- A sampling chamber traps clean formation fluids at the end of the test.
- Analysis of the pressure charts is performed

The DST tool is an arrangement of packers and valves placed at the end of the drill pipe. The packers help in isolating the zone of interest from drilling mud in the hole and to let it produce into the test chamber, drill collar, and drill pipe. The packers also help in reducing wellbore storage effects. (Fig2.16) shows a diagram of operational DST tool and sequence of operations for MFE tool.

DST Pressure Behavior

(Figure 2.17) shows a pressure record from a drill-stem test. Sequences of pressure recording are:

- A. Increase in hydrostatic mud pressure as the tool is lowered into the hole.
- B. Setting of the packers causes compression of the mud in the annulus in the test interval, and a corresponding increase in pressure is noted.
- C. When the tool is opened and inflow from the formation occurs, the pressure behavior is as shown in this section.
- D. After the test tool is closed, a period of pressure buildup results.
- E. . Finally, the test is ended and the packers are pulled loose, causing a return to hydrostatic mud pressure.
- F. Tool is pulled. Fluid recovery from the test may be determined from the contents of the drill pipe or from the amount recovered at the surface if a flowing DST is obtained.



Basics of DST Operations

The drill-stem test often uses two bombs and one or more flow, and shut-in sequences are recorded. Some important factors of the DST chart are:

1. Going into hole
2. Initial flow period
3. Initial shut-in period
4. Final flow period
5. Final shut-in period
6. Going out of hole

In summary, the DST, if properly applied, has become a very useful tool for the Well Completion Engineer

Figure 2.16 Operational DST tool

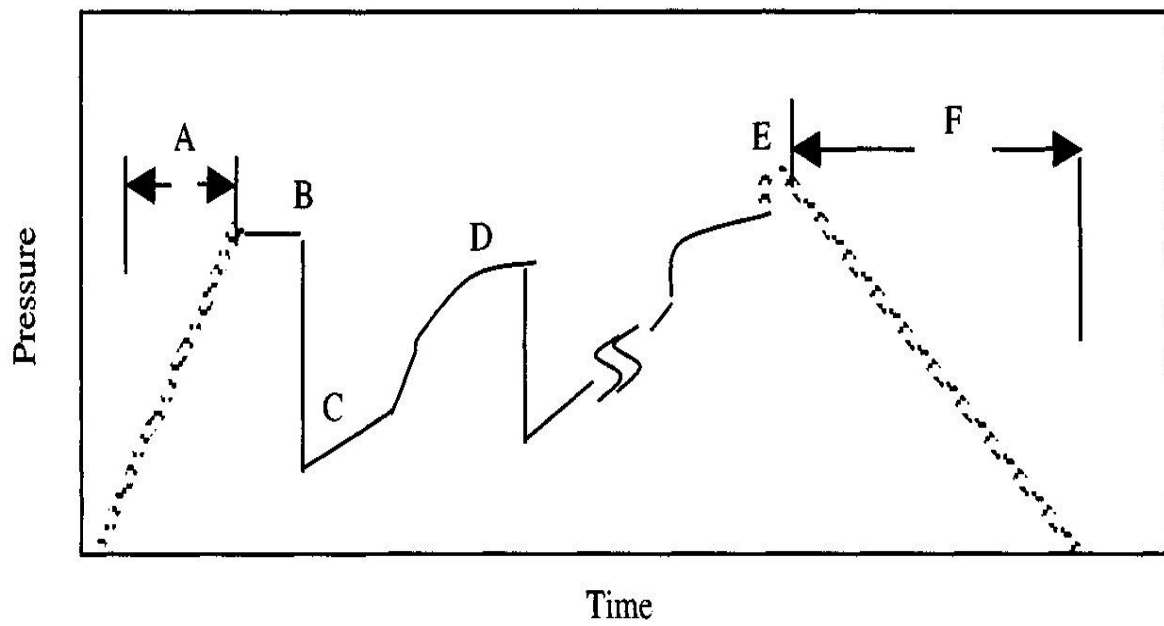


Figure 2.17 DST pressure record

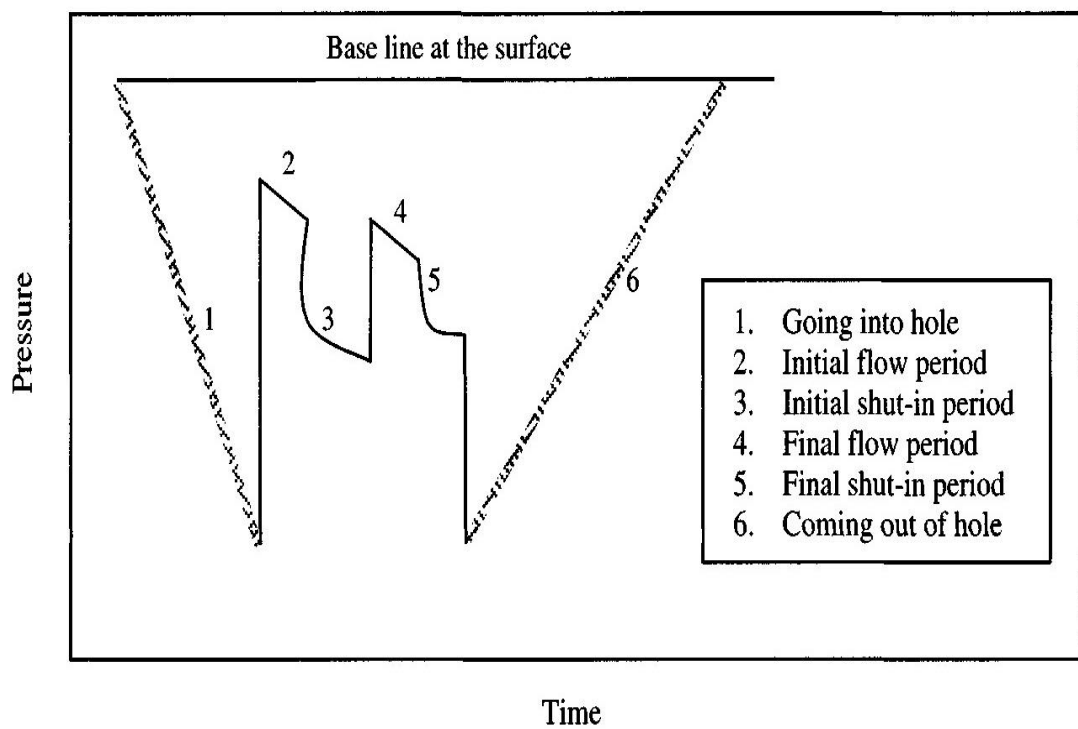


Figure 2.18 DST pressure chart for two-cycle test

Recommended Flow and Shut-in Time for Drill-Stem Tests

The key to DST evaluation is obtaining and recording good data. The DST must be planned to fit the specific situation. Past experience in the area should be studied in planning subsequent tests. The first flow is very short and is designed (usually 5-15 min) to remove any excess pressure, which may have resulted from setting the packers. The first buildup is rather long (usually 30-60 min) since reliable value for the initial reservoir pressure is desired. The second flow is somewhat longer and is designed (usually 60 min) to evaluate the formation for some distance from the well. The second shut-in is usually 30 min to several hours to calculate the transmissibility and other characteristics of the reservoir. If the second extrapolated pressure is less than the pressure of the first shut-in, depletion of the small reservoir should be suspected. If extrapolated pressure P^* is equal to P_i from the two shut-in periods, then depletion results. (Fig 2.18) shows the DST pressure chart for a two-cycle test. The first cycle in (Fig 2.18) includes the initial flow and buildup periods, while the second cycle includes the second flow and final buildup periods. (Fig 2.19 and Fig 2.20) shows tests with more than two cycles are possible. In this figure, the pressure increases upward.

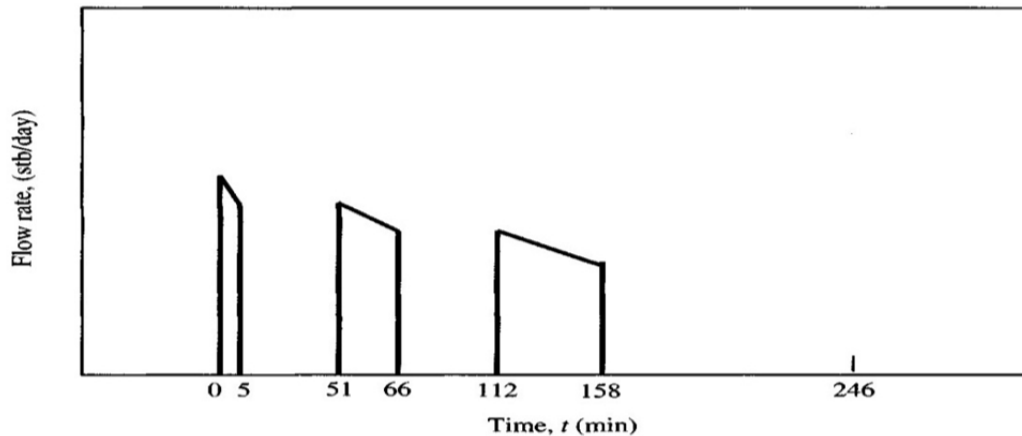


Figure 2.19 Flow rate three-cycle DST

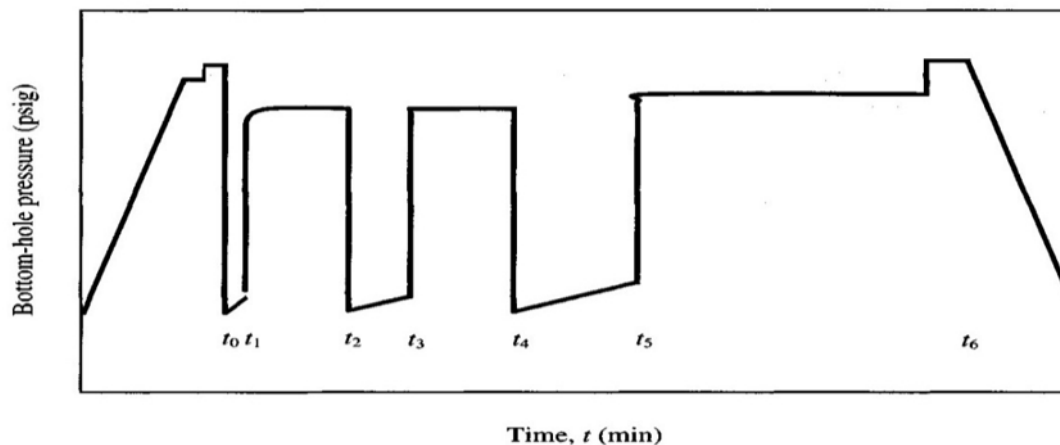


Figure 2.20 Bottom-hole pressure three-cycle DST

Troubleshooting DST Pressure Charts

It is important to carefully examine the DST charts and decide if the test was mechanically and operationally successful. A good DST chart has the following characteristics:

- The pressure base line is straight and clear;
- Recorded initial and final hydrostatic mud pressures are the same and are consistent with depth and mud weight;
- Flow and buildup pressures are recorded as smooth curves. The DST pressure chart will also indicate bad hole conditions and tool malfunctions, and other difficulties can be identified from the DST charts. The actual DST charts on the following pages show examples of DST problems that restrict the calculation possibilities. Included also are sample situations which can be reasonably interpreted by "eyeball" methods.

DST Charts for Barrier Detection

To recognize a poor DST, one must be familiar with DST chart characteristics. Murphy¹² and Timmerman and Van Poollen³ provide such information. A good DST chart has the following characteristics:

- A. the pressure base line is straight and clear;
- B. recorded initial and final hydrostatic mud pressures are the same and are consistent with depth and mud weight; and
- C. flow and buildup pressures are recorded as smooth curves.

DST Analysis Methods, Uses, and Limitation

Analysis of DST provides a practical and economical means for estimating important formation parameters prior to well completion. A proper run and interpreted DST yield more valuable information. DST pressure buildup data are analyzed much like any other pressure buildup data; the techniques of Buildup test. (Fig 2.21) shows various DST analysis methods, uses, and their limitations.

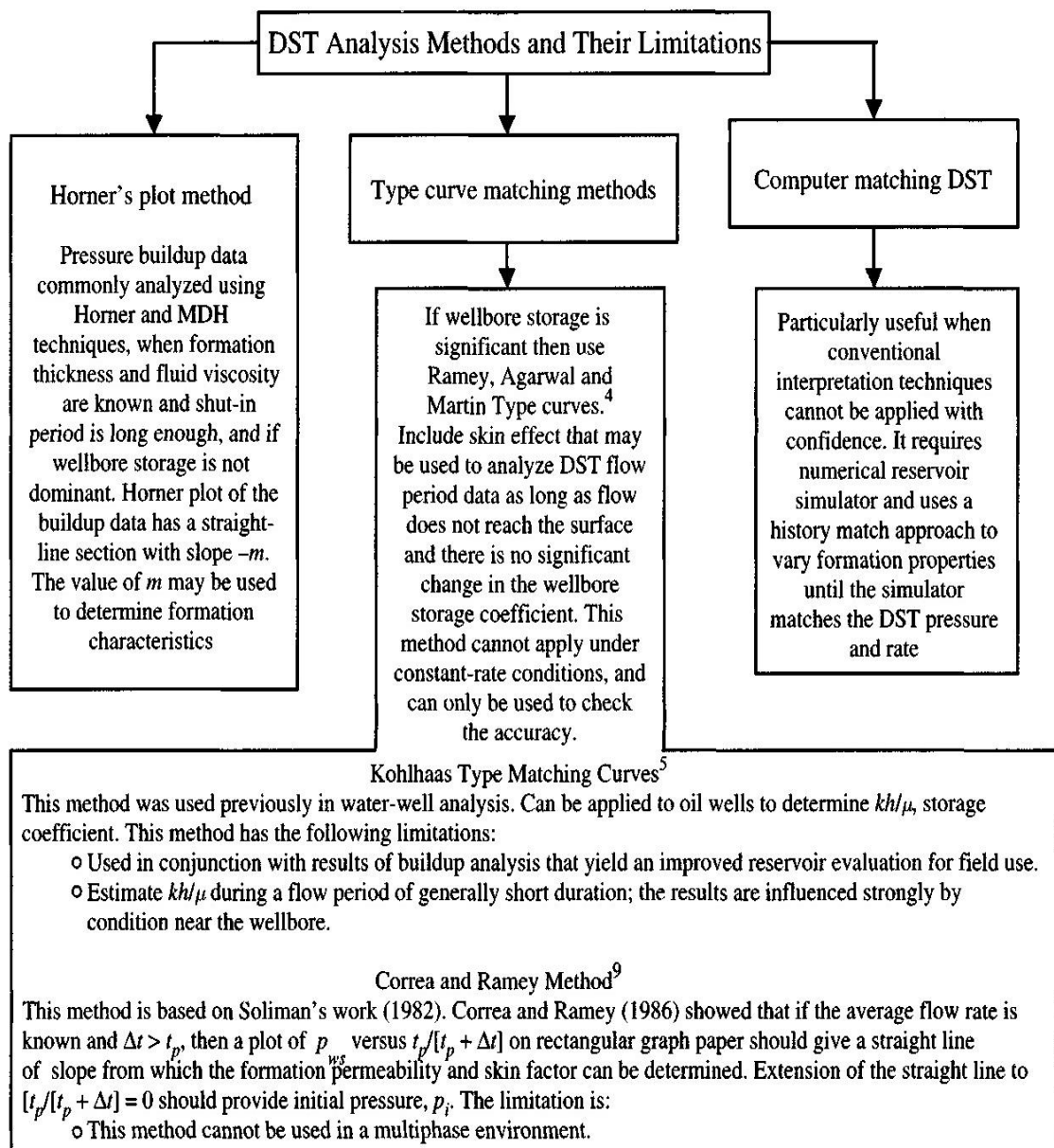


Figure 2.21 Most common methods to analyze DST data and their limitations.

The typical drill stem test will be split into four periods:

- Pre-flow
- Initial shut in period
- Main flow period
- Final shut-in period

Times for each test are dependent on conditions at the well site. Drill stem tests may be run at any time during the drilling operation at the current depth or may be used to test any interval in the hole after TD has been reached. Using these data and based on the evaluation of engineers and geologists, management can base a decision to complete the hole for potential production of oil or gas or proceed with abandonment

Pre-Flow Period

Is a production period to clean up the well and is used to remove any supercharge given to the formation due to mud infiltrating into the prospective formation during the drilling operation.

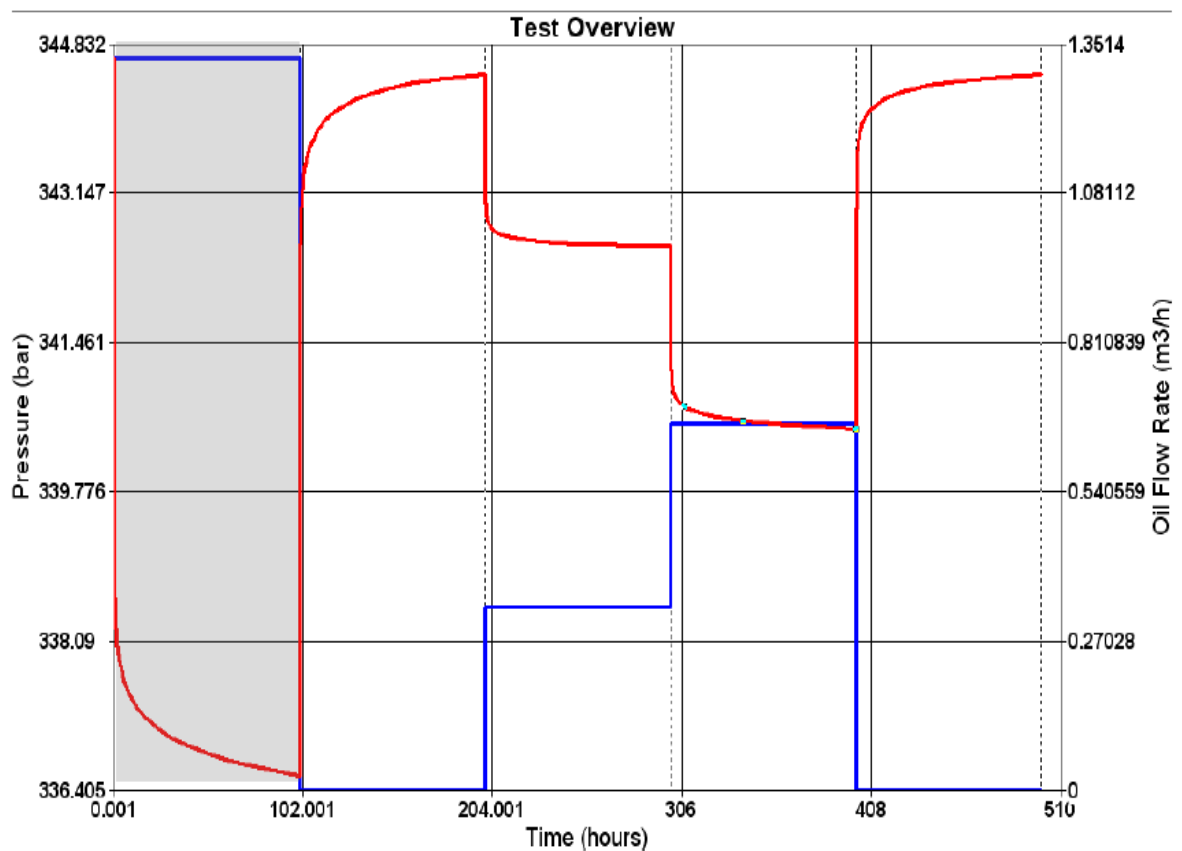


Figure 2.22 Pre-Flow Period

Initial Shut-In

This period is to allow the formation to recover from pressure surges caused during the pre-flow. This is often referred to as "closed-in for the pressure build up".

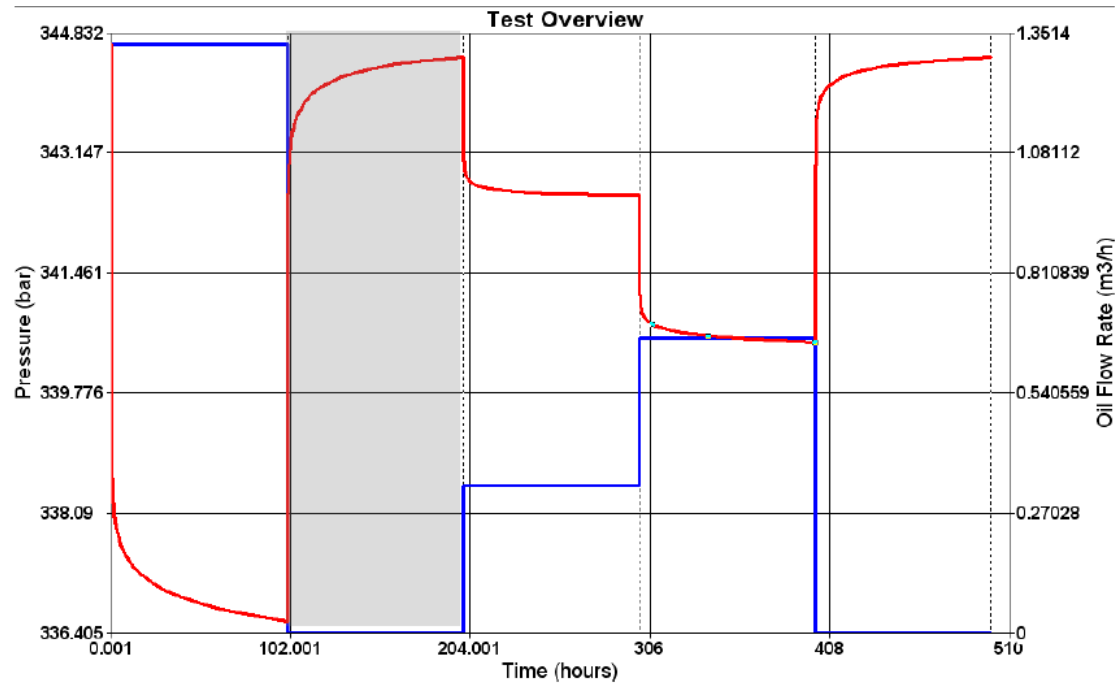


Figure 2.23 Initial Shut-In

Main Flow

A more lengthy production period designed to test the formations flow characteristics more rigorously. Samples of any fluids in the drill string will be gathered for analysis and flowing pressures and temperatures will be recorded.

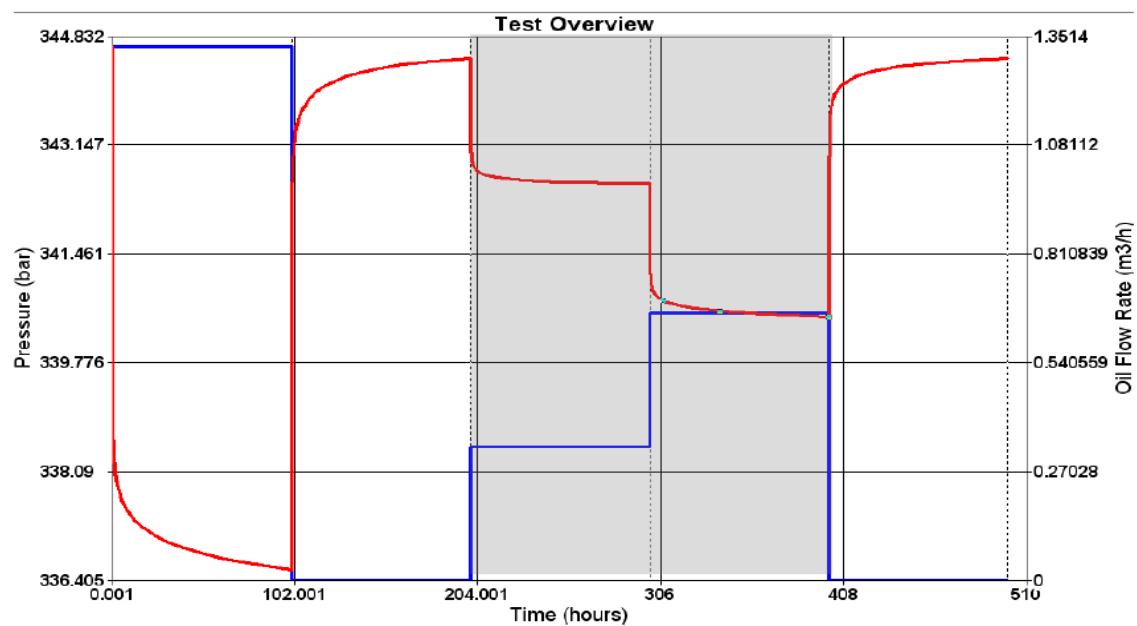


Figure 2.24 Main Flow

Final Shut-In

Formation pressure is recorded over this period. The shape of the pressure build up curve will tell us the permeability of the formation, the degree of formation damage (likely caused during the drilling operation), It will also tell us if we have found a small reservoir but there is no telling if it a big one.

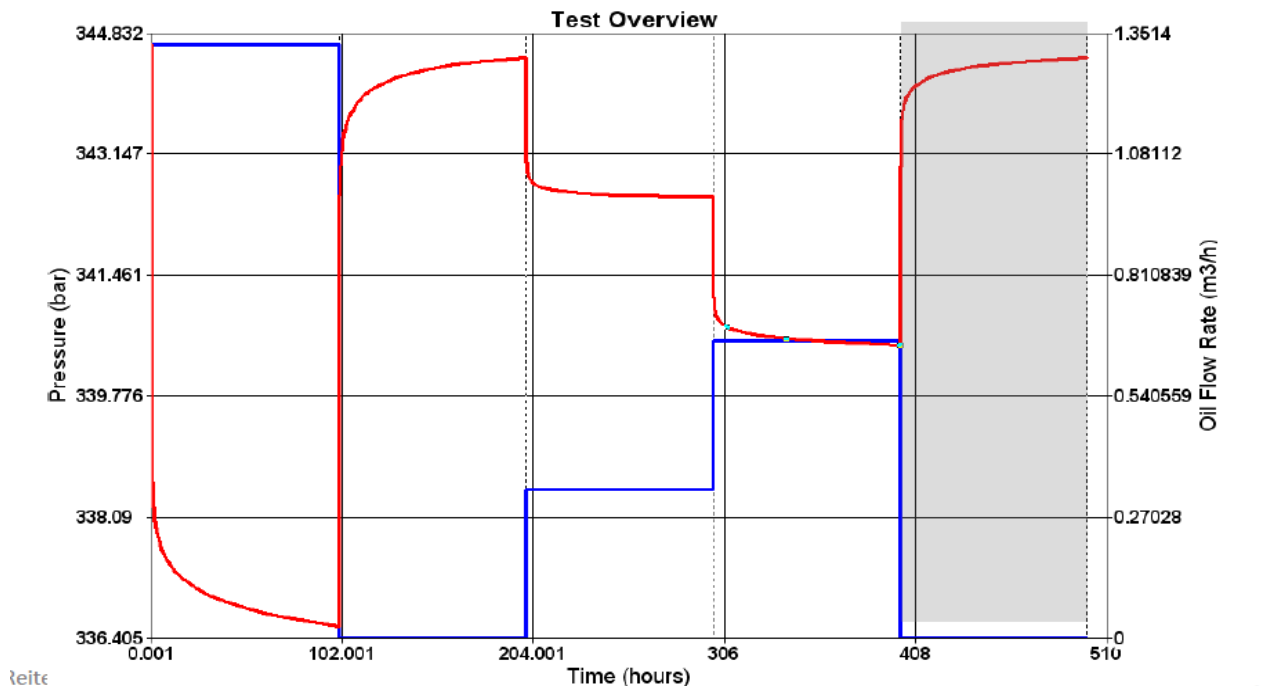


Figure 2.25 Final Shut-In

2.3 Well test interpretation methods:

The pressure response during a transient well test is a function of both the well and reservoir characteristics and the flowrate history. In interpretation terms, the actual pressure and time are unimportant, with analysis performed in terms of pressure change Δp versus elapsed time, Δt :

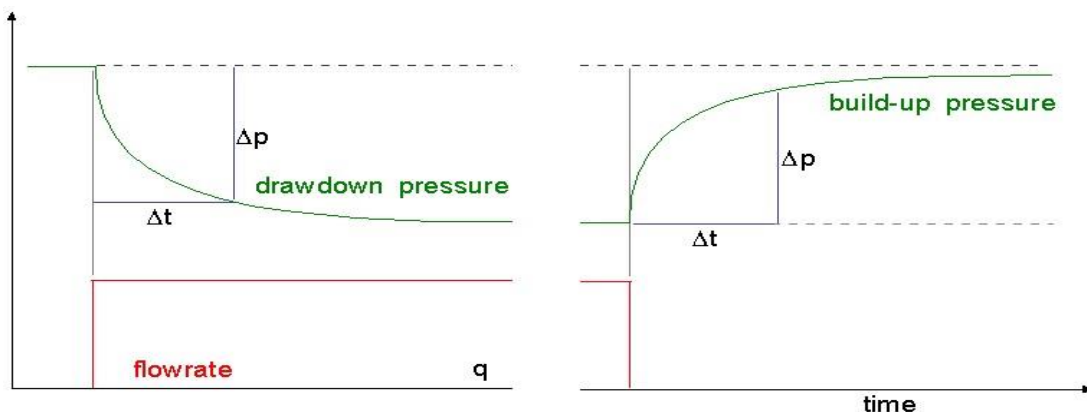


Figure 2.26 WTI Essentials

The change in pressure with respect to time is similar for drawdowns and build-ups, but one is not quite a mirror-image of the other. Although, in principle, either a drawdown or a build-up will reveal the reservoir characteristics, the build-up response is ‘cleaner’ than the drawdown data, which can be adversely affected by even a slight instability in the flow rate.

The linear or Cartesian plot of pressure versus time, as shown above, is of limited value in well testing, but does have specialized uses, as will be seen later. Well test interpretation is predominantly

2.3.1 Conventional Methods:

2.3.1.1 Semi-Log Approach

During radial flow, the pressure change is related to the logarithm of the time. In other words, if pressure is plotted against the log of time, infinite-acting radial flow will give a straight line. For this reason, the classical approach to well test interpretation has been the semi-log plot, of p versus $\log \Delta t$:

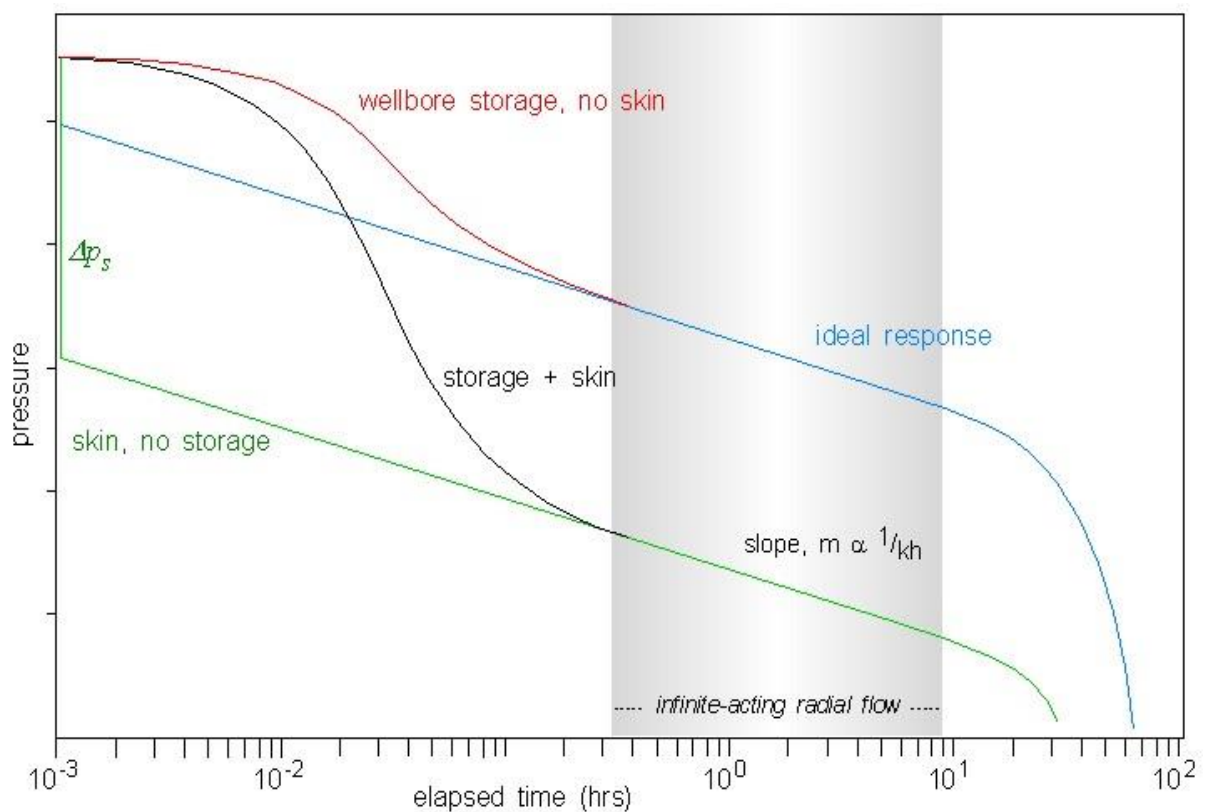


Figure 2.27 Semi-Log Approach

With wellbore storage but no skin the red curve is obtained. Initially production is only from decompression of the wellbore fluid, so the bottomhole pressure remains constant for a short while, as if the well were still shut in. Once there is movement of fluid through the sand face, the bottom hole pressure starts to drop, and once the effects of storage are over the red curve transitions onto the ideal curve.

With skin but no storage, the green curve shows radial flow immediately, parallel to but offset from the ideal blue line. The offset on the y-axis corresponds to Δp_s at this flowrate, and the slope of the straight line cannot be different, as it represents the kh of the system. A typical test will reveal both wellbore storage and skin, corresponding to the black curve transitioning on to the green curve. The storage causes the delay, the skin the offset, and once again the final straight-line slope is unchanged, as permeability is a reservoir property and is unaffected by near-wellbore effects.

In most cases the pressure curve will eventually drop below the radial flow line, as shown to the right of the grey window, if the well is tested long enough. This is because there is no such thing as an infinite reservoir, and as boundaries are seen, but the same flowrate is maintained from the well, the pressure will drop more rapidly. Sometimes the opposite happens, and the boundary is a supporting aquifer or gas cap, in which case the pressure curve tends to stabilize. What is certain is that the radial flow, and its corresponding straight line, cannot last forever.

Until the effects of wellbore storage become insignificant, the pressure response does not reveal information about the reservoir. The 'grey window', containing the radial flow data from which kh and skin are obtained, can be brought forward either physically, by way of downhole shut-in to reduce the wellbore storage, or mathematically, by way of convolution of downhole flowrate and pressure data.

2.3.1.2 MDH Plot

The most simple semi-log plot, in which the time axis is $\log(\Delta t)$, is called the Miller-DyesHutchinson or MDH plot. It is strictly valid only for the first ever drawdown on a well, but can in exceptional circumstances be used for analysis of a later drawdown or even a build-up. In 1998, with computers that can handle superposition rigorously, it should only be used for 'Drawdown #1':

All of the semi-log plots are more convenient plotted with pressure on the y-axis, as this makes no difference to the analysis. So for the MDH, a drawdown plot:

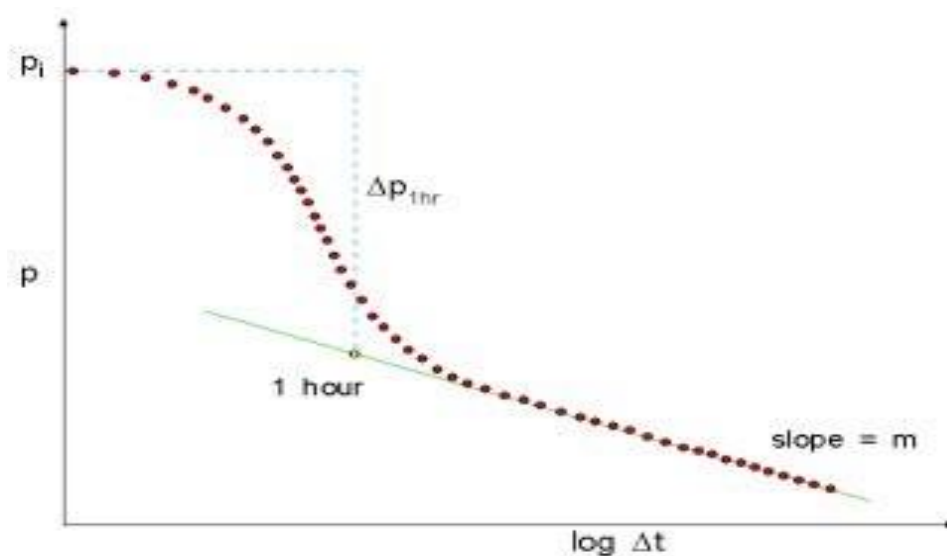


Figure 2.28 MDH Plot

As already mentioned the slope of the straight line is:

$$m = 162.6 \frac{q\mu\beta}{kh} \quad (1)$$

This gives the permeability-thickness product as:

$$kh = 162.6 \frac{q\mu\beta}{m} \quad (2)$$

The value of the pressure on the line at $\Delta t = 1$ hour is used to evaluate the skin. Cross-multiplying the expression on the previous page:

$$S = 1.151 \left[\frac{\Delta p_{1hr}}{m} - \log \left(\frac{k}{\phi\mu C_t r_w^2} \right) + 3.23 \right] \quad (3)$$

2.3.1.3 Horner Plot

The MDH plot, with the simple $\log(\Delta t)$ time function, results directly from the log approximation to the drawdown solution for infinite-acting radial flow. In order to use semi-log analysis for any flow period other than the first drawdown, it is necessary to take account of superposition effects, as discussed in earlier.

In the simplest superposition case of a build-up following a single drawdown, in which an 'elementary drawdown solution' of rate $-q$ (i.e. an injection) overlays a drawdown of rate $+q$, and assuming that both solutions reach IARF, we get the approximate build-up solution:

$$p = p_i - 162.6 \frac{q\mu\beta}{kh} \log \left(\frac{t_p + \Delta t}{\Delta t} \right) \quad (1)$$

So infinite-acting radial flow will be characterized by a linearity between the pressure response and the Horner time function, $\log(t_p + \Delta t)/\Delta t$, which depends upon t_p , the duration of the production period preceding the shut-in.

The coefficient in front of the log term is the same as for the MDH plot, so the straight line slope will again be 'm', and

$$kh = 162.6 \frac{q\mu\beta}{m} \quad (2)$$

as before. The skin calculation requires that the drawdown had reached IARF in the reservoir prior to shut-in, as the last flowing pressure (at t_p) is replaced by its log approximation:

$$= 162.6 \frac{q\mu\beta}{kh} \left[\log \left(\frac{t_p + \Delta t}{\Delta t} \right) + \log \left(\frac{k}{\phi\mu C_t r_w^2} \right) - 3.23 + 0.87 S \right] \quad (3)$$

Taking the pressure on the line again at 1 hour, the skin equation becomes:

$$S = 1.151 \left[\frac{\Delta p_{1hr}}{m} - \log \left(\frac{k}{\phi\mu C_t r_w^2} \right) + \log \left(\frac{t_p + 1}{t_p} \right) + 3.23 \right] \quad (4)$$

The only difference compared to the MDH solution is the second log term, which will typically be of little significance.

Note that the time function is such that the data plots 'backwards', as when Δt is small, at the start of the build-up, Horner time ($\log(t_p + \Delta t)/\Delta t$) will be large, and when Δt tends to infinite shut-in time the Horner time tends to 1, the log of which is 0:

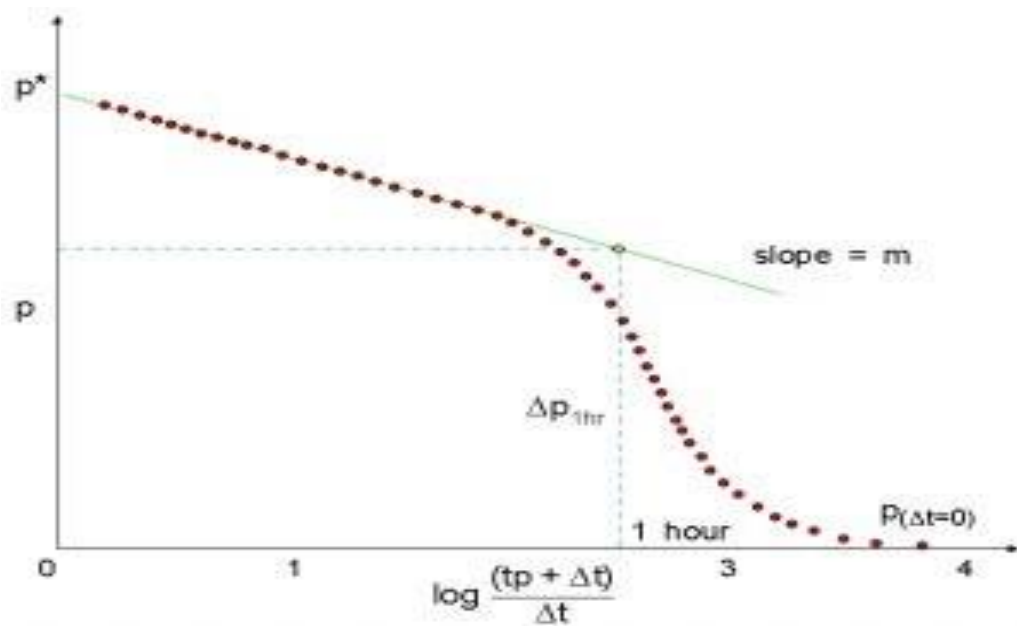


Figure 2.29 Horner Plot

1. Graph the shut-in bottomhole pressure, P_{ws} , vs. the HTR, $(\frac{t_p + \Delta t}{\Delta t})$, on a semilog scale. If a normal semilog scale is used (increasing from left to right), time will increase from right to left. A reversed semilog scale may be used so time will increase from left to right.
2. Identify the data exhibiting IARF.
3. Draw a straight line through the selected data, and find the slope m .
4. Read P_{1hr} from the straight line or its extrapolation at an HTR corresponding to a shut-in time Δt of 1 hour, $HTR_{1hr} = (t_p + 1)/1$.
5. Calculate the permeability from the slope m as.

$$k = \frac{162.6 q \mu \beta}{mh}$$

6. Calculate the skin factor s from the slope m , the flowing bottomhole pressure at the moment of shut-in, P_{wf} , and P_{1hr} :

$$s = 1.151 \left[\frac{P_{1hr} - P_{wf}}{m} - \log \left(\frac{k}{\phi \mu C_t r_w^2} \right) + 3.23 \right]$$

7. Extrapolate the straight line to an HTR of 1. If the reservoir is infinite acting throughout both flow and buildup periods, extrapolating the straight line to an HTR of 1 (corresponding to infinite shut-in time) gives the initial pressure, P_i . If the reservoir is not infinite acting, the extrapolated pressure at an HTR of 1 is called the false pressure, P^* . The MBH (Matthews et al. 1954) method may then be used to estimate the average reservoir pressure from P^* .

2.3.1.4 MBH Method

As noted previously, the buildup test exhibits a semilog straight line which begins to bend down and become flat at the later shut-in times because of the effect of the boundaries. Matthews et al. (1954) proposed a methodology for estimating average pressure from buildup tests in bounded drainage regions. The MBH method is based on theoretical correlations between the extrapolated semilog straight line to the false pressure P^* and current average drainage area pressure p . The authors point out that the average pressure in the drainage area of each well can be related to p^* if the geometry, shape, and location of the well relative to the drainage boundaries are known. They developed a set of correction charts, as shown in (Fig 2.30). The y-axis of these figures represents the MBH dimensionless pressure p_{DMBH} that is defined by:

$$P_{DMBH} = \frac{2.303(P^* - P^-)}{m} \quad (1A)$$

Or

$$P^- = P^* - \left(\frac{m}{2.303}\right) P_{DMBH} \quad (1B)$$

❖ **The following steps summarize the procedure for applying the MBH method:**

1. Make a Horner plot.
2. Extrapolate the semilog straight line to the value of P^* at $(t_p + \Delta t)/\Delta t = 1$.
3. Evaluate the slope of the semilog straight line m .
4. Calculate the MBH dimensionless producing time t_{pDA} from

$$t_{pDA} = \left[\frac{0.000264k}{\phi \mu C_t A} \right] t_p$$

5. Find the closest approximation to the shape of the well drainage area and identify the correction curve.
6. Read the value of P_{DMBH} from the correction curve at t_{pDA}
7. Calculate the value of average drainage area pressure from

$$P^- = P^* - \left(\frac{m}{2.303}\right) P_{DMBH}$$

- Pinson & Kazemi indicate that t_p should be compared with the time required to reach the pseudo-steady state t_{pss} :

$$t_{pss} = \left[\frac{\phi \mu C_t A}{0.000264k} \right] \times (t_{DA})_{pss}$$

- For symmetric closed or circular drainage area, $(t_{DA})_{pss} = 0.1$ as given in previous Table and listed in the fifth column.
- If $t_p \gg t_{pss}$, then: t_{pss} should ideally replace t_p in both the Horner plot and for use with the MBH dimensionless pressure curves.

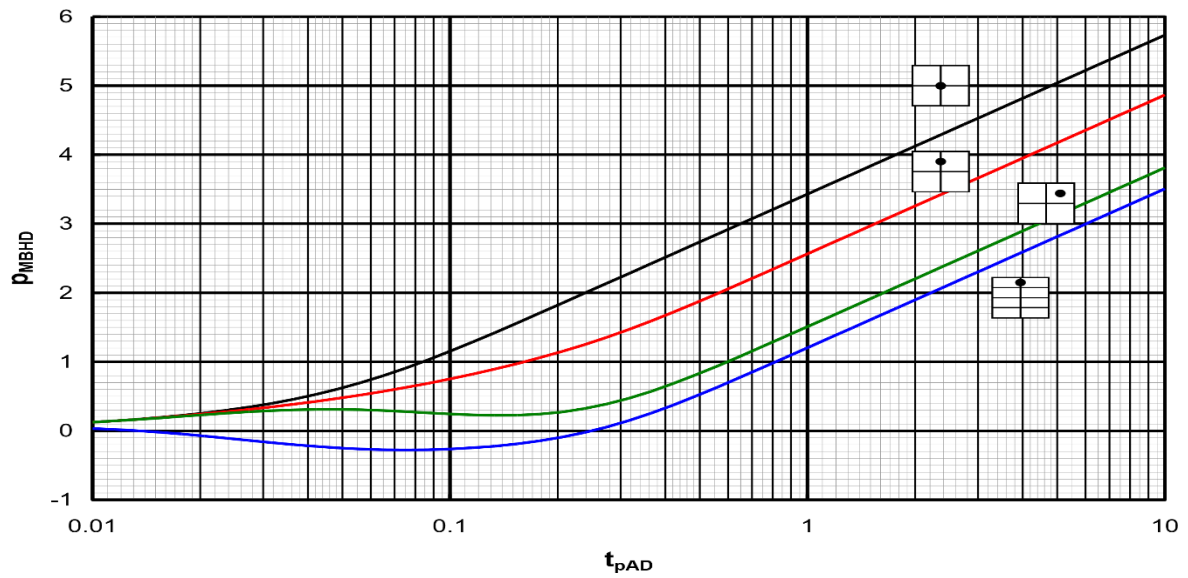


Figure 2.30 Curves for Square Drainage Area

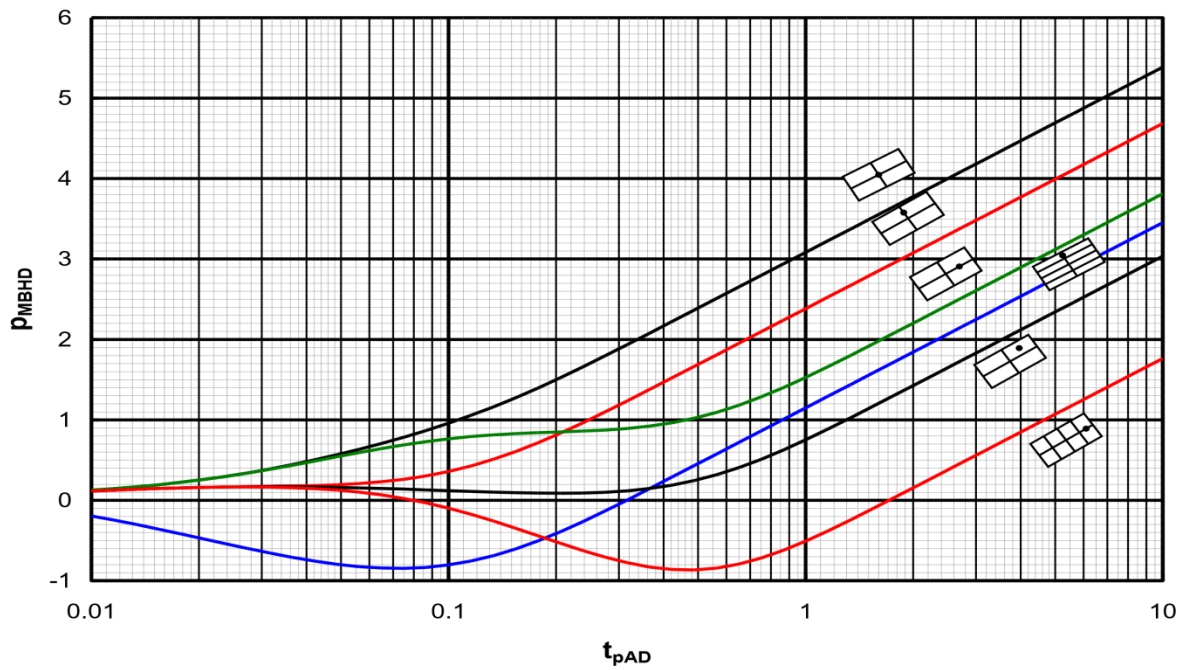


Figure 2.31 Curves for 2x1 Rectangle

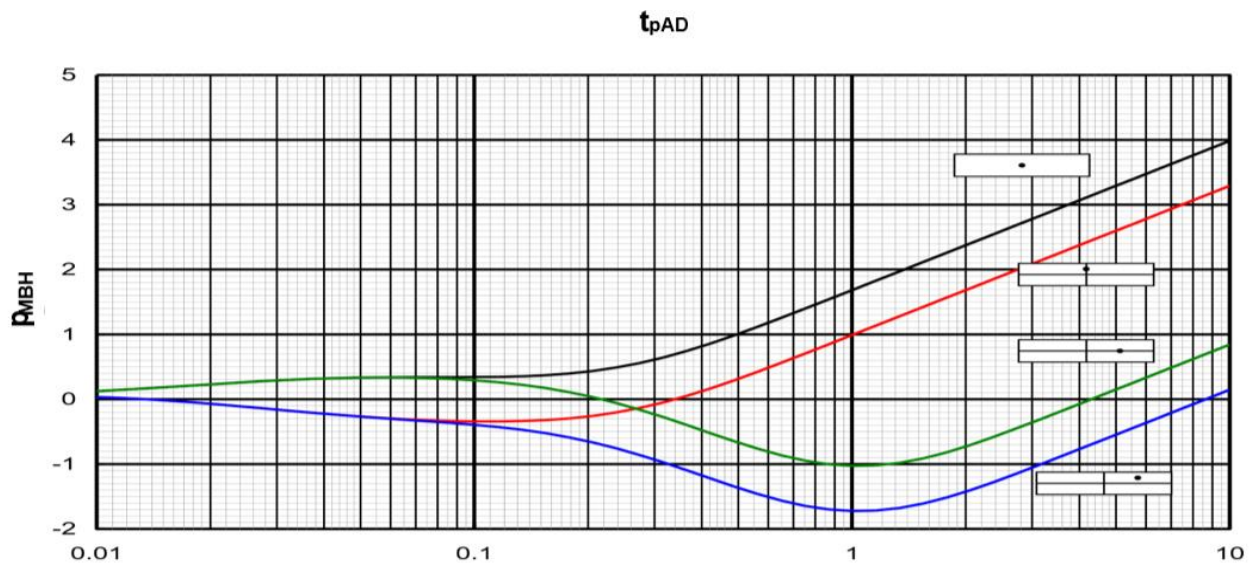


Figure 2.32 Curves for 4x1 Rectangle

2.3.2 Type Curves Methods

Type curves analysis approach was introduced in petroleum industry by Agarwal et al. as a valuable tool when used in conjunction with conventional semilog plots. Type Curves are preplotted family of curves generated by obtaining solutions to the flow equations such as the diffusivity equation, for selected types of formations and selected initial and boundary conditions. Some of these solutions are analytical, others are based on finite difference approximations generated by computer reservoir simulators. Because of the way they are plotted (usually on logarithmic coordinates), it is convenient to compare actual field data plotted on the same coordinates to the type curves. The results of this comparison frequently include qualitative and quantitative descriptions of the formation and completion properties of the tested well. The Type Curves analysis consist of finding the theoretical type curve that matches the actual response from a test well and the reservoir when subjected to changes in production rates or pressures. The match can be found graphically by physically superposing a graph of actual test data with a similar graph of type curves and searching for the type curve that provides the best match.

❖ Application of Type Curves

They allow test interpretation even when wellbore storage distorts most or all of the test data in that case conventional methods fail. Some of the curves are used to help identify the MTR (straight line section), while other type curves are used to estimate the Permeability, Skin Factor, Fracture Length, etc. The type curves are used to double-check the results obtained with conventional methods with those obtained with type curve matching. Since type curves are plots of theoretical solutions to transient and pseudo-steady-state flow equations, they are usually presented in terms of dimensionless variables (PD , tD , rD & CD) rather than real variables (P , t , r & C). The reservoir and well parameters, such as permeability and skin, can then be calculated from the dimensionless parameters defining that type curve.

Any variable can be made “dimensionless” by multiplying it by a group of constants with opposite dimensions, but the choice of this group will depend on the type of problem to be solved.

- A more practical solution then to the diffusivity equation is a plot of the dimensionless PD vs. (t_D/r_D^2) as shown in next Fig. that can be used to determine the pressure at any time and radius from the producing well.
- Next Fig. is basically a type curve that is mostly used in interference tests when analyzing pressure response data in a shut-in observation well at a distance r from an active producer or injector well.
- The subscript “MP” denotes a match point.

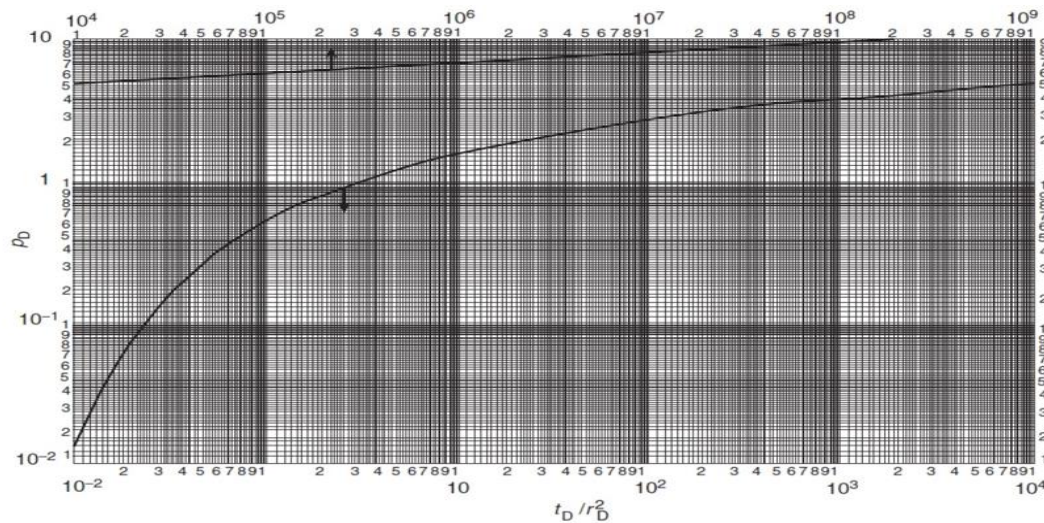


Figure 2.33 Dimensionless pressure for a single well in an infinite system

❖ Type Curve Analysis Procedure

In general, the type curve approach employs the flowing procedure that will be illustrated by the use of previous (Fig 2.33).

Step 1. Select the proper type curve.

Step 2. Place tracing paper over previous (Fig 2.33).and construct a log–log scale having the same dimensions as those of the type curve. This can be achieved by tracing the major and minor grid lines from the type curve to the tracing paper.

Step 3. Plot the well test data in terms of ΔP vs. t on the tracing paper (next (Fig 2.34)).

Step 4. Overlay the tracing paper on the type curve and slide the actual data plot, keeping the X and Y axes of both graphs parallel, until the actual data point curve coincides or matches the type curve.

Step 5. Select any arbitrary point match point MP, such as an intersection of major grid lines, and record $(\Delta P)_{MP}$ and $(t)_{MP}$ from the actual data plot and the corresponding values of $(P_D)_{MP}$ and $(t_D/r_D^2)_{MP}$ from the type curve.

Step 6. Using the match point, calculate the properties of the reservoir from Eqs;

$$\left(\frac{P_D}{\Delta p}\right)_{MP} = \frac{kh}{141.2Q\beta\mu} \quad \& \quad \left(\frac{t_D/r_D^2}{t}\right)_{MP} = \frac{0.0002637k}{\phi\mu C_t r_w^2}$$

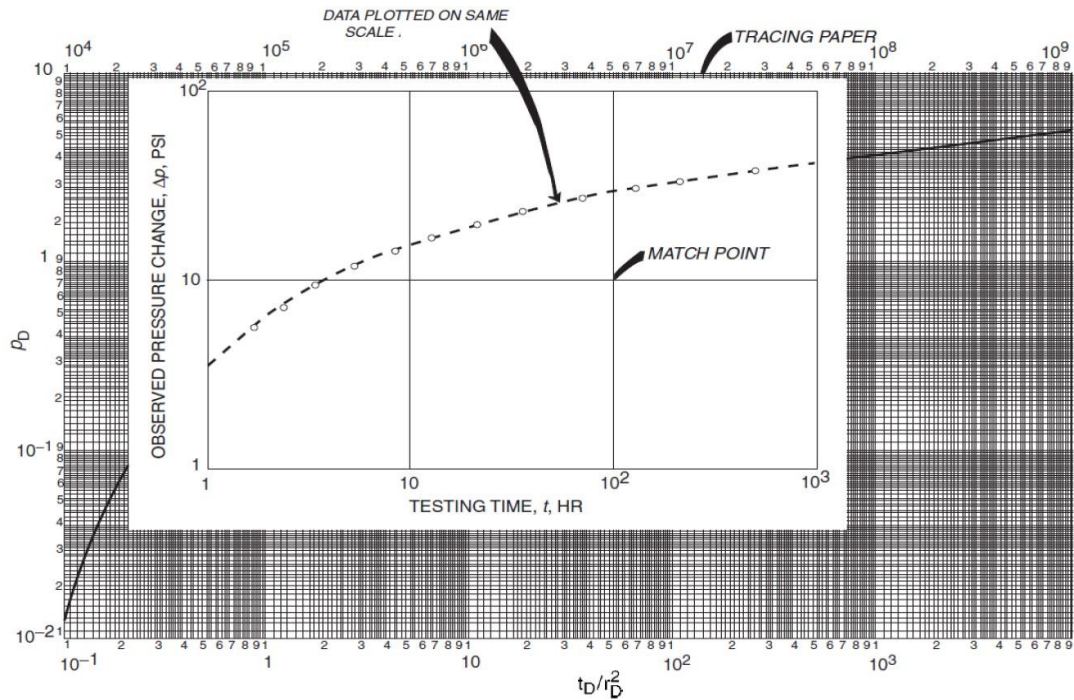


Figure 2.34 Tracing paper

❖ Gringarten Type Curve

During the early-time period where the flow is dominated by the wellbore storage, the wellbore pressure is described by:

$$P_D = \frac{t_D}{C_D} \quad (1)$$

$$\log(P_D) = \log(t_D) - \log(C_D) \quad (2)$$

This relationship gives the characteristic signature of wellbore storage effects on well testing data which indicates that plot of P_D vs. t_D on log-log scale will yield straight line of unity slope.

At the end of the storage effect, which signifies the beginning of the infinite-acting period, the resulting pressure behavior produces the usual straight line on semilog plot as described by:

$$P_D = \frac{1}{2} [\ln(t_D) + 0.080901 + 2s] \quad (3)$$

It is convenient when using the type curve approach in well testing to include the dimensionless wellbore storage coefficient in the above relationship.

Adding and subtracting $\ln(C_D)$ inside the brackets of the above equation gives:

$$P_D = \frac{1}{2} [\ln(t_D) - \ln(C_D) + 0.080901 + \ln(C_D) + 2s] \quad (4)$$

$$P_D = \frac{1}{2} \left[\ln\left(\frac{t_D}{C_D}\right) + 0.080901 + \ln(C_D e^{2s}) \right] \quad (5)$$

Eq. above describes the pressure behavior of a well with wellbore storage and skin in homogeneous reservoir during the transient (infinite-acting) flow period. Gringarten et al. expressed the above equation in the graphical type curve format shown in (Fig2.35A)

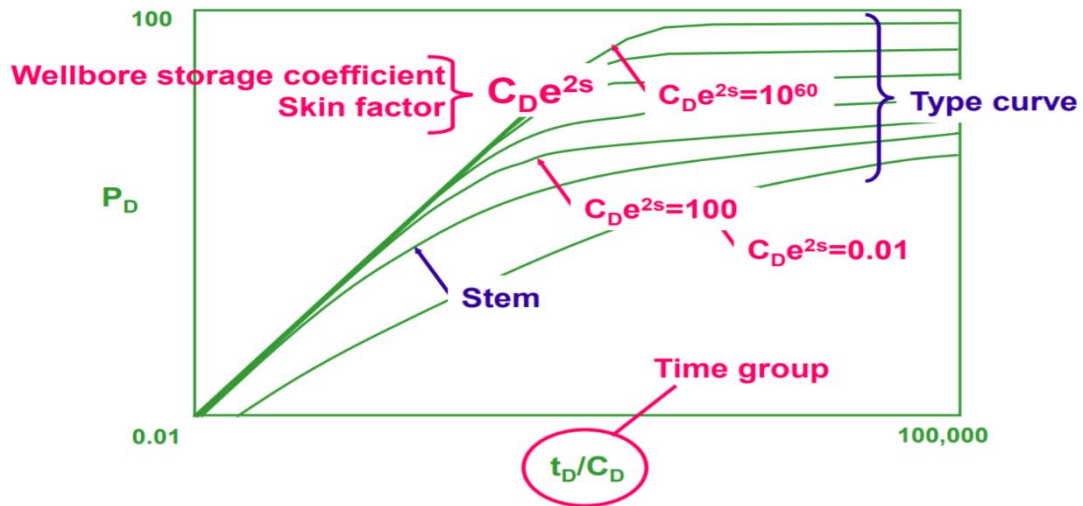


Figure 2.35A Gringarten Type Curve

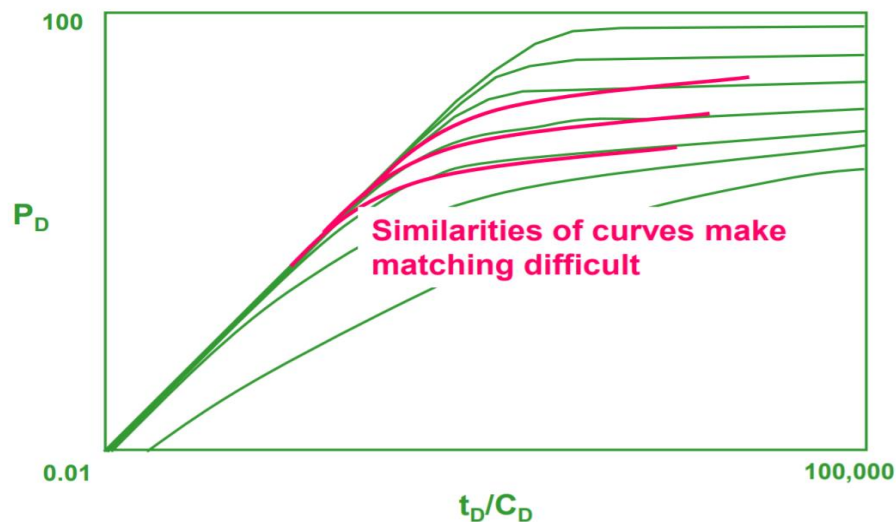


Figure 2.35B Gringarten Type Curve

- In previous (Figure 2.35B)., the dimensionless pressure P_D is plotted on log–log scale versus the dimensionless time group t_D/C_D .
- The resulting curves, characterized by the dimensionless group $C_D e^{2s}$, represent different well conditions ranging from damaged wells to stimulated wells.
- Previous (Fig 2.35B). shows that all the curves merge, in early time, into a unit-slope straight line corresponding to pure wellbore storage flow. At later time with the end of the wellbore storage-dominated period, curves correspond to infinite-acting radial flow.

- There are three dimensionless groups that Gringarten et al. used when developing the type curve:
- Dimensionless pressure PD;
- Dimensionless ratio tD/CD;
- Dimensionless characterization group CDe2s.
- There are three dimensionless groups that Gringarten et al. used when developing the type curve:
 - 1) dimensionless pressure PD.
 - 2) dimensionless ratio tD/CD.
 - 3) dimensionless characterization group CDe .

- The above three dimensionless parameters are defined mathematically for both drawdown and buildup tests as follows:

❖ **For Drawdown Test**

- Dimensionless pressure PD:

$$P_D = \frac{kh(P_i - P_{wf})}{141.2q\beta\mu} = \frac{kh\Delta p}{141.2q\beta\mu} \quad (6)$$

- Taking logarithms of both sides of the above equation gives:

$$\log(P_D) = \log(P_i - P_{wf}) + \log\left(\frac{kh}{141.2q\beta\mu}\right) \quad (7)$$

$$\log(P_D) = \log(\Delta p) + \log\left(\frac{kh}{141.2q\beta\mu}\right) \quad (8)$$

- Dimensionless ratio tD/CD:

$$\frac{t_D}{C_D} = \left(\frac{0.0002637kt}{\phi\mu C_t r_w^2}\right) \left(\frac{\phi h C_t r_w^2}{0.8396C}\right) \quad (9)$$

- Simplifying gives:

$$\frac{t_D}{C_D} = \left(\frac{0.0002951kh}{\mu C}\right) t \quad (10)$$

- Taking logarithms gives:

$$\log\left(\frac{t_D}{C_D}\right) = \log(t) + \log\left[\frac{0.0002951kh}{\mu C}\right] \quad (11)$$

- Eqs indicate that plot of the actual drawdown data of log(ΔP) vs. log(t) will produce a parallel curve that has an identical shape to plot of log(PD) vs. log(tD/CD).
- When displacing the actual plot, vertically and horizontally, to find a dimensionless curve that coincides or closely fits the actual data, these displacements are given by the constants of Eqs as:

$$\left(\frac{P_D}{\Delta p}\right)_{MP} = \frac{kh}{141.2Q\beta\mu} \quad (12)$$

$$\left(\frac{t_D/C_D}{t}\right)_{MP} = \frac{0.0002951kh}{\mu C} \quad (13)$$

- Eqs above can be solved for the Permeability k (or the Flow Capacity kh) and the wellbore storage coefficient C respectively:
- The mathematical definition of dimensionless characterization group CDe^{2s} is given below and it is valid for both drawdown & buildup tests:

$$C = \left[\frac{0.0002951kh}{\mu} \right] \left(\frac{t}{t_D/C_D} \right)_{MP} \quad (14)$$

$$k = \frac{141.2q\beta\mu}{h} \left(\frac{P_D}{\Delta p} \right)_{MP} \quad (15)$$

$$C_D e^{2s} = \left[\frac{5.615C}{2\pi\phi\mu C_t r_w^2} \right] e^{2s} \quad (16)$$

$$s = \frac{1}{2} \ln \left[\frac{(C_D e^{2s})_{MP}}{C_D} \right] \quad (17)$$

- When the match is achieved, the dimensionless group CDe^{2s} describing the matched curve is recorded.

❖ For Buildup Tests

- All type curve solutions are obtained for the drawdown solution. Therefore, these type curves cannot be used for buildup tests without restriction or modification.
- The only restriction is that the flow period t_p before shut-in must be somewhat large. However, Agarwal empirically found that by plotting the buildup data $P_{ws}-P_{wf}$ at $\Delta t = 0$ versus equivalent time Δt_e instead of the shut-in time Δt , on log-log scale, the type curve analysis can be made without the requirement of a long drawdown flowing period before shut-in.
- Agarwal introduced the equivalent time Δt_e as defined by:

$$\Delta t_e = \frac{\Delta t}{1 + (\Delta t/t_p)} = [\Delta t/t_p + \Delta t]t_p \quad (18)$$

- Agarwal's equivalent time Δt_e is simply designed to account for the effects of producing time t_p on the pressure buildup test.
- The concept of Δt_e is that the pressure changes $\Delta P = P_{ws}-P_{wf}$ at time Δt during a buildup test is the same as the pressure change $\Delta P = P_i-P_{wf}$ at Δt_e during a drawdown test.

- Thus, graph of buildup test in terms of $P_{ws}-P_{wf}$ vs. Δt_e will overlay graph of pressure change ΔP versus flowing time t for drawdown test.
- Therefore, when applying the type curve approach in analyzing pressure buildup data, the actual shut-in time Δt is replaced by the equivalent time Δt_e .
- In addition to the characterization group CDe^{2s} as defined by Eq. the following two dimensionless parameters are used when applying the Gringarten type curve in analyzing pressure buildup test data.
- Dimensionless pressure P_D :

$$P_D = \frac{kh(P_{ws} - P_{wf})}{141.2q\beta\mu} = \frac{kh\Delta p}{141.2q\beta\mu} \quad (19)$$

- Taking the logarithms of both sides of above equation gives:

$$\log(P_D) = \log(\Delta p) + \log\left(\frac{kh}{141.2q\beta\mu}\right) \quad (20)$$

- Dimensionless ratio tD/CD :

$$\frac{t_D}{C_D} = \left(\frac{0.0002951kh}{\mu C} \right) \Delta t_e \quad (21)$$

- Taking the logarithm of each side of Eq. gives:

$$\log \left(\frac{t_D}{C_D} \right) = \log(\Delta t_e) + \log \left[\frac{0.0002951kh}{\mu C} \right] \quad (22)$$

- Similarly, a plot of actual pressure buildup data of $\log(\Delta P)$ vs. $\log(\Delta t_e)$ would have a shape identical to that of $\log(PD)$ vs. $\log(tD/CD)$.
- When the actual plot is matched to one of the curves then:

$$\left(\frac{P_D}{\Delta p} \right)_{MP} = \frac{kh}{141.2Q\beta\mu} \quad (23)$$

- which can be solved for the Flow Capacity kh or the Permeability k :

$$k = \left[\frac{141.2Q\beta\mu}{h} \right] \left(\frac{P_D}{\Delta p} \right)_{MP} \quad (24)$$

- And

$$\left(\frac{t_D/C_D}{\Delta t_e} \right)_{MP} = \frac{0.0002951kh}{\mu C} \quad (25)$$

- Solving for C gives: The recommended p

$$C = \left[\frac{0.0002951kh}{\mu} \right] \left(\frac{\Delta t_e}{t_D/C_D} \right)_{MP} \quad (26)$$

$$C_D = \left[\frac{0.8936}{\phi h C_t r_w^2} \right] C \quad (27)$$

$$s = \frac{1}{2} \ln \left[\frac{(C_D e^{2s})_{MP}}{C_D} \right] \quad (28)$$

The recommended procedure for using the Gringarten type curve is given by the following steps:

1. Using the test data, perform conventional test analysis and determine:
 - Wellbore storage coefficient C and CD .
 - Permeability k .
 - Skin factor s .
 - False pressure P^* .
 - Average pressure P^- .
 - Shape factor CA .
 - Drainage area A .
2. Plot ΔP vs. t for drawdown test or ΔP vs. Δt_e for buildup test on log-log tracing paper with the same size log cycles as the Gringarten type curve.
3. Check the early-time points on the actual data plot for the unit-slope (45° angle) straight line to verify the presence of the wellbore storage effect. If a unit-slope straight line

presents, calculate the wellbore storage coefficient C and the dimensionless CD from any point on the unit-slope straight line with coordinates of $(\Delta P, t)$ or $(\Delta P, \Delta t_e)$, to give:

- For drawdown:

$$C = \frac{Q\beta}{24} \left(\frac{t}{\Delta p} \right) \quad (29)$$

- For buildup:

$$C = \frac{Q\beta}{24} \left(\frac{\Delta t_e}{\Delta p} \right) \quad (30)$$

- Estimate the dimensionless wellbore storage coefficient from:

$$C_D = \left[\frac{0.8936}{\phi h C_t r_w^2} \right] C \quad (31)$$

4. Overlay the graph of the test data on the type curves and find the type curve that nearly fits most of the actual plotted data. Record the type curve dimensionless group (CDe2s)MP.
5. Select match point MP and record the corresponding values of (PD, ΔP)MP from the Y axis and (tD/CD, t)MP or (tD/CD, Δt_e)MP from the X axis.
6. From the match point, calculate k , C , CD & s .
7. Check the agreement between the conventional well testing analysis and that of the Gringarten type curve approach.

2.3.3 The pressure derivative Method

The pressure derivative application in oil well test analysis involves the combined use of existing type curves in both the conventional dimensionless pressure form (pD) and the new dimensionless pressure derivative grouping ($P'_D(t_D/C_D)$). Thus, this new approach has combined the most powerful aspects of the two previously distinct methods into a single-stage interpretive plot. Use of the pressure derivative with pressure behavior type curves reduces the uniqueness problem in type curve matching and gives greater confidence in the results. Features that are hardly visible on the Horner plot or that are hard to distinguish because of similarities between a reservoir system and another are easier to recognize on the pressure derivative plot.

❖ Pressure Derivative Analysis Methods

Bourdet et al.³ developed a new set of type curves (see Figure 2.40) based on the pressure and pressure derivative. In (Fig 2.36), at early time, the curves follow a unit-slope log-log straight line. When infinite-acting radial flow is reached at late time, the curves become horizontal at a value of ($P'_D(t_D/C_D) = 0.5$). Between these two asymptotes, at intermediate times, each $C_D e^{2s}$ curve produces a specific shape and is different for varying values of Dimensionless groups are :

$$P'_D = \frac{kh}{141.2q\mu\beta} \Delta p \text{ and } \frac{t_D}{C_D} P'_D = \frac{kh}{141.2q\mu\beta} \Delta t \Delta p \quad (1)$$

$C_D e^{2s}$. Thus, it is easy and simple to identify the correct $C_D e^{2s}$ curve corresponding to the data. By matching the two straight lines (unit-slope and the late-time horizontal lines) a unique match point is provided. The double plot provides as a check, as the two data set must match on their respective curves. The matching procedures for pressure buildup and drawdown tests are as follows.

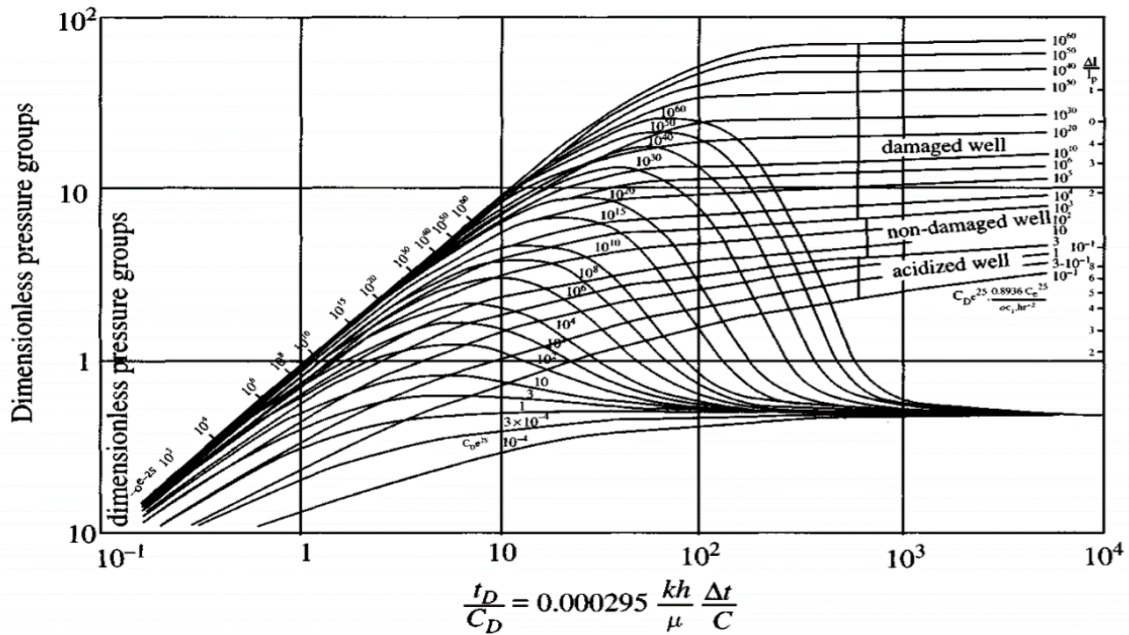


Figure 2.36 Derivative and pressure type curves for a well with wellbore storage and skin in infinite-acting homogeneous reservoir.³

❖ Pressure Buildup Test Data Matching Procedure

- Plot ΔP versus Δt on 3 x 5-cycle log-log paper.
- Calculate the pressure derivative of the field data.
- Plot $\Delta t'(\Delta P')$ versus Δt on same 3 x 5-cycle log-log paper.
- Select the best match by sliding the actual test data plot both horizontally and vertically.
- Note the values of the match points:

$$(P_D)_{M'}, (\Delta P)_{M'}, \left(\frac{\Delta t}{t_D/C_D} \right)_{M'}, (C_D e^{2s})_{M'} \quad (2)$$

- Determine the formation permeability, k , from pressure match points:

$$k = \frac{141.2 q \mu \beta}{h} \frac{(P_D)_M}{(\Delta P)_M} \quad (3)$$

- Estimate the wellbore storage, C , from time match point:

$$C = 0.000295 \frac{kh}{\mu} \left(\frac{\Delta}{t_D/V_D} \right)_M \quad (4)$$

- Calculate the dimensionless wellbore storage, C_D , from

$$C_D = 0.8936 \frac{C}{\phi h C_t r_w^2} \quad (5)$$

- Estimate the skin factor, s , from curve match point:

$$S = 0.5 \ln \left[\frac{(C_D e^{2s})_M}{C_D} \right] \quad (6)$$

❖ Pressure Drawdown Test Data Matching Procedure

- Plot $\Delta P = (p_i - p_{wf})$ versus t on 3 x 5-cycle log-log paper.
- Calculate the pressure derivative of the field data.
- Plot $t'(\Delta P')$ versus t on same 3 x 5-cycle log-log paper.
- Select the best match by sliding the actual test data plot both horizontally and vertically.
- Note the values of the match points:

$$(P_D)_{M'} \quad (\Delta P)_{M'} \quad \left(\frac{t}{t_D/C_D} \right)_M \quad (C_D e^{2s})_M \quad (7)$$

- Determine the formation permeability, k , from pressure match points:

$$k = \frac{141.2 q \mu \beta}{h} \frac{(P_D)_M}{(\Delta P)_M} \quad (8)$$

- Estimate the wellbore storage, C , from time match point:

$$C = 0.000295 \frac{kh}{\mu} \left(\frac{\Delta t}{t_D/V_D} \right)_M \quad (9)$$

- Calculate the dimensionless wellbore storage, C_D , from

$$C_D = 0.8936 \frac{C}{\phi h C_t r_w^2} \quad (10)$$

- Estimate the skin factor, s , from curve match point:

$$S = 0.5 \ln \left[\frac{(C_D e^{2s})_M}{C_D} \right] \quad (11)$$

2.4 Well test analysis models:

2.4.1 Wellbore Models

2.4.1.1 Constant wellbore storage model

Constant wellbore storage assumes that the difference between the sandface flow rate and the surface flow rate is proportional to the speed of the pressure change.

(Fig 2.37) illustrates the behavior of the sandface rate during the opening and shut-in of a well. (Fig 2.38) illustrates the response with various wellbore storage constants. The form or the width of the hump is governed by the parameter group $C_D e^{2s}$, the position of the curves in time is governed by the wellbore storage coefficient C .

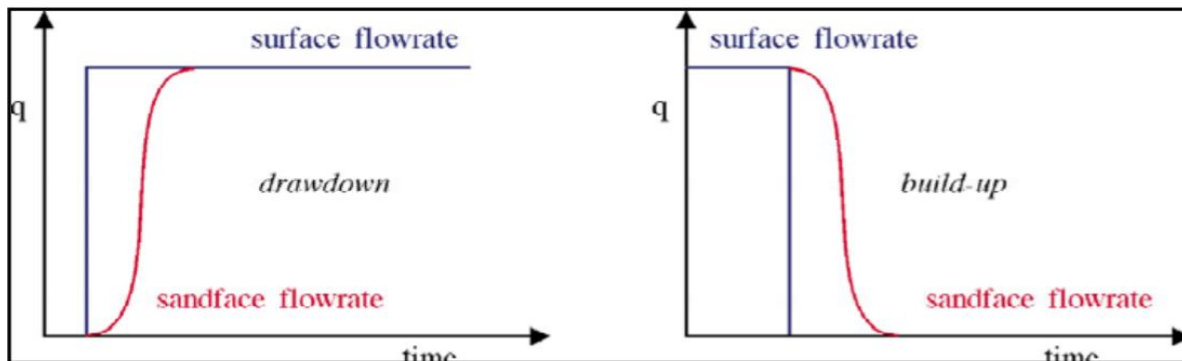


Figure 2.37 Wellbore Storage

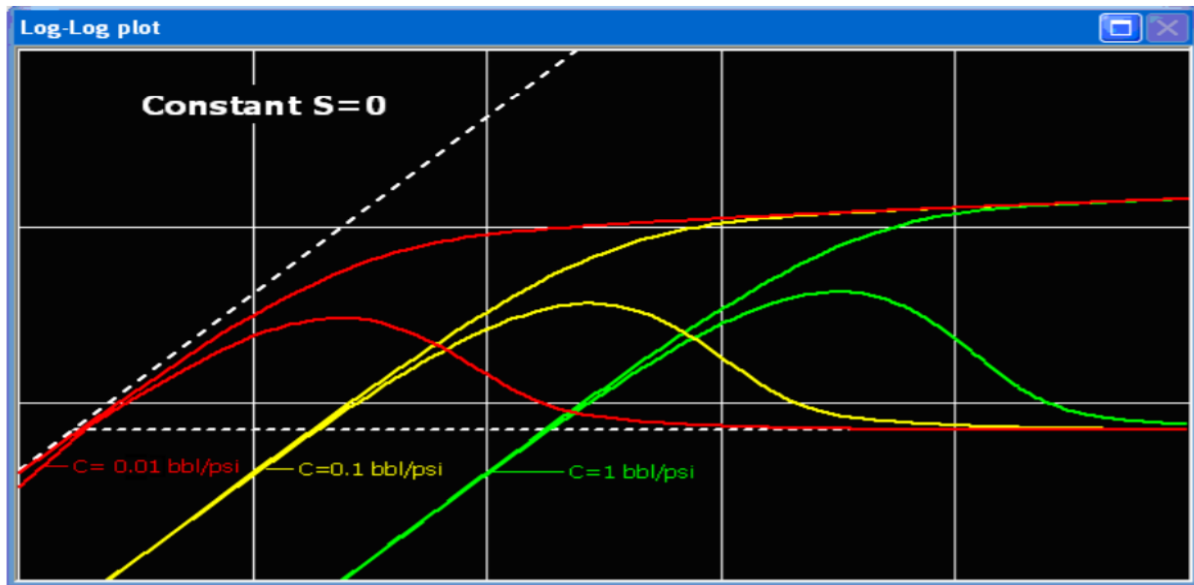


Figure 2.38 Wellbore Storage

2.4.1.2 Change wellbore storage model

Wellbore storage may vary. This is the case when fluid compressibility varies in the wellbore during the test operation. A typical case is tight gas reservoirs, where the pressure drop in the well will be considerable and the compressibility will vary during both production and shut-in periods. In such case the wellbore storage may vary considerably during the flow period being analyzed. As another example, an oil well flowing above bubble point condition in the reservoir may see gas coming out of solution in a wellbore below bubble point pressure. Initially oil compressibility would be dominating and this would gradually change to gas as more and more gas is produced in the wellbore. We would have the phenomenon of 'increasing' wellbore storage. When, the well is shut in the reverse will happen. First, the gas first dominates, and then later the oil compressibility takes over. The response will exhibit decreasing storage

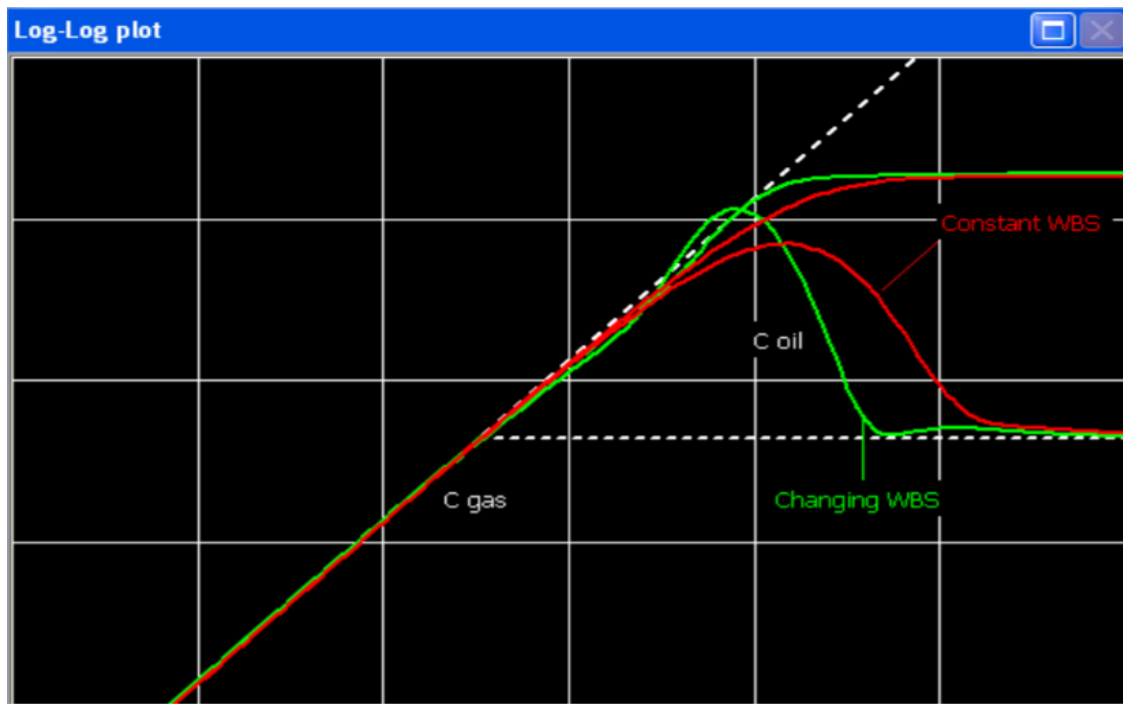


Figure 2.39 Production increasing storage

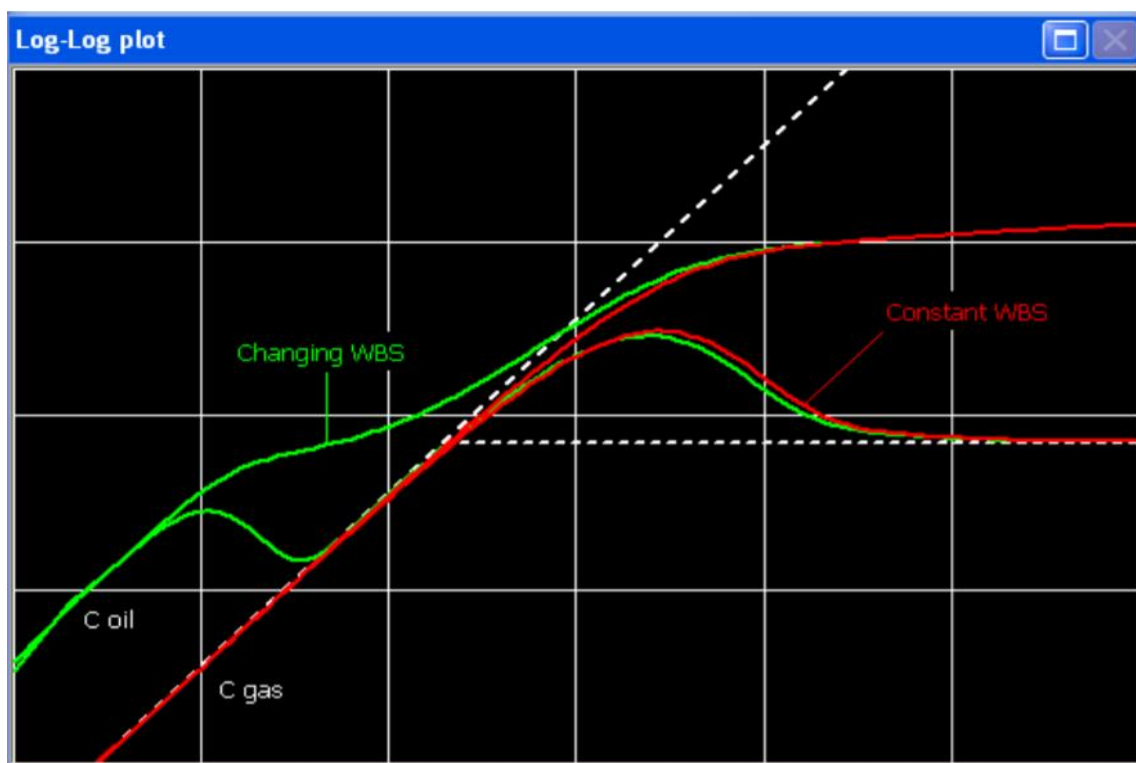


Figure 2.40 Build-up decreasing storage

2.4.2 Well Models

2.4.2.1 Vertical fully penetrating well

The simplest model is a vertical well fully penetrating the reservoir producing interval. This is the model used to derive the basic equations in Chapter two. This model is sometimes called ‘wellbore storage & skin’, reference to the original type-curves of the 1970’s. The reason is that the two only parameters affecting the loglog plot response will be the wellbore storage and the skin factor. However wellbore storage is a wellbore effect and skin is used in complement of all other models. So we will stick to the term ‘vertical well’, considering that ‘fully penetrating’ is the default status of a vertical well. The behavior of a vertical well in a homogeneous infinite reservoir has already been presented. (Fig 2.41) and (Fig 2.42) illustrate The loglog and semilog plots below show the response for various values of the skin factor (S).

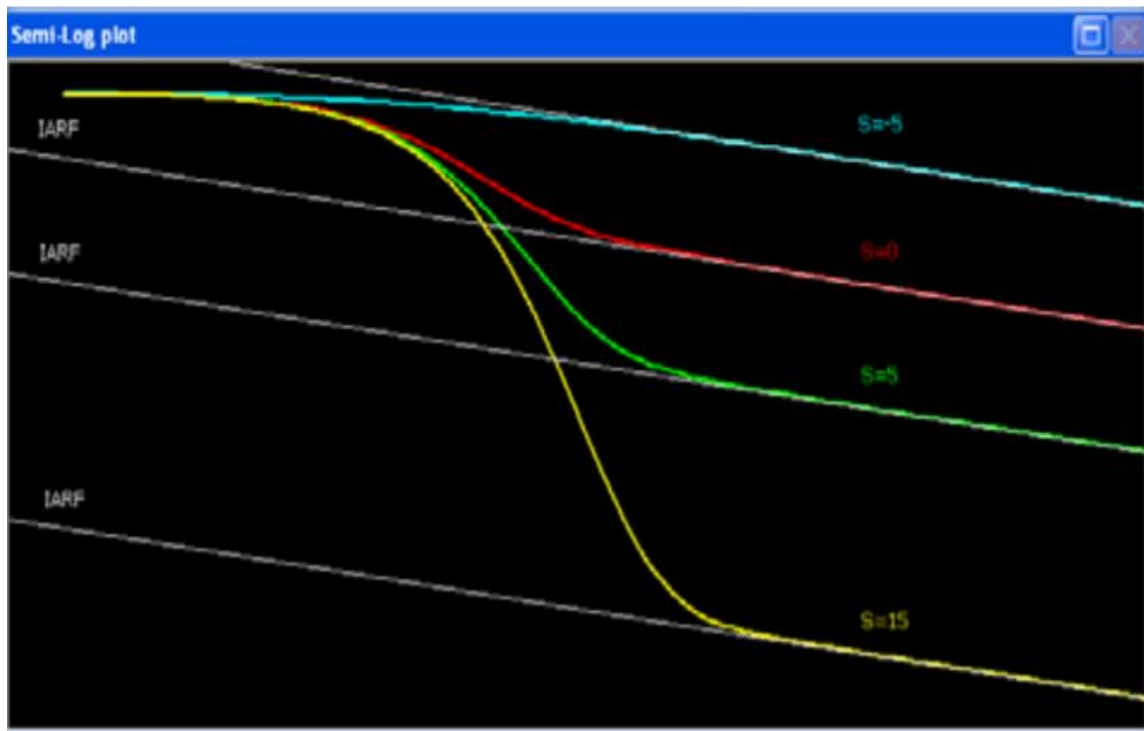


Figure 2.41 Loglog plot, skin

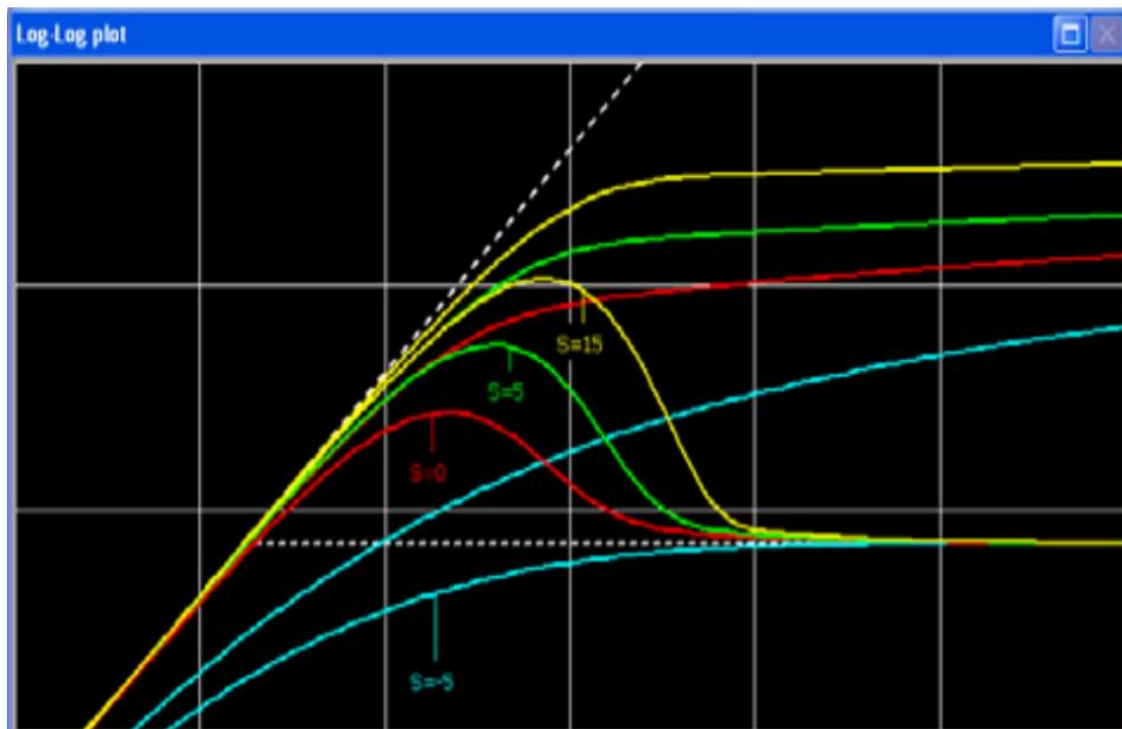


Figure 2.42 Semilog plot, skin.

2.4.2.2 Fractured wells

To improve the productivity of a well, there are two basic stimulation choices; either acidize or fracture. Many factors are considered when selecting such a treatment, but the general rule is 'high permeability; acidize, low permeability; fracture'. To acidize, injectivity is needed to enable the fluid to enter the formation without exceeding maximum pressures governed by the nature of the completion. To fracture it is necessary to pump fluid against higher resistance, so that the bottom hole pressure rises above the fracture gradient of the formation. Again the operation is limited by the maximum pressure allowed by the completion. Once the fracture is initiated, the key is to maintain a high bottom hole pressure by pumping rapidly, so that the fracture propagates away from the wellbore. During the treatment a 'proppant' such as sand or ceramic beads are included in the fracturing fluid, so that, as the fracture 'screens out', the induced fracture faces will remain open. It is also assumed in the analysis of the fracture behavior that it is internally propped to a constant dimension, i.e. that there is no variation in fracture width with height or length. At present there is no way to know if this is true or not, but like all mathematical models, the fracture models are as good as can be handled analytically, and they typically reproduce the pressure response due to the fracture quite accurately. There are two fractured models: the high, or 'infinite conductivity' and the 'finite conductivity'. In the high conductivity we assume that the pressure drop along the inside of the fracture is negligible. In the low conductivity case we simulate diffusion within the fracture. The high conductivity fracture model can be divided into two sub-categories: the Infinite-Conductivity model assumes no pressure drop along the fracture. The Uniform Flux model assumes a uniform production per unit length of fracture. The Uniform Flux model assumes a uniform production per unit length of fracture. Originally the uniform flux model was published because it was fairly

easy to calculate. The infinite conductivity fracture was solved semi-analytically (at high CPU cost) but it was shown that an equivalent response could be obtained by calculating the (fast) uniform flux solution at an off-centered point in the fracture ($X=0.732.X_f$). So in most software packages the generation of the two models only differs by the point at which the same uniform flux solution is calculated. These solutions differ only slightly when plotted on a loglog scale. Purists consider that the uniform flux solution is physically incorrect and only the infinite conductivity solutions should be used. In real life the uniform flux transients generally offer a better match, and this can be explained by the fact that the productivity of the uniform flux fracture, for a given length,

Is slightly lower than the infinite conductivity, and that this, possibly, better simulates the slight pressure losses in the fracture. If the solutions only differ slightly in terms of pressure response, the rate distribution is quite different. By definition the rate profile of the uniform flux solution stays constant and uniform. In the infinite conductivity case the rate will be uniform at early time, but at late time most of the flow will come from the extremity of the fracture. It makes sense physically. The extreme parts of the fracture are 'facing' most of the reservoir volume. The original publications on fracture solutions were without wellbore storage and skin. It is not that it was absent, but the solution with two additional parameters (C and S) was too complex to be turned into readable type-curves especially as the influence of skin is particularly messy. Also, the particular interest of this solution was in the specific linear flow that such a configuration may produce, and which is independent of storage and skin. However, most software today accommodates storage and skin effects. A tricky part of the skin modeling is to know where it comes from; either fracture or perforations. Many publications have been written on this problem. The behavior is the same but the values of the skin depend on the reference length; X_f for the fracture skin and r_w for the sandface skin. For both models, after the end of wellbore storage and unless the fracture length is too

small, the behavior is dominated by a linear and uniform flow from the reservoir, towards the fracture and orthogonally to the fracture plane. On a loglog plot, the linear flow is characterized by a $1/2$ -unit slope in both the pressure and derivative curves. The derivative is lower than the pressure, this shift corresponding to a factor 2 on a linear scale. (Fig 2.43) illustrates the behavior of an infinite conductivity fracture with different fracture lengths and wellbore storage.

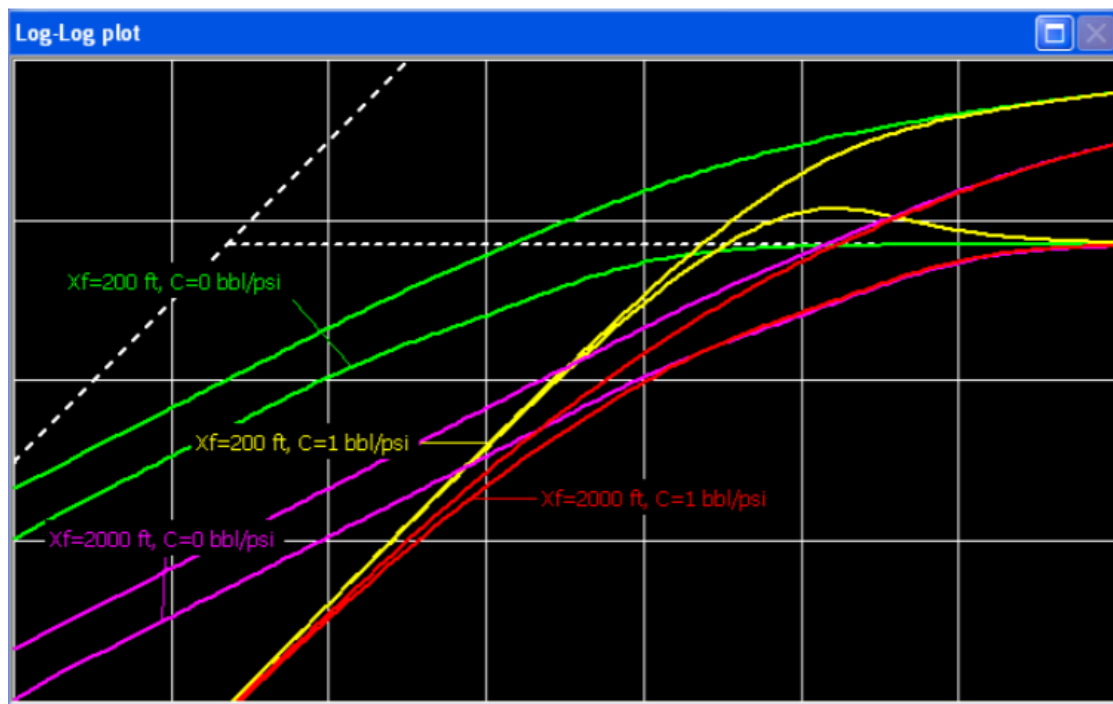


Figure 2.43 Infinite conductivity fracture behavior

2.4.2.3 Limited entry well

This model assumes that the well produces from a perforated interval smaller than the interval thickness:

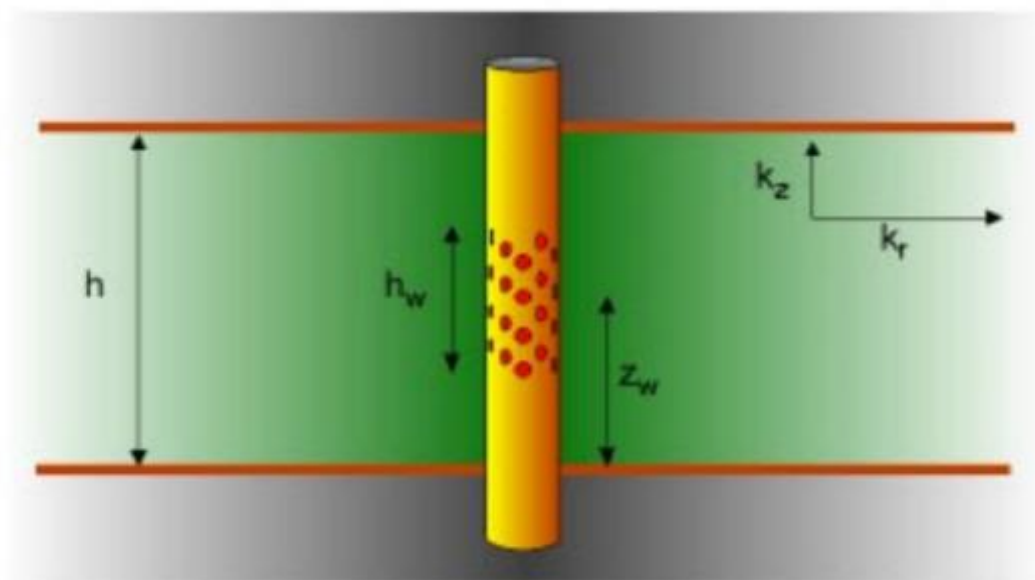


Figure 2.44 Limited Entry

In theory, after wellbore storage, the response can be initially radial in the perforated interval thickness h_w , shown as '1' below. This will give a derivative match equivalent to the small mobility $k h_w$, and it can be imagined that if there were no vertical permeability this would be the only flow regime. In practice this flow regime is often masked by storage.

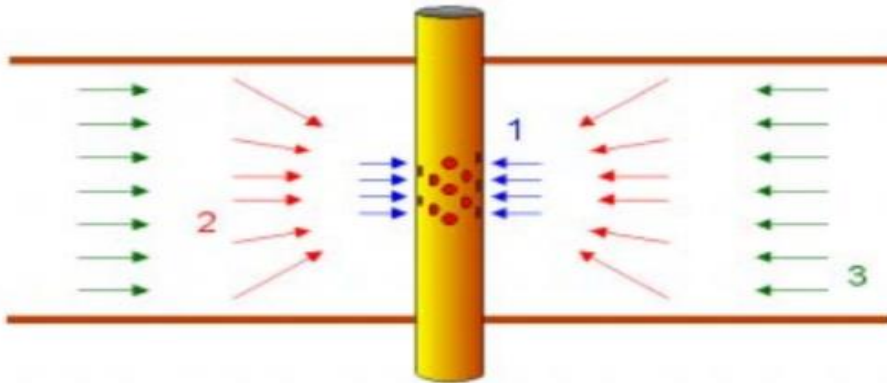


Figure 2.45 Limited Entry Flow Regimes

In flow regime '2' there is a vertical contribution to flow, and if the perforated interval is small enough a straight line of slope $-1/2$ may be established in the pressure derivative, corresponding to spherical or hemi-spherical flow. (As with radial flow, there is no special log-log shape corresponding to spherical flow.) Finally, when the upper and lower bed boundaries have been seen, the flow regime becomes radial again, and the mobility now corresponds to the normal kh . Schlumberger Introduction to Well Testing (March 1998) 5-39 In any model where there is a vertical contribution to flow, there must also be a pressure drop in the vertical direction, and vertical permeability has to be considered along with the radial permeability. The pressure drop due to the flow convergence (flow regime 2) is a 'near-wellbore' effect, so typically looks like an additional skin. If the spherical flow is seen in the data it may be possible to separate the 'true' and 'geometric' components of the apparent skin, but sometimes the first flow regime seen after storage is the final radial flow:

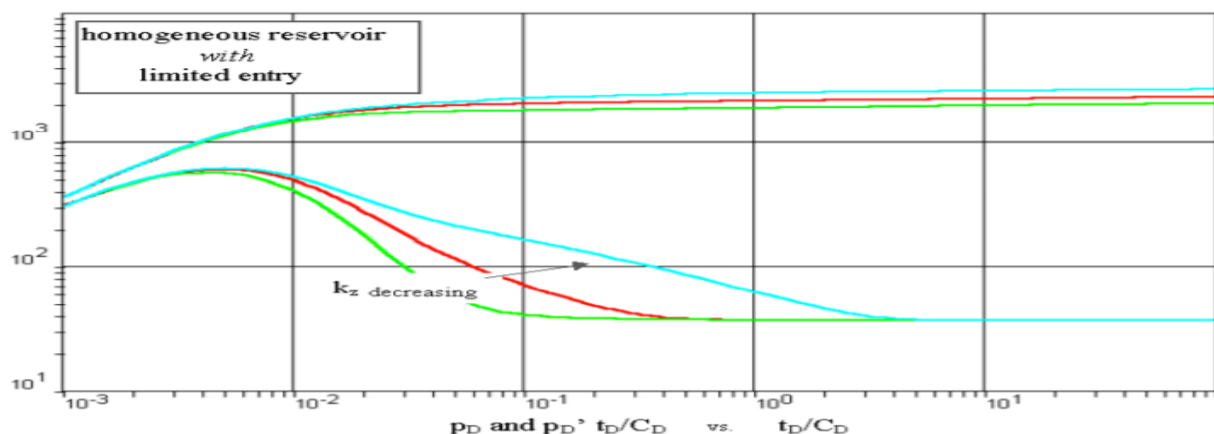


Figure 2.46 Limited Entry Response

With a high enough vertical permeability the spherical flow may not be seen at all, as shown by the green curve, but this also depends on h_w/h , the fraction of the producing interval that is perforated, and of course the storage. As k_z decreases the $-1/2$ spherical flow derivative becomes evident, as the duration of the spherical flow regime increases, and does the overall pressure drop increases, shown by the log-log curve moving up the page. The apparent skin also increases, as shown by the separation of the log-log and derivative curves.

2.4.2.4 Horizontal wells

The well is assumed to be strictly horizontal, and is defined with the same parameters as a limited entry well:

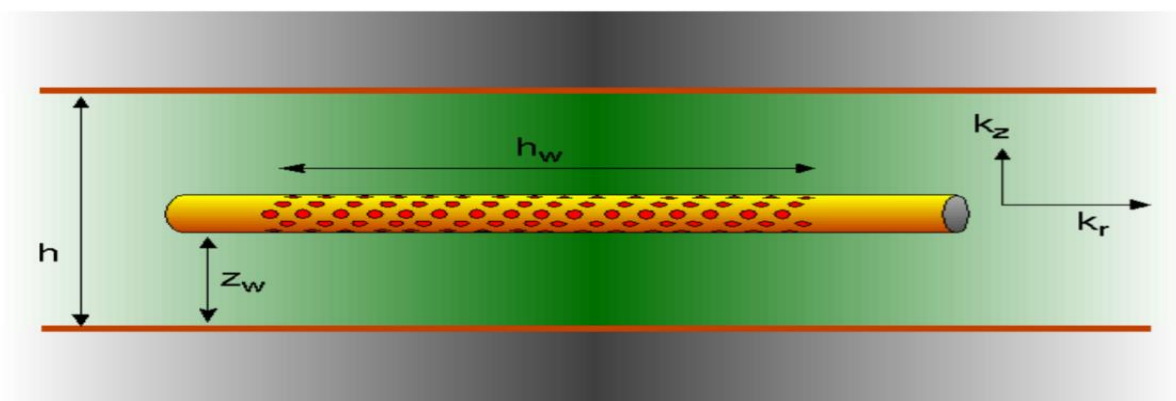


Figure 2.47 Horizontal Well

The first flow regime, often obscured by wellbore storage, is pseudo-radial flow in the vertical sense, analogous to radial flow in a vertical well. The average permeability combines a vertical and a radial (horizontal) component, and the 'thickness' corresponds to the producing well length.

The second flow regime is linear flow, corresponding to horizontal flow between the upper and lower bed boundaries. Both log-log and derivative curves will follow a $1/2$ -unit slope. The final flow regime is radial flow equivalent to that in a vertical well.

The flow regimes are summarized next:

Horizontal Well Flow Regimes

Looking end-on into a horizontal well is equivalent to looking down on a vertical well. The first flow regime after storage in a vertical well is radial flow, and in a horizontal well the same applies. However due to permeability anisotropy the flow around the wellbore is not circular, but elliptical, as the pressure front will typically propagate more slowly in the vertical direction:

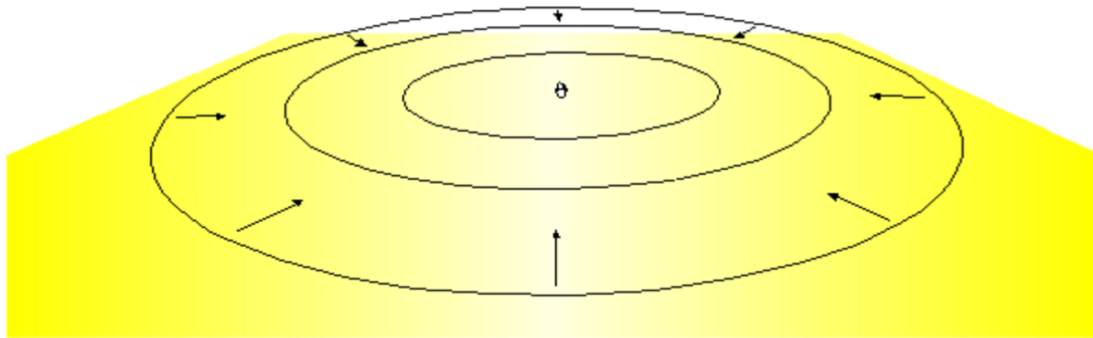


Figure 2.48 Horizontal Well Flow Regimes

Once the pressure front has reached the upper and lower bed boundaries the flow becomes linear, equivalent to the parallel faults geometry in a vertical well, but because of the finite length of the horizontal wellbore it can not stay linear. Eventually the pressure front is sufficiently far from the wellbore that the dimensions of the horizontal section become irrelevant, and the flow again becomes radial, equivalent to normal radial flow in a vertical well.

Horizontal Well Log-Log Responses In a reservoir with no gas cap or aquifer, the well would typically be positioned as centrally as possible between the upper and lower bed boundaries, in which case the boundaries would be seen simultaneously and there would be a clean transition from radial to linear flow:

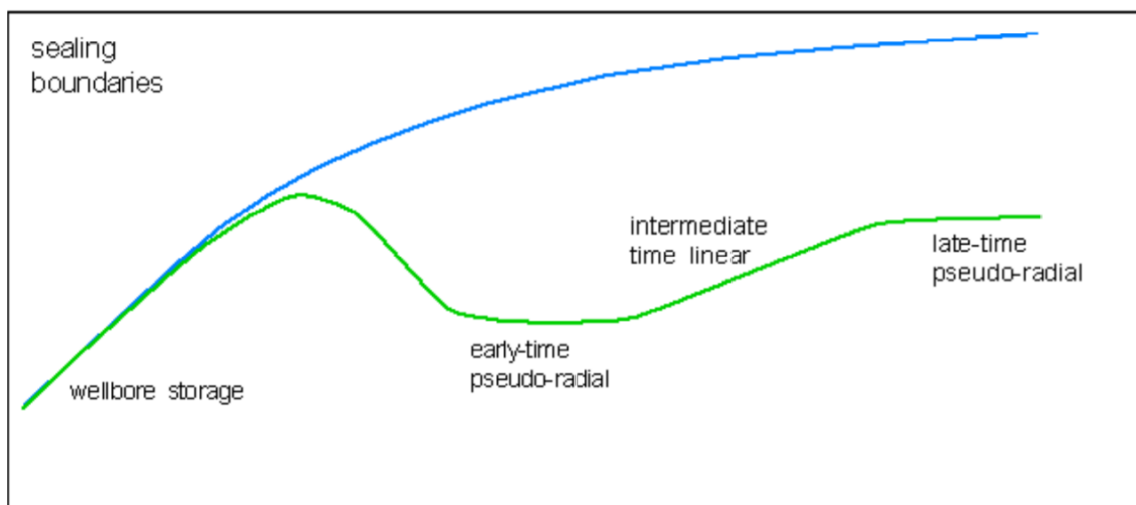


Figure 2.48 Horizontal Well Responses

However, it can be imagined that if the well is closer to one or other boundary, there will first be a doubling of the derivative, as if seeing a fault in a vertical well, before the second boundary brings on the linear flow.

If the upper or lower boundary is a gas cap or an aquifer, the well will probably be positioned close to the other, sealing boundary. In that case there will again be a doubling

of the derivative, similar to the 'fault' response in a vertical well, followed by a constant pressure response:

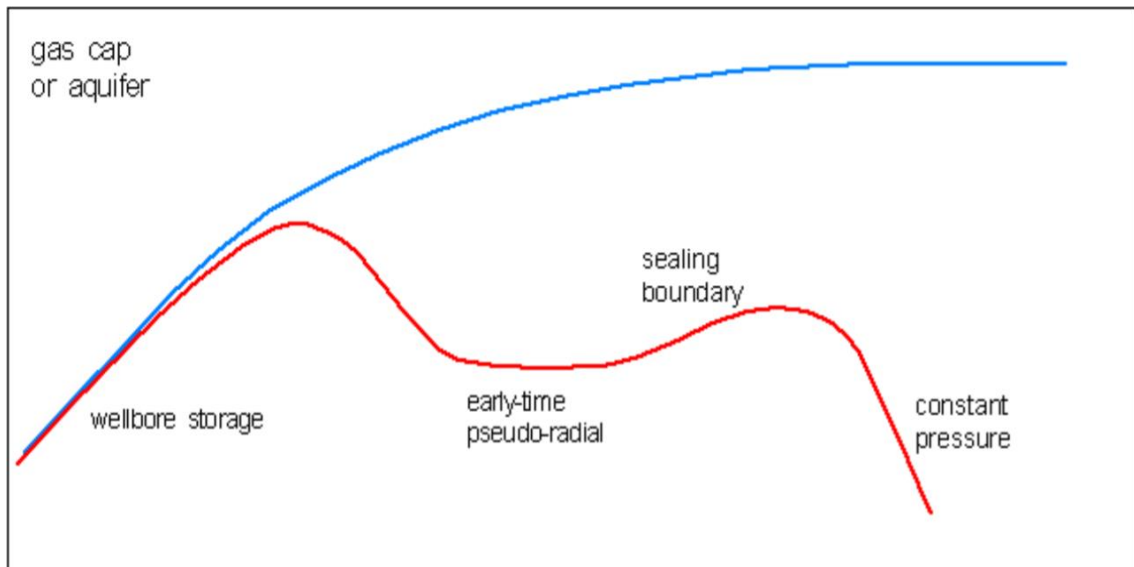


Figure 2.49 Horizontal Well Responses

In each case the doubling of the derivative will almost certainly not be fully developed before the arrival of the next flow regime, be it linear flow or a constant pressure boundary.

2.4.3 Reservoir Models

2.4.3.1 Homogeneous Reservoir

The homogeneous reservoir is the simplest possible model assuming everywhere the same porosity, permeability and thickness. The permeability is assumed isotropic. That is, the same in all directions. The governing parameters are: kh Permeability-thickness product, given by the pressure match. ϕc_t Reservoir storativity, input at the initialization of a standard test or as a result in interference tests. S Skin. Wellbore storage, linear flow (high conductivity fracture), bilinear flow (low conductivity fracture), spherical flow, horizontal well (linearity after early time radial flow). These regimes are coupled with a hump caused by the storativity and the skin. In addition, we have the line source well with no skin or wellbore storage used for the analysis of interference tests.

When infinite acting radial flow (IARF) is established the Bourdet derivative stabilizes and follows a horizontal line. (Fig 2.50) illustrates the various homogenous behaviors on a loglog plot commonly seen in pressure transient analysis. (Fig 2.51) shows the line source solution. (Fig 2.52) illustrates the semilog behavior of wellbore storage and skin in a homogeneous reservoir.

This first flow regime is typically over very quickly, and is frequently masked by wellbore storage. If not, it will develop as an IARF response and the pressure derivative will stabilize horizontally (Fig 2.53). Once the fissure system has started to produce, a pressure differential is established between

the matrix blocks and the fissures. The matrix is still at initial pressure p_i , and the fissure system has a pressure p_{wf} at the wellbore the matrix blocks then start to produce into the fissure system, effectively providing pressure support, and the drawdown briefly slows

down, as this extra energy tends to stabilize the pressure, thus a transitional dip in the derivative is created (Fig 2.54). The total system radial flow (IARF) is established when any pressure differential between the matrix blocks and the fissure system is no longer significant, and the equivalent homogeneous radial flow response is observed. A second IARF stabilization in the pressure derivative is therefore developed after the transitional dip, called by some the derivative valley. According to the mathematics, this takes place when the pressure inside the matrix blocks is the same as in the fissure system; however, this can never be true at all points in the reservoir, as there would be no production into the fissure system.

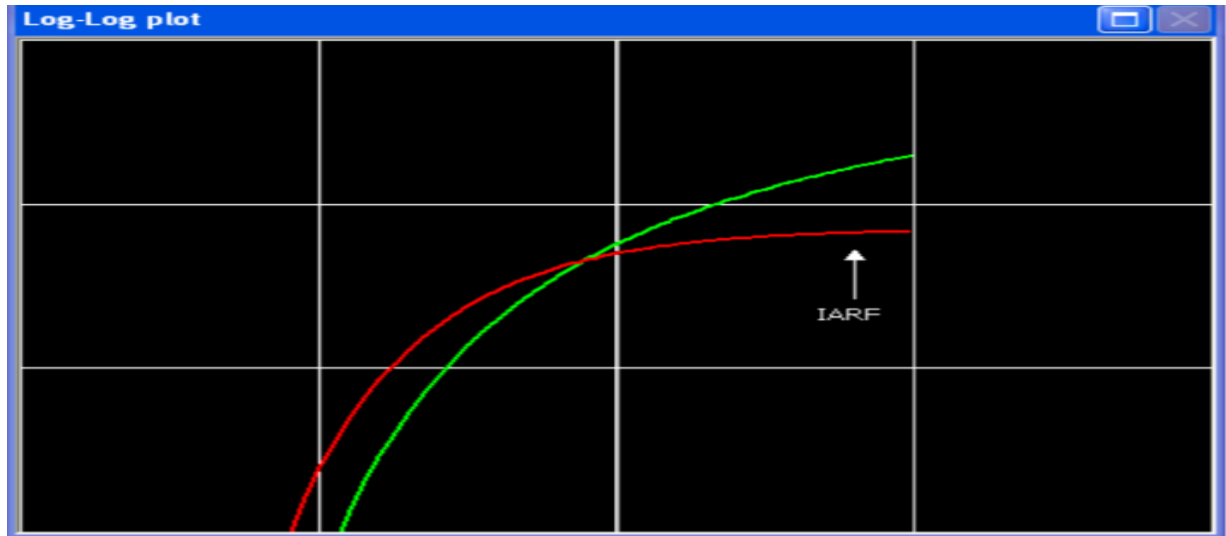


Figure 2.50 Homogeneous loglog plots

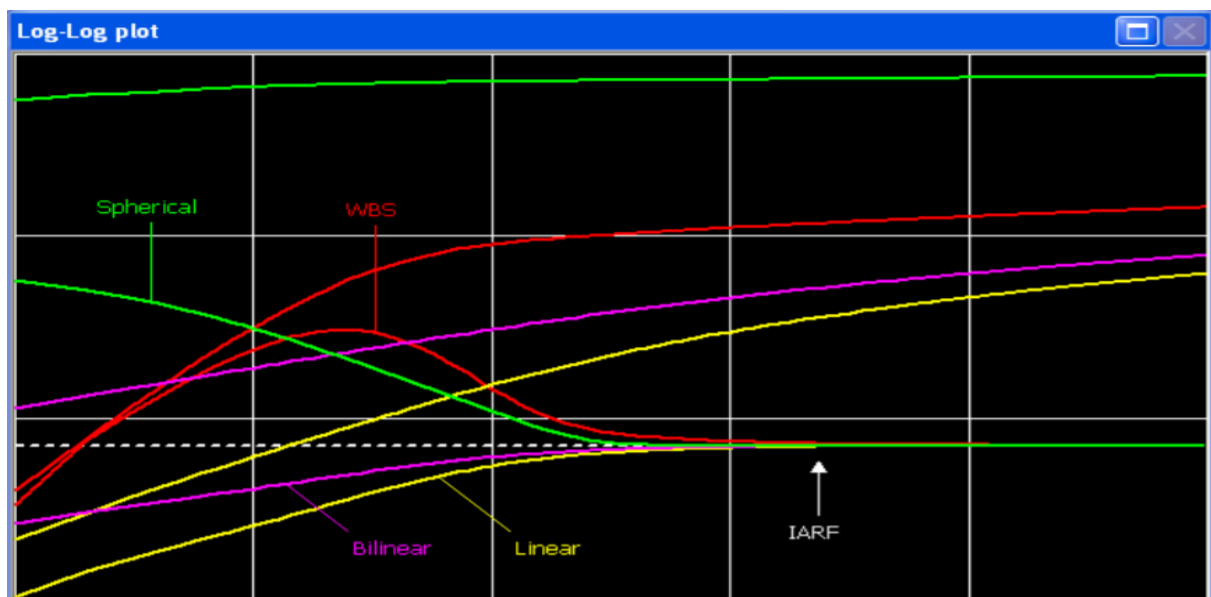


Figure 2.51 Line source

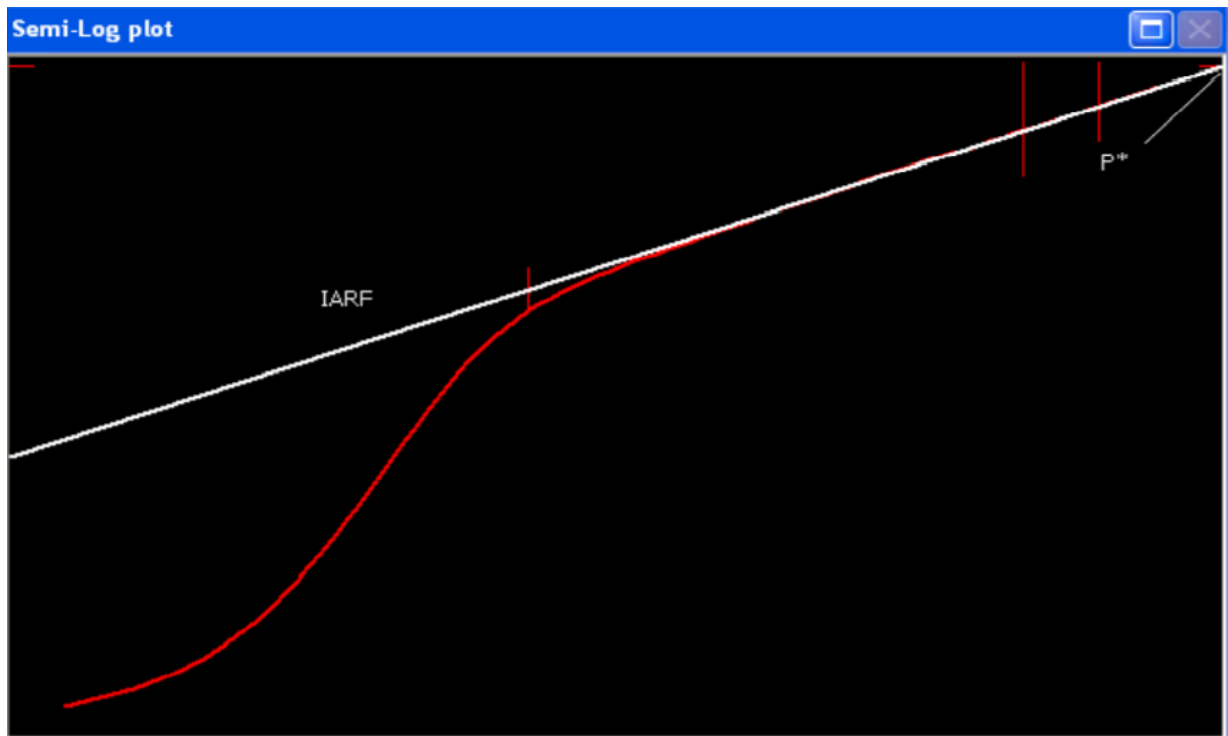


Figure 2.52 Homogeneous semilog plot

2.4.3.2 Heterogeneous:

2.4.3.2.1 Double porosity

The double-porosity (2Φ) models assume that the reservoir is not homogeneous, but made up of rock matrix blocks with high storativity and low permeability. The well is connected by natural fissures of low storativity and high permeability. The matrix blocks cannot flow to the well directly, so even though most of the hydrocarbon is stored in the matrix blocks it has to enter the fissure system in order to be produced. The double-porosity model is described by two other variables in addition to the parameters defining the homogeneous model: ω is the storativity ratio, and is essentially the fraction of fluids stored in the fissure system (e.g. $\omega=0.05$ means 5%). λ is the interporosity flow coefficient that characterizes the ability of the matrix blocks to flow into the fissure system. It is dominated by the matrix/fissures permeability contrast, k_m/k_f . When the well is first put on production, after any well dominated behavior, the first flow regime to develop is the fissure system radial flow, i.e. the fissure system is producing as if this system was there alone, and there is no change in the pressure inside the matrix blocks.

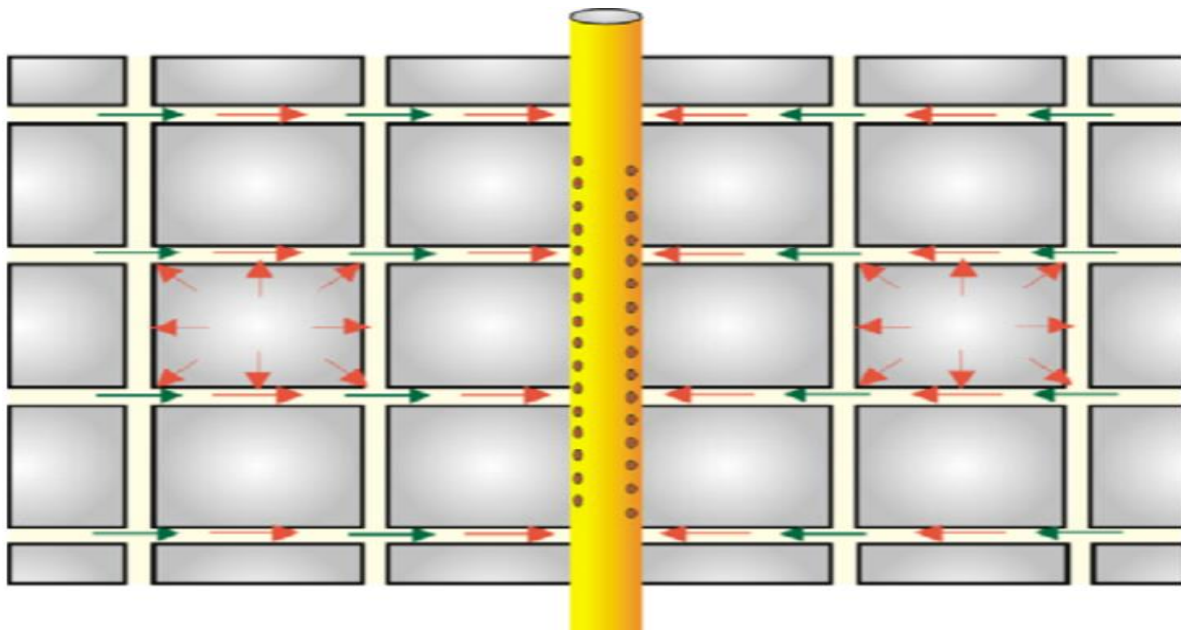


Figure 2.53 Fissure system production

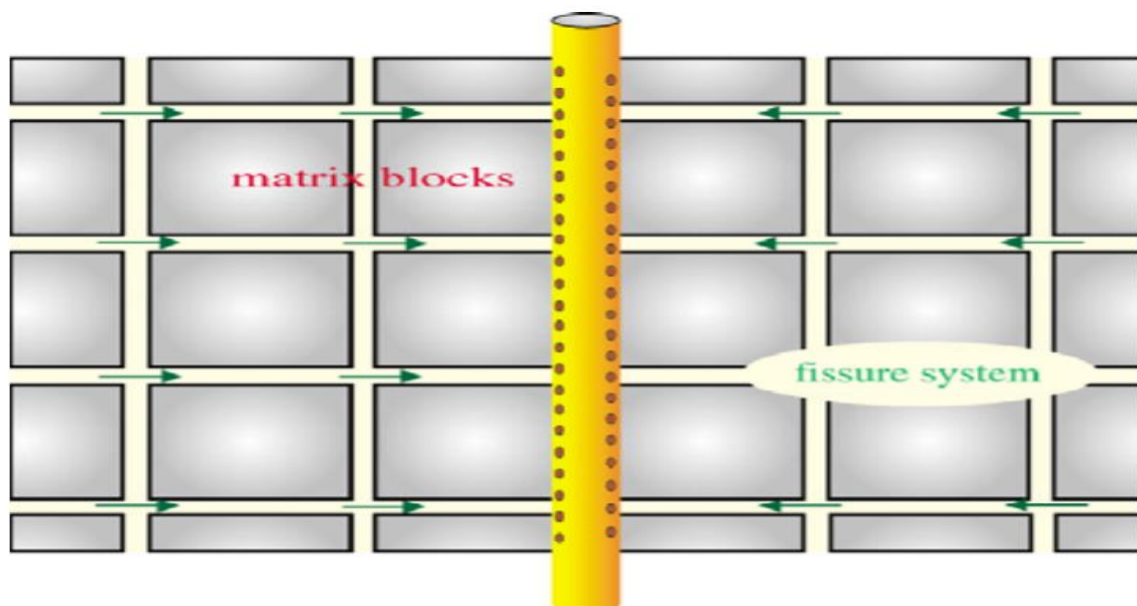


Figure 2.54 Total system production

2.4.3.2.2 Double permeability

When is a layered reservoir not a layered reservoir? When each layer has the same properties, in which case the behavior of the system will be the equivalent behavior of the summed interval. In the double-permeability (2K) model the reservoir consists of 2 layers of different permeabilities, each of which may be perforated. Crossflow between the layers is proportional

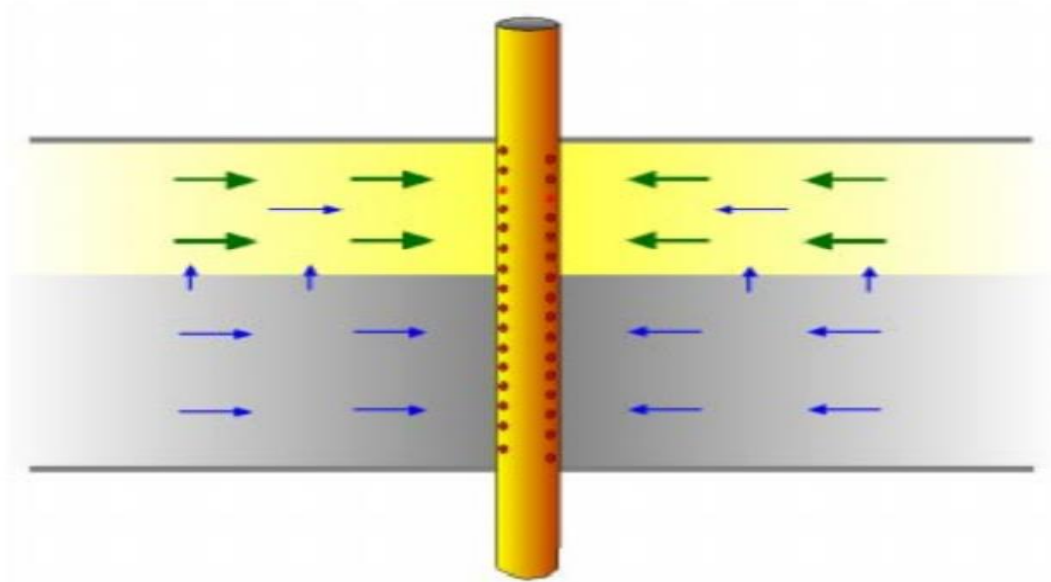


Figure 2.55 Double Permeability

At early time there is no pressure difference between the layers and the system behaves as 2 homogeneous layers without crossflow, in infinite-acting radial flow, with the total kh of the 2 layers. As the most permeable layer produces more rapidly than the less permeable layer, a Δp develops between the layers and crossflow begins to occur. Eventually the system behaves again as a homogeneous reservoir, with the total kh and storativity of the 2 layers

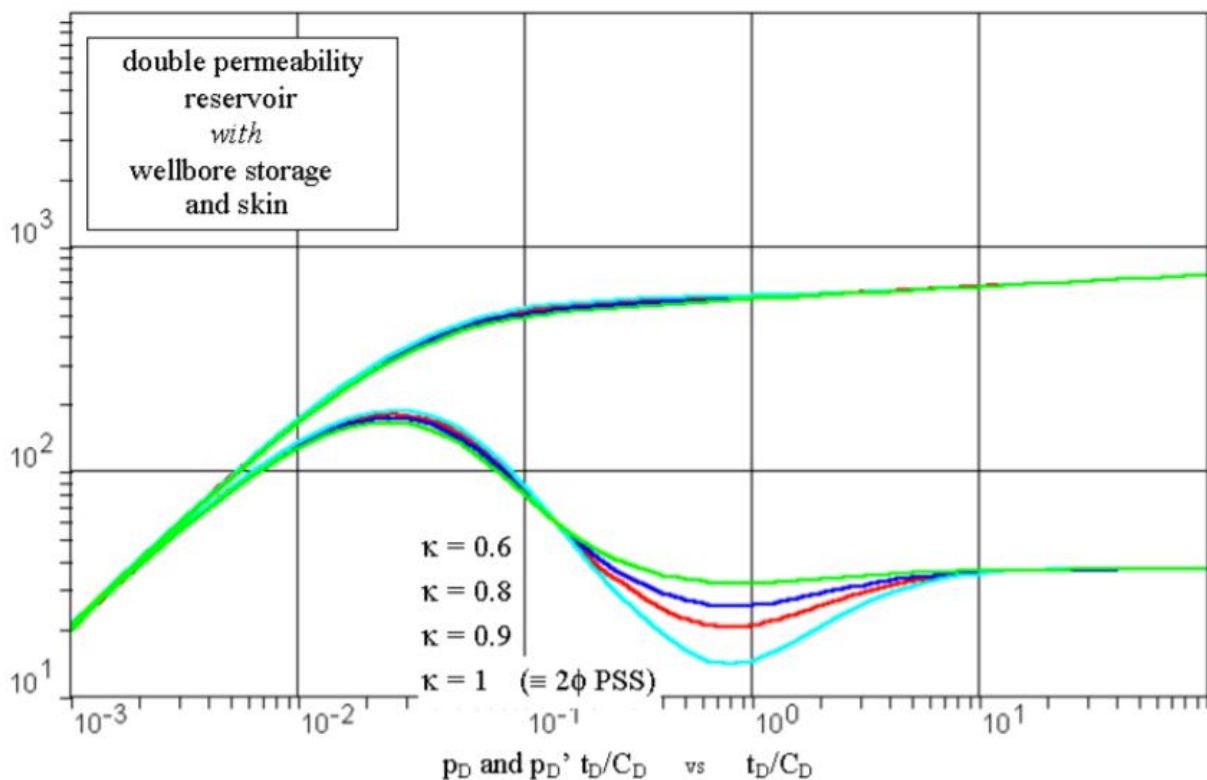


Figure 2.56 Double Permeability Type-Curve

2.4.3.2.3 Composite reservoirs

Up to this point the models assumptions were uniform with constant saturations, mobility and effective permeability. In most cases this assumption is valid within the time limits of a well test and radius of investigation. However, in some cases it will be necessary to consider a variation in the mobility in the lateral direction. The most classical cases where observation of a change in mobility in the reservoir area are:

- Injection of a fluid different to the reservoir fluid.
- Change in saturation due to an aquifer.
- Change in saturation due to a gas cap.
- Change in lateral saturation due to production below bubble or dew point.
- Compartmentalization.
- Actual changes in reservoir characteristics (k , Φ).

The analytical solutions which model these cases are called composite models. Their geometry is quite straightforward and they are governed by two simple parameters. The most common analytical composite models are the radial composite (Fig 2.57A) and the linear composite (Fig 2.57B). The radial composite geometry is centered at the well, and r_i is the radius of the inner compartment. For the linear composite reservoir (of infinite extent), the corresponding parameter will be L_i , the distance between the well and the linear composite limit.

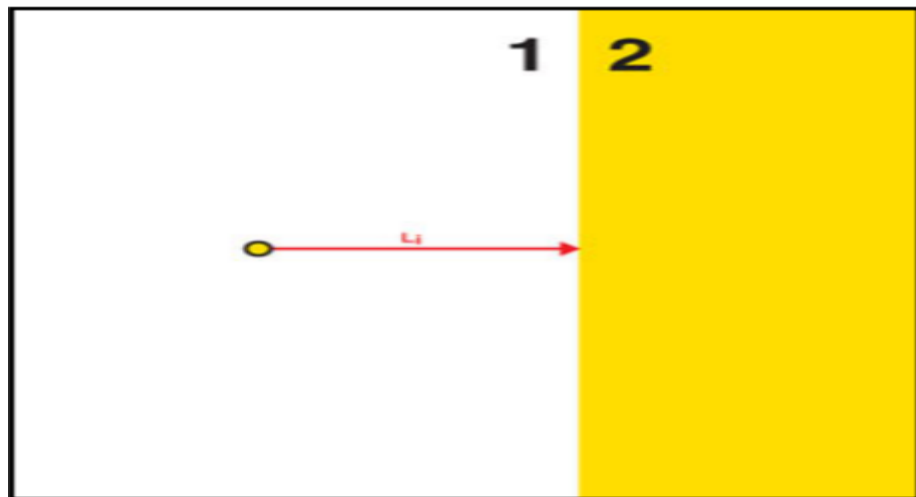


Figure 2.57A Radial composite reservoir

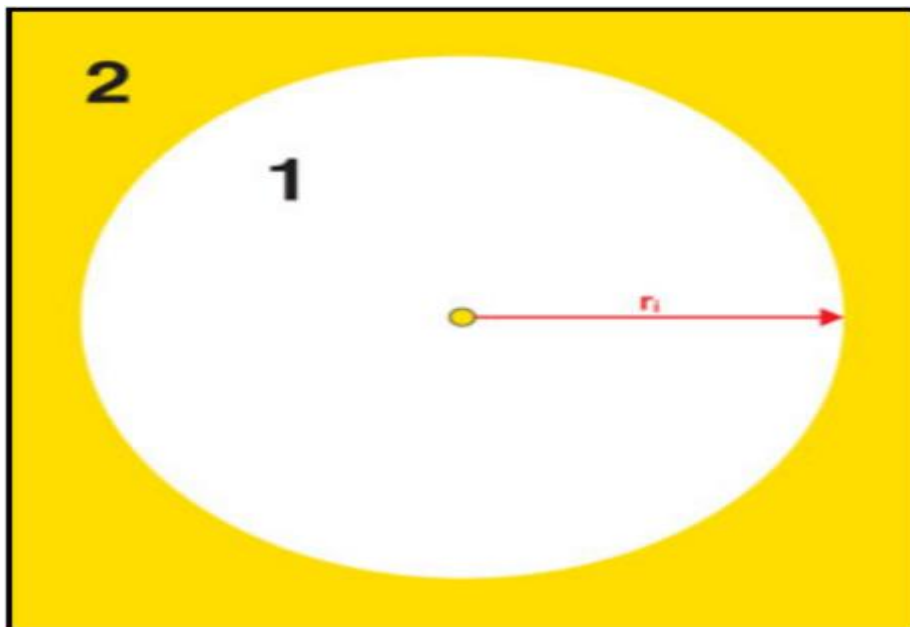


Figure 2.57B Linear composite reservoir

2.4.4 Reservoir Boundaries Models

1. Pressure front has not reached the fault

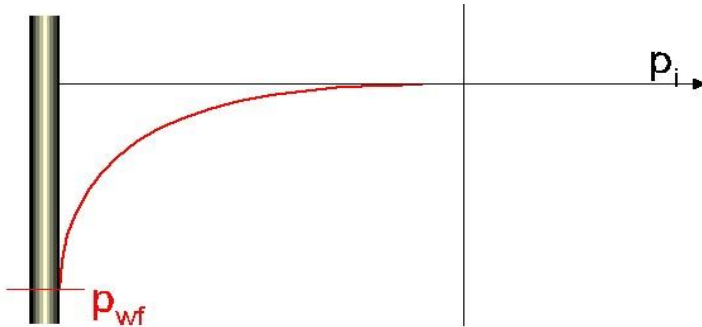


Figure 2.58A Boundary Modeling

2. Reflection has not yet reached the wellbore:

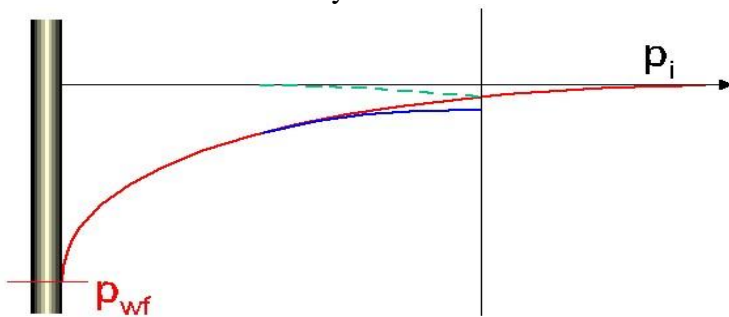


Figure 2.58B Boundary Modeling

3. Boundary is seen at the wellbore:

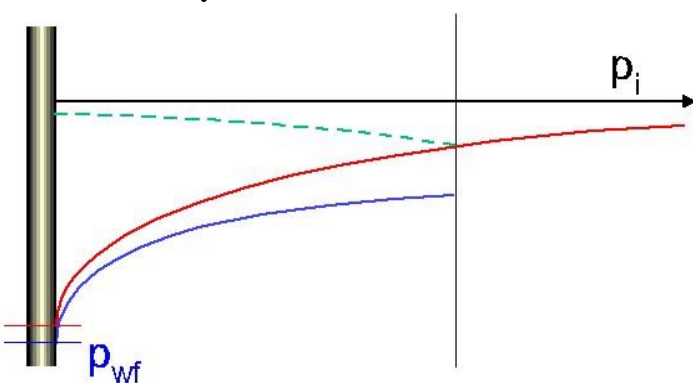


Figure 2.58C Boundary Modeling

The wellbore pressure corresponds to the superposition of the infinite response and its own 'reflection' from the fault. The reflection is equivalent to the infinite-acting response of an 'image' well, at an equal distance on the other side of the fault. Single boundaries are modeled with a single image well, multiple boundaries with an escalating number of image wells.

2.4.4.1 Linear Boundaries

Sealing Fault: The solution is constructed by superposing 2 infinite responses. In reality, the nature of the reservoir beyond the fault is irrelevant, but in the model the reservoir is replaced by an infinite virtual reservoir, which extends beyond the fault. The virtual image well has the same production history as the active well, so that the Δp each side of the boundary is symmetrical, and nothing will flow across it:

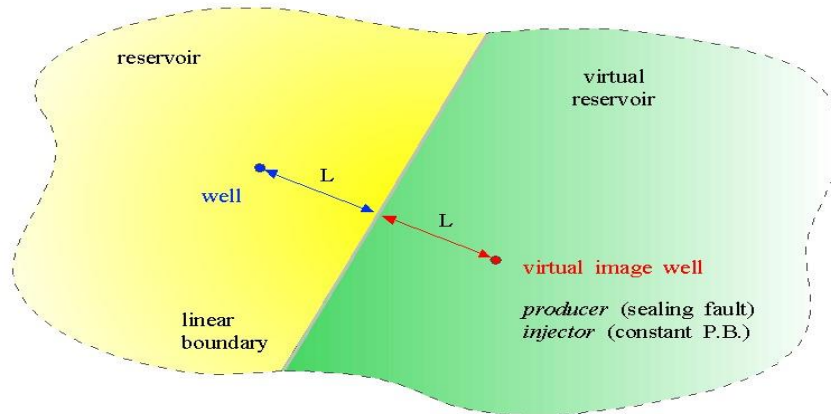


Figure 2.59 Linear Boundaries

- **Constant Pressure Boundary:** The configuration is exactly as above, except the production history at the image well is the inverse of the active well; i.e., if the active well is a producer the image well is an injector, and vice versa. Any point on the boundary is equidistant from the 2 wells, so the Δp from one is balanced by the Δp from the other, and the pressure along the boundary is constant. Note that for the image well approach to be rigorous, the image well(s) should have the same wellbore storage, skin, etc. as the active well. However, the image wells are typically represented by straightforward line sources, which is technically incorrect. Fortunately, the pressure regime around any well, outside the skin-damaged zone, will be almost identical to that around a line source well, with no storage and no skin, as the inner boundary conditions affect only the pressure internal to the wellbore. The deliverability of the reservoir is not changed by the presence of a well, and the only distortion will be the effect on the early-time flowrate in the reservoir, which will not change instantaneously.
- **Pressure Response: When** the semi-log approximation holds for both active and image wells, the overall derivative, which is the sum of the individual derivatives, becomes:

Sealing fault : twice that of infinite system

Constant pressure boundary : tending to 0

In the sealing fault case, the late-time response is identical to the response of an infinite system with a permeability of half the actual reservoir permeability. In the constant pressure response, the derivative is tending to zero, as the pressure stabilizes.

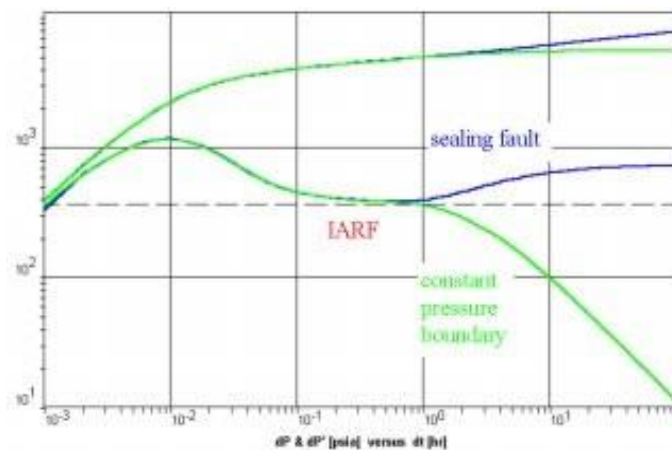


Figure 2.60 Linear Boundary Response

The semi-log response for the sealing fault is a second straight line with double the slope of the IARF line, as seen in the doubling of the derivative.

The constant pressure response is seen to be stabilizing to a value sometimes called the 'average reservoir pressure.

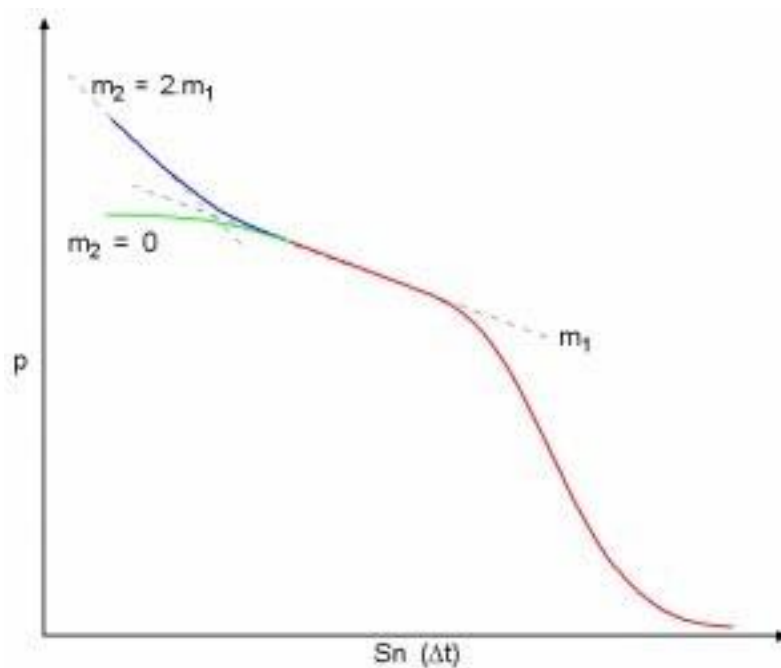


Figure 2.61 Semi-Log Response

2.4.4.2 Circular Boundaries

- **Closed Circle :** The well is at the center of a reservoir limited by a sealing circular boundary, radius r_e . Unlike linear faults, this model has a radial symmetry and can be solved without the need for image wells:

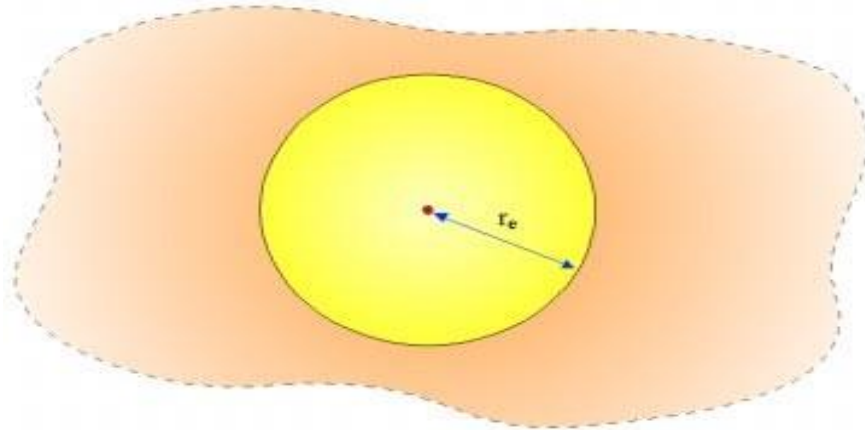


Figure 2.62 Circular Boundaries

When the boundary is seen during a drawdown, the pressure response will transition from radial flow to pseudo-steady state flow, corresponding to depletion and approximated in dimensionless terms by:

$$p_D = 2\pi t_{DA} + a$$

where a is a constant, and t_{DA} is the dimensionless time, in which r_w^2 is replaced by the reservoir area 'A'. During pseudo-steady state flow, Δp is proportional Δt , for a constant flowrate, so there will be a straight line on a linear plot and a unit slope straight line on the log-log plot. The derivative, $2\pi t_{DA}$, is also proportional to Δt , and also follows a unit-slope straight line, as seen overleaf. The build-up response is actually the difference between 2 drawdown responses, at the same point in space but shifted in time.

When the pseudo-steady state approximation holds for both responses the pressure becomes constant, equal to the average reservoir pressure, and the derivative tends to zero.

This is precisely the response of a reservoir with a constant pressure boundary:

The drawdown response in a closed circle (or any closed reservoir) is unmistakable, a unit-slope straight line in late time, on both the log-log and the derivative. The build-up response is the same as for a constant pressure circular boundary, as seen below. (It is too steep to be a linear constant pressure.)

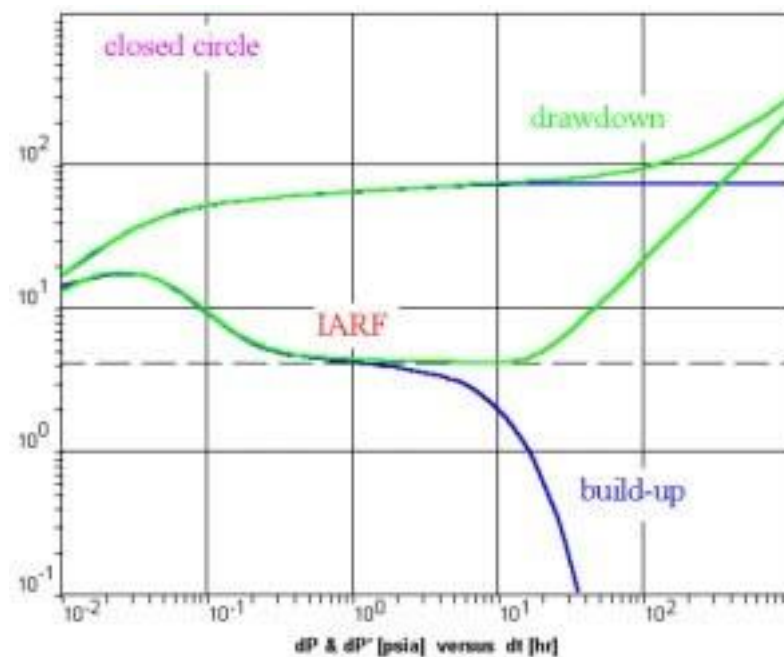


Figure 2.63 Closed Circular Boundary

- **Constant Pressure Circle:** The geometry is the same as for the closed circle, but the pressure at the boundary radius (r_e) is constant. The model again has radial symmetry, and is solved with no image wells.

The qualitative behavior is the same as for a constant pressure linear boundary, namely a pressure stabilization indicated by a plunging derivative, but for a circular boundary the trend is sharper. Drawdowns and build-ups look the same:

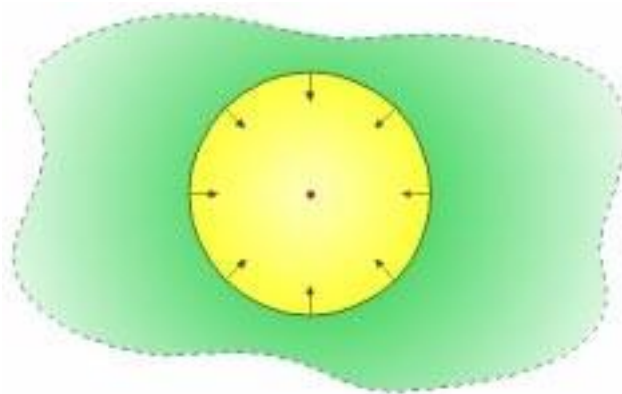


Figure 2.64A Constant Pressure Circle

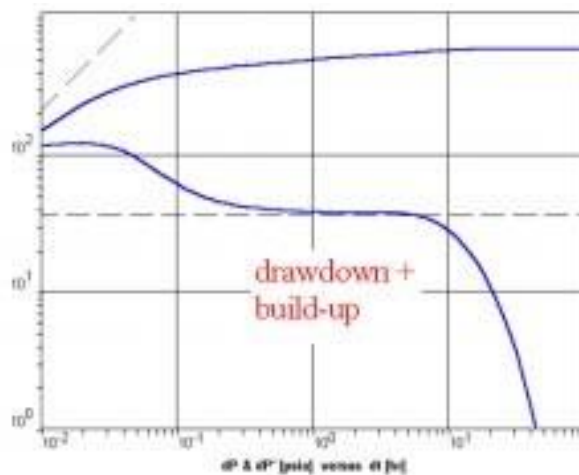


Figure 2.64B Constant Pressure Circle

2.4.4.3 Intersecting Faults

If the first fault is far enough away, infinite-acting radial flow is established after wellbore storage. Until a fault is seen, it will have no effect on the pressure curve. Similarly, the first fault will always cause the derivative to double, as until it is seen the second fault will have no effect. The final stabilization level is determined by the angle between the faults, θ :

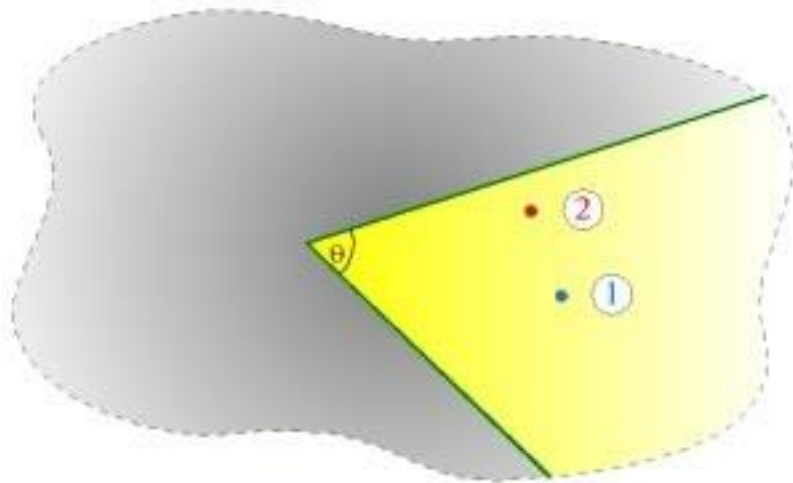


Figure 2.64C Constant Pressure Circle

If the well is centered (1), there will be a single jump to the final stabilization, at a value $360/\theta$ times the initial radial flow stabilization. If the well is much closer to one fault (2), the single fault doubling of the derivative may be seen before a second jump.

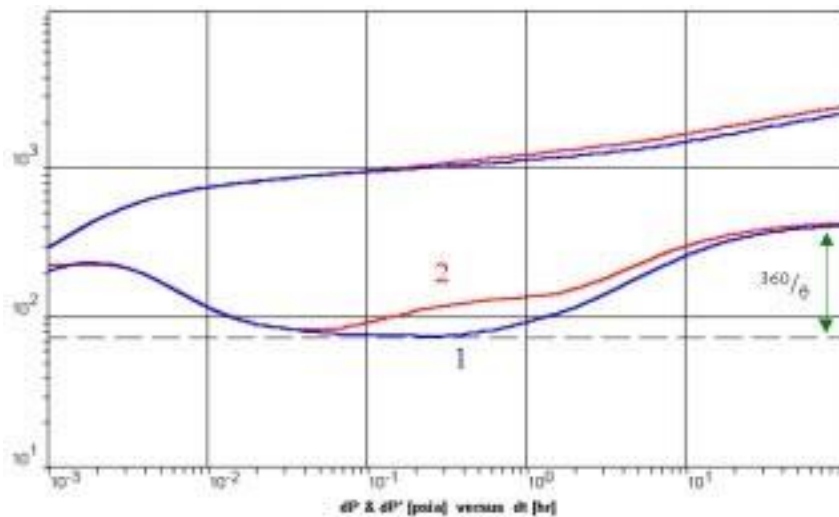


Figure. 2.65 Intersecting faults

When at least one of the ‘faults’ is a constant pressure, the pressure will stabilize and the derivative will tend to zero. The constant pressure boundary will dominate the pressure response, so that nothing more distant will be observed. The total jump in the derivative, between infinite-acting radial flow and the final stabilization, is equal to $360/\phi$. The flow structure in the ‘wedge’ is a fraction of radial flow, so the flow capacity of the system has reduced by that fraction. Just as a single fault reduces the ‘infinite’ reservoir by a factor of 2, and the derivative doubles, faults at 60° would reduce it by a factor of 6, for example, so the total increase in the derivative from the IARF value would be 6. Interestingly, the same rule applies for parallel faults.

2.4.4.4 Parallel Faults (Channel)

The well is either between parallel faults or in a channel:

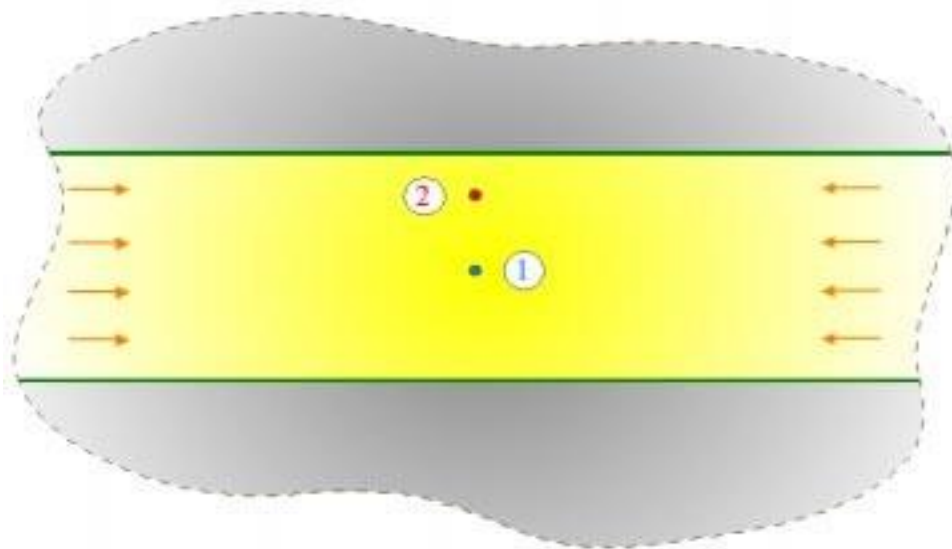


Figure 2.66A Parallel Faults

The late time behavior will be linear flow, resulting in a $1/2$ -unit slope on both the log-log and derivative plots, as for a fracture in early time. Before that there may be infinite-acting radial flow, and there may be a doubling of the derivative due to the first fault being a lot closer than the second:

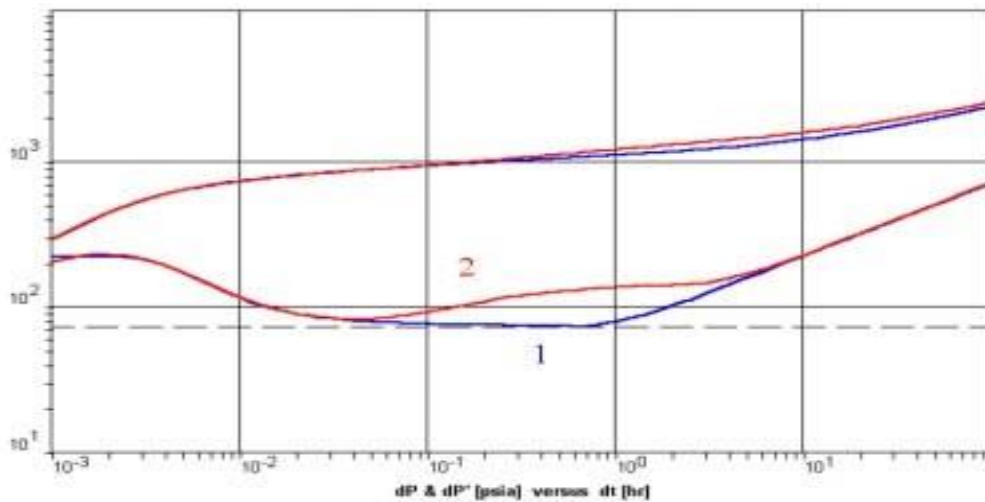


Figure 2.66B Parallel Faults

Note that the $360/\theta$ rule still applies to the total jump in the derivative; in this case, when θ is 0° , it is infinite, and the derivative increases continually at a $1/2$ -unit slope.

2.4.4.5 Mixed Boundary Rectangle

The mixed boundary or composite rectangle has each of the 4 sides either sealing, constant pressure or infinite:

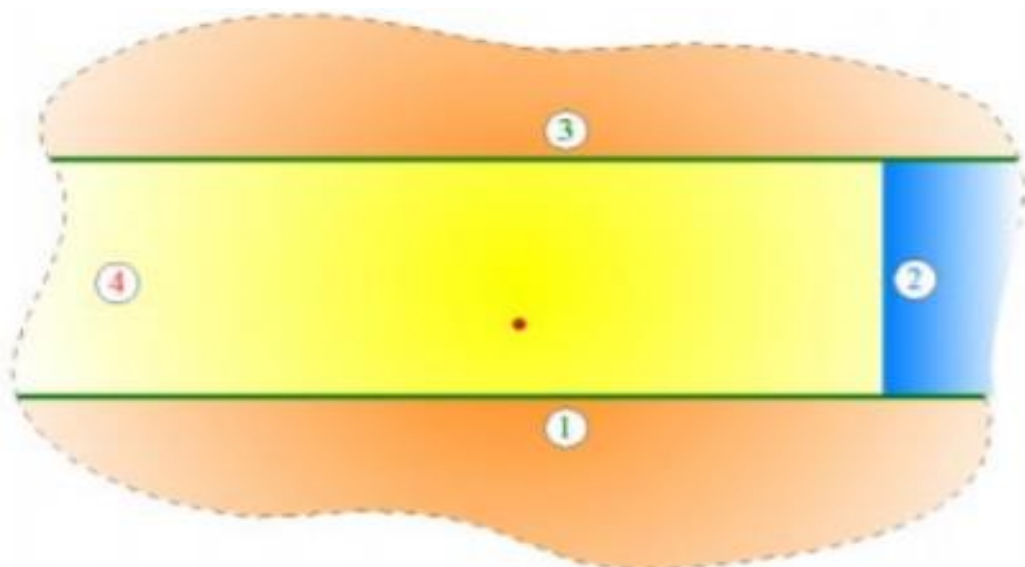


Figure 2.67A Mixed Boundary Rectangle

In this case sides 1 and 3 are sealing faults, 2 is constant pressure and 4 is infinite. The derivative response clearly depends upon the nature of the boundaries and their configuration, but in this case it would be as shown below:

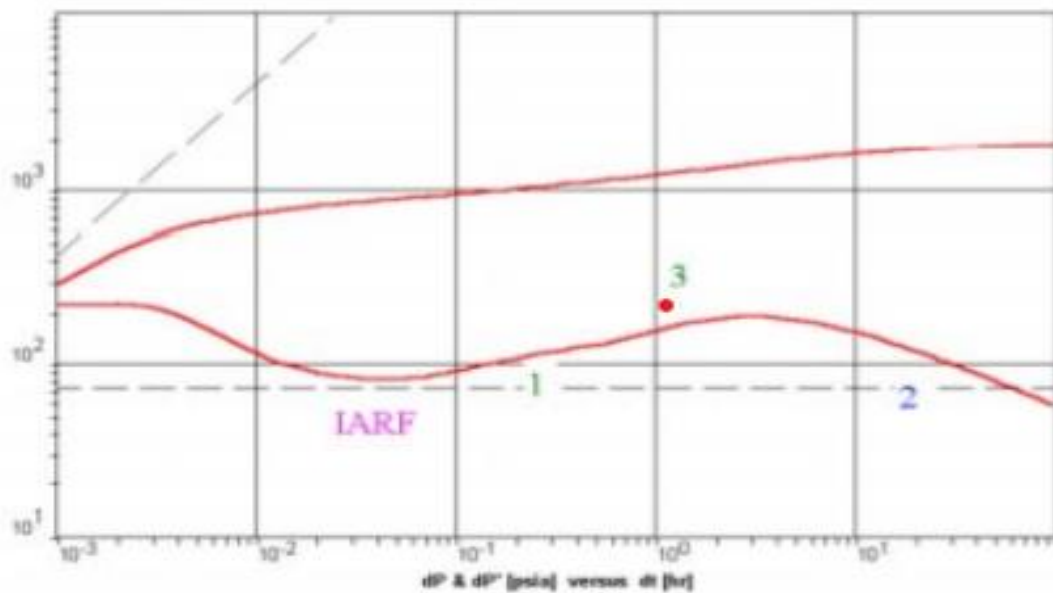


Figure 2.67B Mixed Boundary Rectangle

Note that the decline in the derivative due to the constant pressure boundary is very gradual, as the support is 'competing' with a rapid linear pressure drop along the channel.

CHAPTER THREE

3. Methodology

3.1. Introduction

This project is focused on well test analysis to characterize Qishan clastic member reservoir in Sharyoof field. In order to achieve the aims and objectives of the project, the procedure for buildup test to determine key well and reservoir parameters is given in the (Table 3.1) data available. Data were obtained from Sh-2 in the Sharyoof field and analyzed using well test analysis software Ecrin to assess different scenarios of analytical models then select the most suitable approach that gives the best match.

This section briefly discusses the workflow of the project to achieve the aims and objectives described above.

3.2 Data Required

General data requirement to achieve project are the following:

1. Well data, such as type of well completion, drilling report, stimulation type, and type of artificial lift used, wellbore schematic, etc.
2. Reservoir data, such as pressure, temperature, datum, fluid contacts, etc.
3. Test data, such as pressure gradient data, and variation of fluid rate versus time.
4. Detailed flow rate data prior to and during the test period.
5. Gauge data, such as variation of pressure and temperature data versus time, start and end test date, gauge type, etc.
6. Fluid Property data, (FVF, μ , Co, Cw, Cg or Ct)
7. Petrophysics data, such as Logs, pore volume compressibility, Core analysis data, etc.
8. Geology and Geophysics such as structure maps, boundaries, natural fracturing, layering, fluid contacts..., etc.

The data available that used in this project is shown in Table. 3-1

No	Data Required
1.	DST-2 Drillstem test data sharyoof-2 lower S1A
2.	Wireline Logging Data sharyoof-2(las file)
3.	Completion data

Table 3.1 Data available for the project

3.3. Software Used Description

This study utilizes different software packages, described as the following:

3.3.1 Microsoft Office Package:

Microsoft Office 2021 (Excel, Word and PowerPoint) is used to handle the data, writing graduate project and making presentations for the group discussion and the final graduate project defense



3.3.2 KAPPA ECRIN: is a software that trains and consults in Dynamic Data Analysis; namely, transient and production analysis, production log analysis, data management, modeling and history. Programs, computer-aided well test analysis by use of nonlinear regression became handy and. Ecrin by ETS Company offers analytical and numerical well Investigate possible geological models present. Reinterpretation of performed well tests is conducted using Ecrin Kappa Sapphire software. Well Test software helps you conduct gas and oil pressure transient analysis and serves as an everyday well test data interpretation tool. Decipher reservoir-flow characteristics and predict future deliverability based on buildup and short-term drawdown well test information. Use diagnostic plots, as well as G Function and DFIT analyses for minifrac tests, to identify flow regimes and estimate reservoir parameters. Leverage analytical and numerical models to match the pressure history and generate forecasts.

Kappa Ecrin Software is used In this project to do and interpret some models and analysis the well test to obtain the main Reservoir properties such as Effective permeability, Formation transmissibility, Skin factor, Average Reservoir pressure, Boundary conditions ,Formation heterogeneities including faults and fractures.

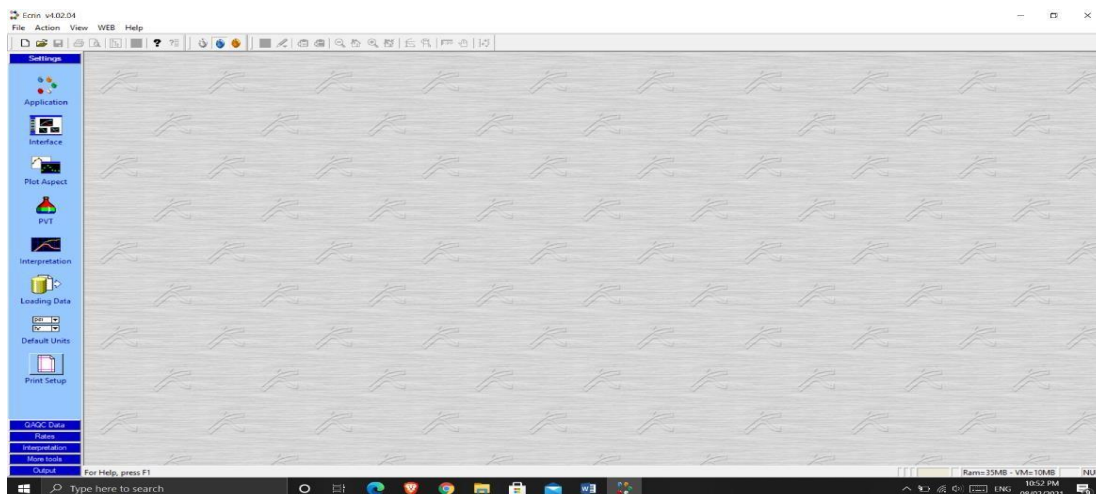


Figure 3.1 shows the display window of Ecrin software

3.3.3 TECHLOG 2015.3: Techlog is a Schlumberger owned Windows based software platform intended to aggregate all the wellbore information. It allows the user to interpret any log and core data. It addresses the need for a single platform able to support all the wellbore data and interpretation integration workflows, reducing the need for a multitude of highly specialized tools. By bringing the whole workflow into a single platform risk and uncertainty can be assessed throughout the life of the wellbore. With the Techlog Quanti module, you can perform log quality control and precomputations of fluid properties followed by a full petrophysical analysis. This workflow can be saved and reused for future work, incorporating Monte Carlo for uncertainty analysis.

Schlumberger techlog is used in this project to do some interpretations, review the wireline logging data then to make sure to identify and determine the top and the bottom of each production zones and Reservoir properties as net pay zone, porosity, permeability, hydrocarbon saturation.

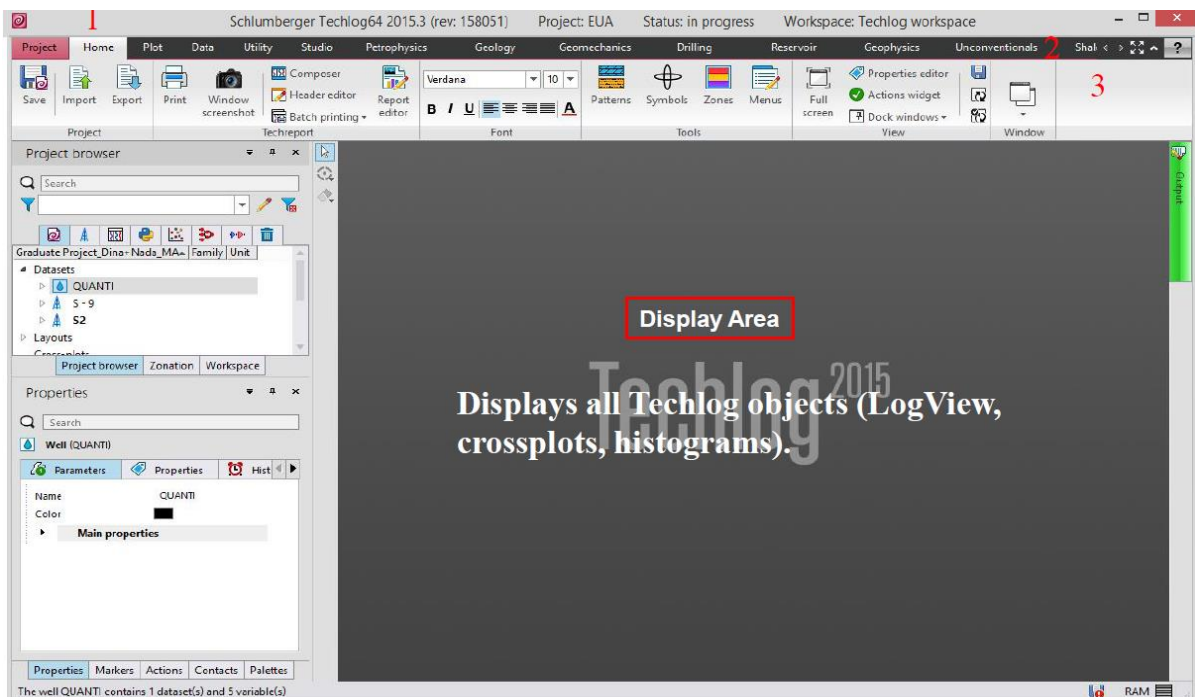


Figure 3.2 shows the display window of TECHLOG 2015.3

3.4. Steps of Study

1. Gather the data required for the interpretation.
 2. Upload PTA data to Ecrin software.
 3. Analysis, quality control, and setting up the data for interpretation.
 4. Break up the test data based on the change in the pressure responses.
 5. Characterize the flow regimes that appear in the test data.
 6. Choose the reservoir model to apply for interpretation.
 7. Determine the parameters that describe the reservoir model by applying manual straight-line and log-log approaches.
 8. Mimic or history-match the pressure response.
 9. If proper, estimate confidence intervals.
 10. Interpret the computed model parameters, and confirm the results.
- Discuss results and make conclusion and recommendations.

3.5. Expected Outcome

The results that we are expected from the well test analysis is to find the following outcome that will use to characterize the reservoir:

1. Recognized if there is any reservoir boundary near sharyoof-2.
2. Estimating distance to and investigating nature of reservoir boundaries
3. Estimating effective permeability at in-situ conditions.
4. Degree of damage or evaluating stimulation treatment effectiveness.
5. Estimating initial or average drainage area pressure.

CHAPTER FOUR

4. Interpretation and Results

4.1 Introduction

This chapter presents the results and analysis of Sharyoof-2 well test data that available which is DST data. Kappa Ecrin and Tech-log and EXCEL2016 are the main tools used for the analysis. The pressure transient analysis was done through EXCEL 2016 and the well test software, Ecrin, as well as Techlog used to analysis petrophysical properties and all the analysis in this chapter was done to characterize reservoir and find out the location and type of boundaries if it is available that would help in understanding the reservoir fluid movements and improve reservoir development plans. Therefore, to successfully interpret a well test result either manually or by the use of computer aided software such as Ecrin sapphire used in this study, we need to understand the well, reservoir and boundary models. In this study, Qishn Clastic is classified into units (S1A, S1B, S1C, S2 and S3). In this study we selected lower S1A unit for well test analysis. The analysis and discussion results of Sharyoof-2 well will present as the following:

4.1.1 Sharyoof-2 Well Summary Overview

4.1.1.1 Drilling and Completion summary

Sharyoof-2 is located in the central-southern part of sharyoof field and it was drilled in November 2000 and encountered oil in the Qishn formation at a depth of approximately 1455.5 m RKB. The 12¼ hole section was drilled down to TD at 1634.5 m RKB and 9 5/8th casing was set. Sharyoof-2 well was perforated over a 3 m interval and completed as ESP pump and the total depth and completion are illustrated in Wellbore Diagram (Fig. 4.1). Sharyoof-2 is producing from Qshin calstic and put on production in December 2001. It is noted that all intervals were perforated instead of net pay that in turn effected on increase water cut.

Well Completion	
Sharyoof-2 Perforated Interval	1455 -1460m RKB A_Upper 1463 -1472m RKB SI A_Lower 1484 -1487m RKB SIC Sand
ESP	Dual Reda ESP
Tubing String	5" drillpipe

Table 4.1 Well Completion

Wellhead Remains
Installed

13-3/8" Casing Cement
Top Job at 30m RKB

20" Casing
At 12m RKB

13-3/8" Casing
At 281.5m RKB

Top of 9-5/8" Cement
at +/- 1300m RKB

Perforations at
1455-60m RKB
Perforations at
1463-72m RKB

Cement Plug at
1425-1475m RKB

Perforations at
1484-87m RKB

Bridge Plug at
1478m RKB

9-5/8" Casing
At 1634.5m RKB

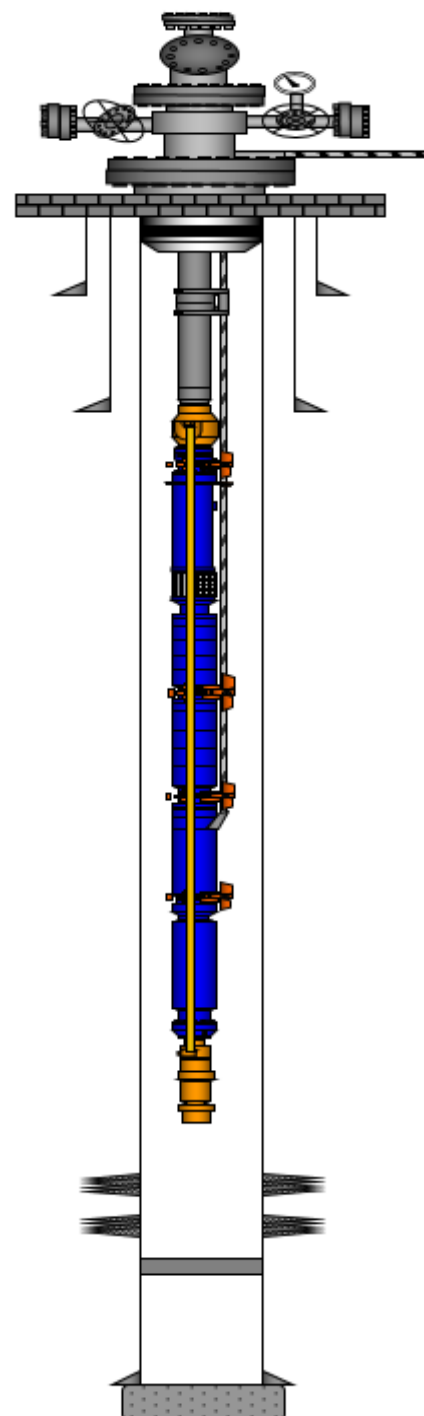


Figure 4.1 Sharyoof-2 Completion Schematic

4.1.1.2 Petrophysical Analysis summary

Based on the petrophysical analysis, three hydrocarbon-bearing zones have been identified. Two zones are indicated in the S1A unit while the third is recognized at the S1C unit (Fig. 4.2).

The first hydrocarbon-bearing zone is a unique clean-sand zone, located at upper part of S1A unit (depth range of 1455.5 - 1460 m) and exhibits good properties values as the Table (4.2) permeability values (range from 2700 up to 3800 mD.)

The second zone is occupied at the lower part of S1A unit of Qishn formation between depths of 1462.5 m and 1472 m. it has good properties permeability range of 1700 mD -3100 mD.

A 100% water-bearing thin shaley zone, with much lower petrophysical parameters, is found separating these two zones.

The third zone is located at the upper part of S1C unit (depth range of 1483.5 m - 1487 m). it shows average permeability 1900 md . The lower part of the S1C is mainly water-bearing. In S1B zone No hydrocarbon content is detected at this well.

Simandux equation was used to calculate the water saturation. The important parameters of Archie equation are cementation factor ($m=1.8$), saturation exponent ($n=2$), tortuosity factor ($a=1$), and formation water resistivity ($R_w=0.98$) . The water saturation was calculated using the values of the calculated parameters and the well log values

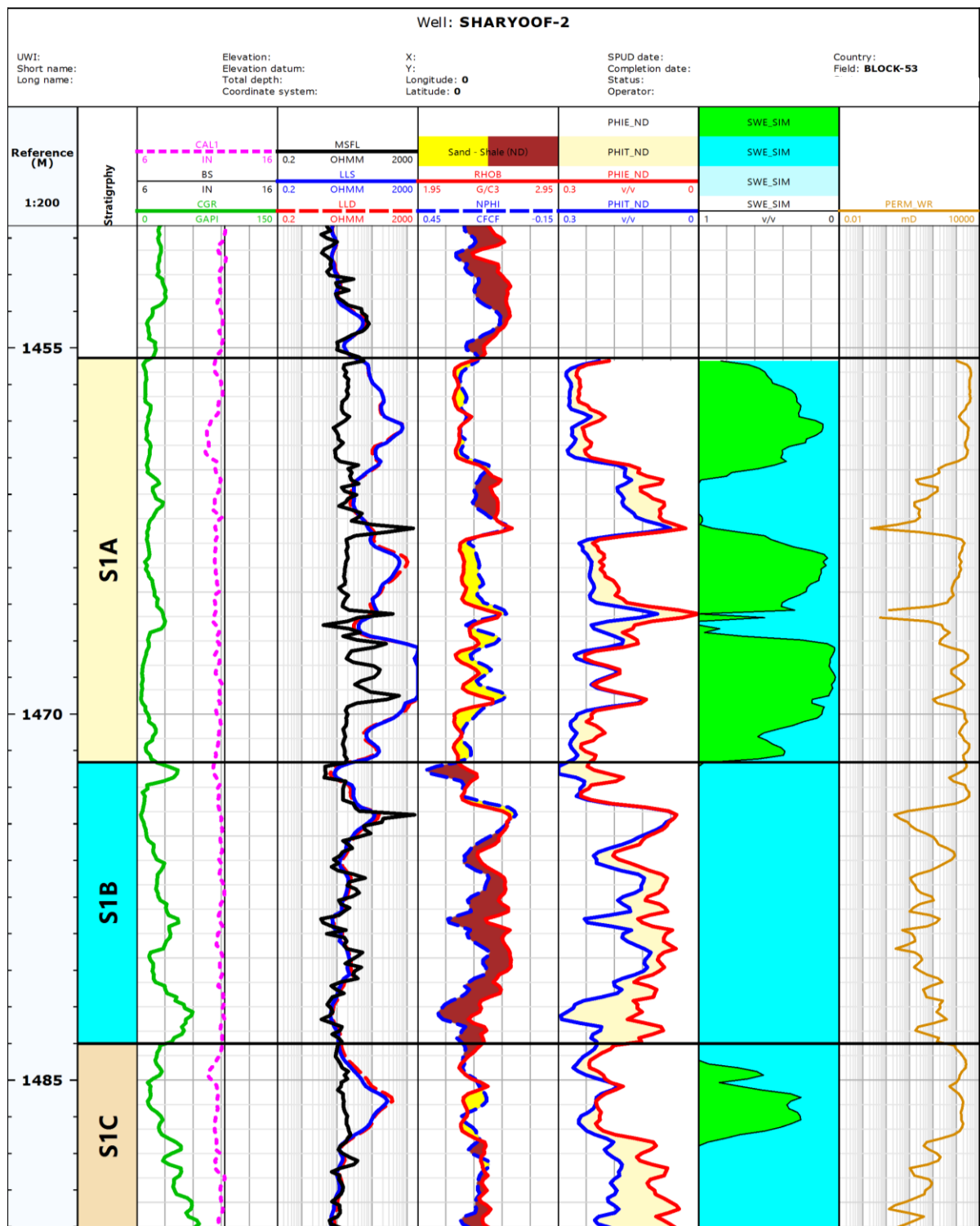


Figure 4.2 Sharyoof-2 well CPI

Sharyoof-2 Petrophysical Properties Summary

Zones	Top	Bottom	Gross	Net Reservoir	Net Pay	Av_Shale Volume	Av_Porosity	Av_Water Saturation
	m	m	m	m	m	Linear		simandux
S1A	1455.41	1471.98	16.57	11.4	10.7	0.2	0.21	0.2
S1B	1471.98	1483.5	11.52	3.4	0	0.1	0.17	0.99
S1C	1483.5	1494	10.5	2.9	2.1	0.14	0.2	0.33

Table 4.2 summarize Petrophysical properties using well log analysis

4.2 DST Overview

An ESP assisted DST-2 was performed on the well over the period 28th November – 1st December 2000. The well was perforated over a 3m intervals. The well was perforated over the S 1A Lower sand and produced dry oil at 4700 bopd for 23 hours. After a 22 hours build-up period (that was analysed) the bridge plug was drilled out and another plug set above the S1A_Lower perforations . The S1A_Upper sand was perforated and the well-produced water cut oil for 6 hours before producing dry oil at 5800 bopd for 15 hours. A 15 hours build-up period followed before the well was plugged back and temporarily suspended. During the entire Sharyoof-2 ESP production testing a pressure gauge installed in the Sharoof-1 monitored the communication between the wells. However the first stage 3hour 42minute was running into the hole and cleaning the well , the second stage 23hour was "drawdown" main flow period, the third stage 22hour was "buildup" main shut-in period, the four stage 12hour was running out of the hole.

Just only DST-2 data for S1A lower is available so the analysis was done on S1A lower build up

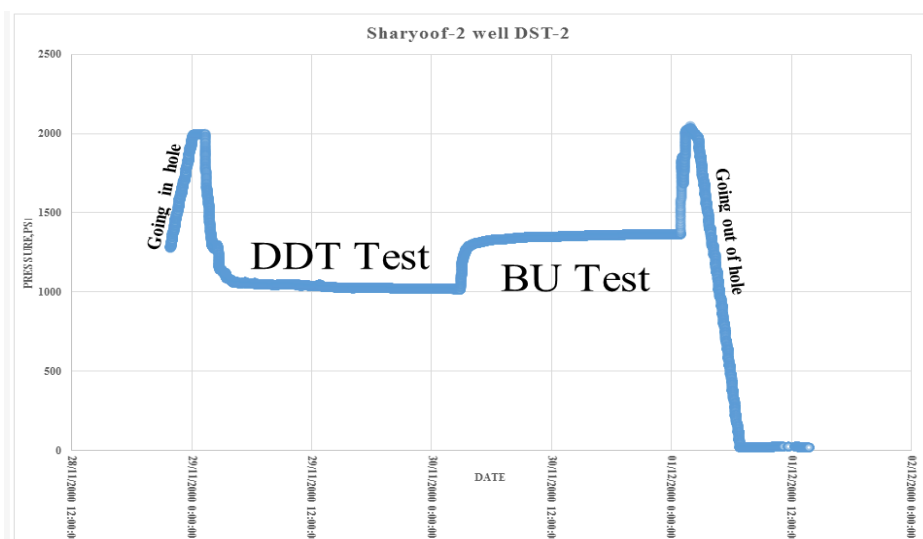


Figure 4.3 DST_2 Lower S1A history plot

4.2.1 Well Test Information

In this project some value parameters are very important that were used in calculation which are oil flow rate (q), oil formation volume factor (Bo), oil viscosity factor (μ), oil compressibility factor (Co), net pay (h), porosity (Φ), water saturation (Sw), Wellbore radius (rw). However (table 4.3) listed the parameters used for equations of well test.

Parameter	Symbol	Result	Unit
Oil flow rate	q	4700	STB/D
Oil formation volume factor	Bo	1.069	BBL/STB
Oil viscosity factor	μ	4.98	CP
Oil compressibility factor	Co	6.2×10^{-6}	Psi ⁻¹
Net pay	h	26.5	Ft
Porosity	Φ	21	%
Water Saturation	Sw	25	%
Wellbore radius	rw	1.02	Ft

Table 4.3 Well and Test Information

4.2.2 Data Validation

Two Downhole gauges were used during the test. The pressure, temperature and time data from both gauges was inputted into Microsoft Excel sheet and Ecrin software for comparison. First is the Pressure data, during the test, there was a difference change 2-10psi between Sharyoof-2 gauges. Both are located at 1433m RKB, therefore the pressure difference is attributed to a systematic in one or both gauges. Second is the temperature data, during the test, there was a 1-3 °F difference between the temperatures recorded by the two gauges. Third is the time data, during the test, there was 5 minutes difference between the times recorded by the two gauges, meaning that at the beginning SLSR 799 recorded 5 minutes before SLSR 840.

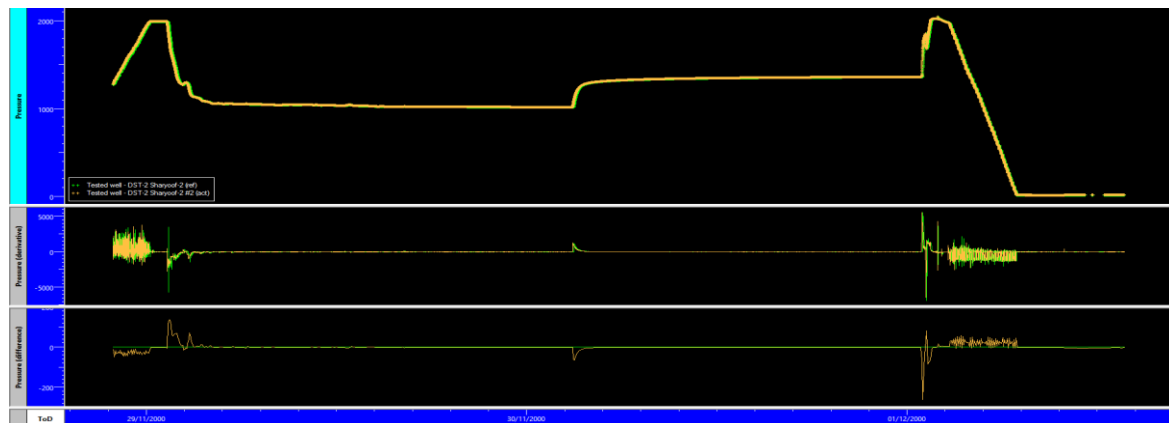


Figure 4.4 pressure gauge comparison

4.3 Pressure Transient Analysis (PTA)

Pressure Transient Analysis (PTA) testing is a primary source of dynamic reservoir data. However, initially called well test interpretation. This type of analysis was performed on data acquired during operations referred to as a well test. In addition, the pressure response, preferably from downhole measurement, and it was generally acquired during pressure build-ups are recorded. In this project we used PTA to predict future deliverability, understand skin damage, permeability and reservoir geometry, and evaluate the presence of limits or boundaries nearby.

Pressure build up analysis in Sharyoof-2 well is using the Horner plot and pressure derivative plot. The first approach is to make a well history plot using software Ecrin 4.20 and EXCEL 2016 by inputting reservoir data, petrophysics, and well flow rate data. History plot is made to interpret the state of the actual reservoir. Figure (4.5&4.6) represents that the top graph shows pressure vs time while the bottom graph shows the oil flow rate vs time.

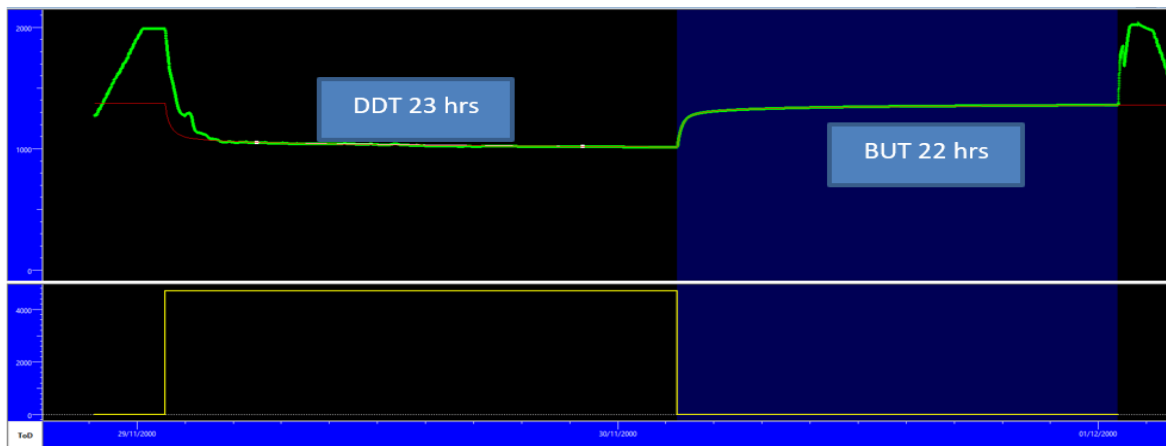


Figure 4.5 History plot using Ecrin 4.2

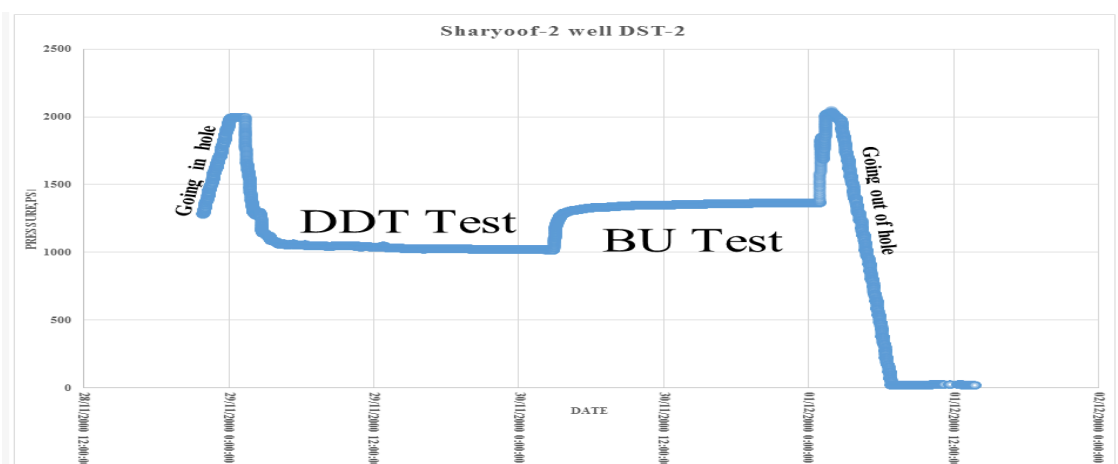


Figure 4.6 History plot using EXCEL 2016

The second approach was done using software Ecrin 4.20 which number of different reservoir models have been used in the analysis of sharyoof-2 well buildup data. During the present analysis three different models were used for interpreting the data generated from the 22 hours Pressure Buildup Study. The three models selected for interpretation of data are: Radial - infinitely acting, Single fault and intersection fault model. All the model's analysis is given below

4.3.1 Pressure Buildup Analysis Using Semi-log method

The method we used to analyze the pressure buildup tests are Horner and MDH Plot methods by using Semi-log on two programs (MS Excel and Kappa Ecrin Software). The Semi-log technique of both Horner and MDH Plot methods used in this project to determine reservoir parameters like permeability, skin factor, and other parameters by plotting pressure data on Semi-logarithmic graphs to simplify the interpretation of pressure transient data. The programs were used to determine the best infinite-reservoir acting by the relationship which between the shut-in pressure and logarithm of the shut-in time. MS Excel sheet and Kappa Ecrin Software were using to identify: Wellbore storage effect, and Middle time region “straight line”. However, we compared the results that we obtained from both programs MS Excel and Kappa Ecrin Software.

4.3.1.1 Semi log analysis using Ms EXCEL 2016:

4.3.1.1.1 Horner Plot method

The Horner Plot on Semi-logarithmic graph with Horner ratios ($t_p + dt/dt$) on (the X-axis) and shut-in bottom hole pressure P_{ws} on (Y-axis).

Horner plot was be made from semi-log plot as shown in Figure (4.7) we put the correct Straight line that represents the good transient state behavior MTR then determine the slope of the semi log straight line, m and calculate the permeability .Extrapolate the straight line to Horner time equal to 1 (infinite shut-in time) and read off P_i (discovery well) the results of analysis are illustrated in table (4.4). To identify the dominant flow regimes influencing the pressure buildup behavior, a log-log plot was generated for Buildup #1. Wellbore storage ETR (early time region), dominates the first $3\frac{1}{2}$ log cycles, after which, the pressure get straight line throughout the remainder of the test MTR middle time region (middle times) and LTR (late time region) not observed fig.(4.8&4.9) then calculate wellbore storage coefficient and in turn period of wellbore storage .

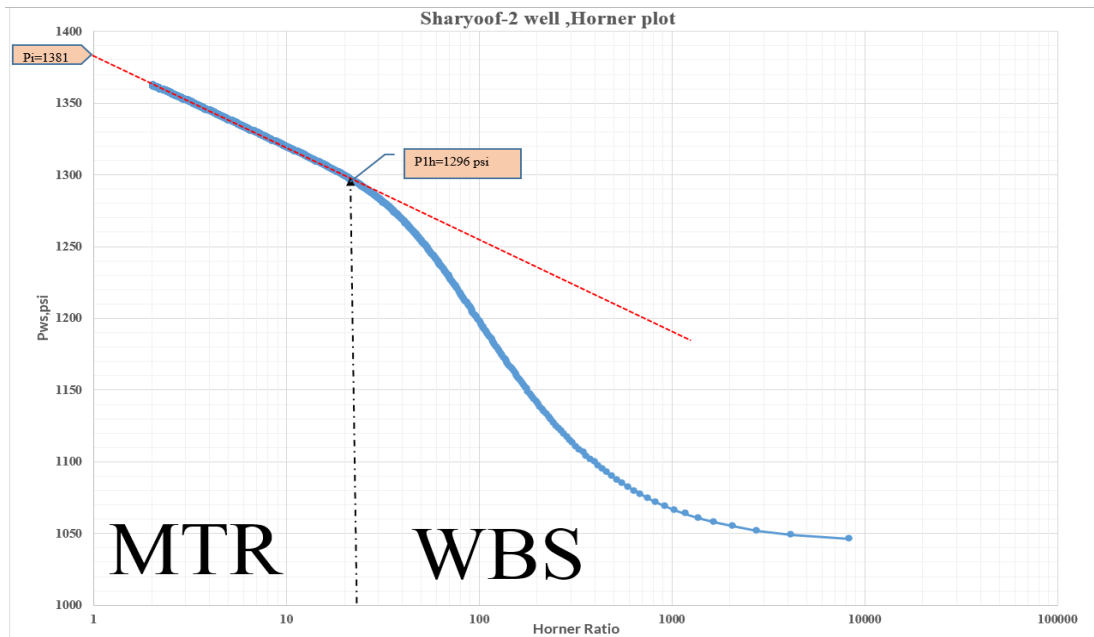


Figure 4.7 Horner Plot Using Ms EXCEL2016

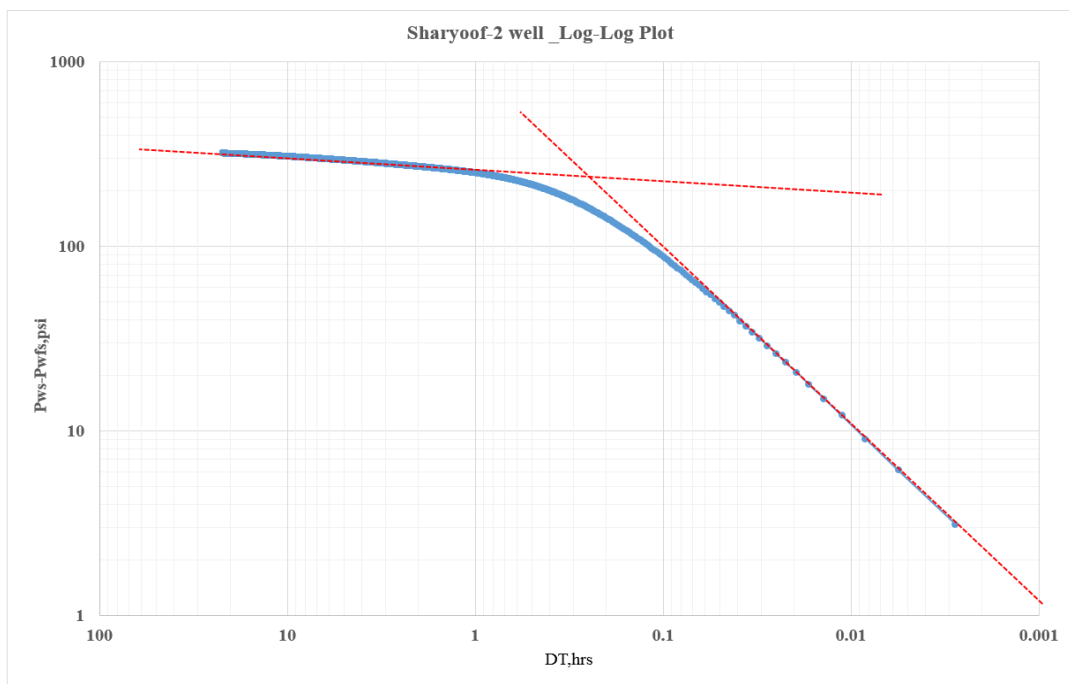


Figure 4.8 Log-log plot

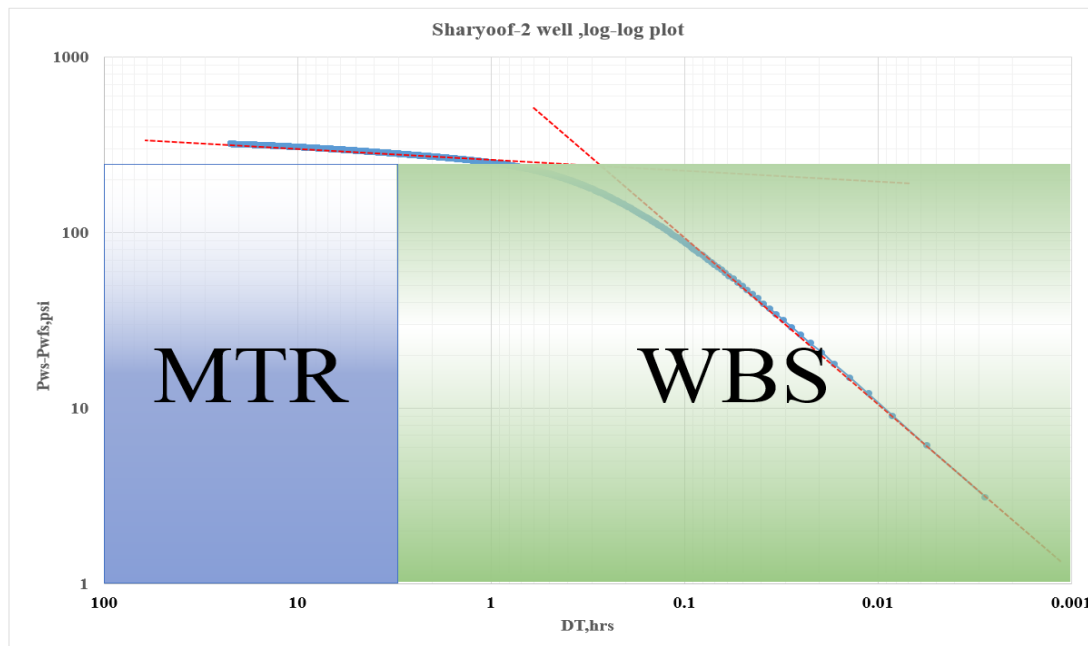


Figure 4.9 Log-log plot

Horner Result Using Ms. Excel							
Parameter	Symbol	Result	Unit	Parameter	Symbol	Result	Unit
Intercept Pressure	Pi	1381	Psia	Flow Efficiency	FE	1.43	
Pressure at one hour	P1hr	1296	Psia	Damage Ratio	DR	0.70	
Slope	m	63		Radius of investigation	Rinv	13443.785	ft
Effective Permeability	k	2437	md	Productivity Index	PI	9.7	bbl/d/Psia
Formation Transmissibility	kh	64578	md.ft	Wellbore Storage	Cs	0.21	BPD/Psia
Skin Factor	S	-2.7		End of the wellbore storage distortion	Twbs	3.17	hours
Pressure Drop due to skin factor	DP Skin	146.581	psi				

Table 4.4 Horner Plot Result Using Ms. Excel

It is clearly from Horner plot figure (4.7) the data at the end of the buildup show no deviation from a straight line that would indicate the presence of a boundary so no indication of any boundary effect and to confirm that we have to use derivative method by using Ecrin software 4.20 as below.

4.3.1.1.2 Miller-Dye-Hutchinson MDH Plot method

MDH Plot on the Semi-logarithmic graph with the logarithm of time (dt) on the (X-axis) and shut-in bottom hole pressure Pws on (Y-axis) .

MDH plot Pws vs Dt was be made from semi-log plot as shown in Figure (4.10) we put the correct Straight line that represents the good transient state behavior MTR then determine the slope of the semilog straight line, m and calculate the permeability. Extrapolate the straight line to tp production and read off Pi (discovery well) the results of analysis are illustrated in table (4.5)

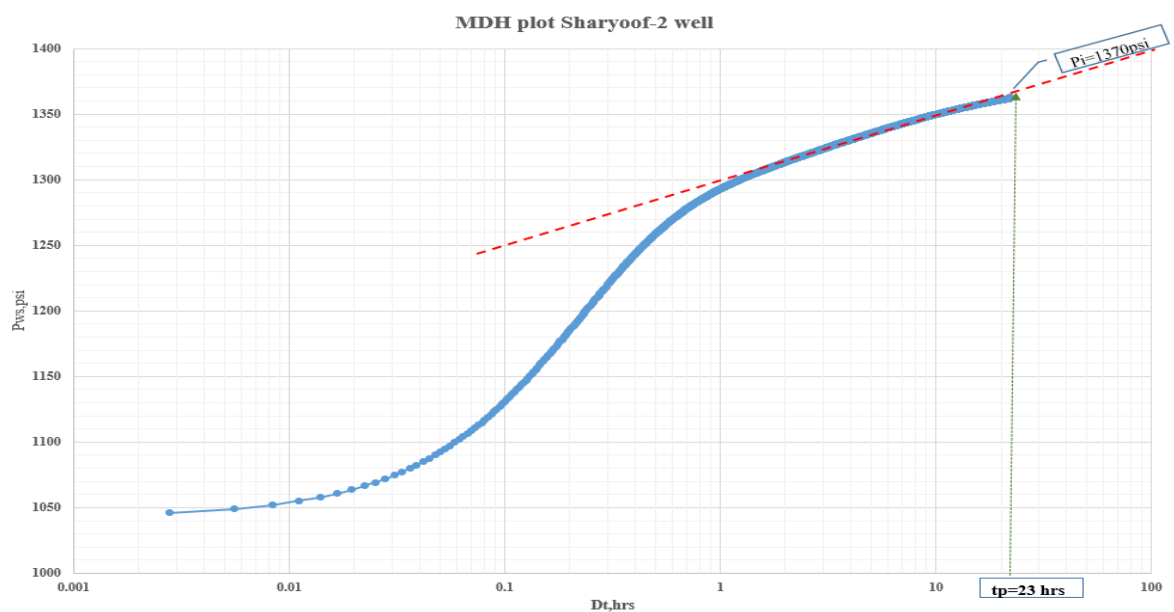


Figure 4.10 MDH Plot Method

MDH Result Using Ms. Excel							
Parameter	Symbole	Result	Unit	Parameter	Symbole	Result	Unit
Intercept Pressure	Pi	1370	Psia	Flow Efficiency	FE	1.2	
Pressure at one hour	P1hr	1300	Psia	Damage Ratio	DR	0.83	
Slope	m	50		Radius of investigation	Rinv	15090.61	ft
Effective Permeability	k	3070.5	md	Productivity Index	PI	12.02	bbl/d/Psia
Formation Transmissibility	kh	81368	md.ft	Wellbore Storage	Cs	0.21	BPD/Psia
Skin Factor	S	-1.5		End of the wellbore storage distortion	Twbs	2	hours
Pressure Drop due to skin factor	DP Skin	-65.18	psi				

Table 4.° MDH Plot Result Using Ms. Excel

In summary, both the Horner method and the MDH method were valuable tools for interpreting pressure-transient data in this project. By utilizing semi-log and analyzing the slopes and intercepts, we inferred key reservoir parameters and gain a better understanding of reservoir behavior. Two scenarios are listed below show the Horner and MDH calculation methods. (Table 4.٦) shows comparation and summarize of the difference values estimated of well test interpretation parameters of lower Qishn Clastic S1A by both Methods of Horner and MDH.

Parameter	Symbol	Semi-log Results		
		Horner Method	MDH Method	Unit
Intercept Pressure	Pi	1381	1370	Psia
Pressure at one hour	P1hr	1296	1300	Psia
Slope	m	63	50	
Effective Permeability	k	2437	3070.5	md
Formation Transmissibility	kh	64578	81368	md.ft
Skin Factor	S	-2.7	-1.5	
Pressure Drop due to skin factor	DPskin	-146.6	-65.18	Psia
Flow Efficiency	FE	1.43	1.2	
Damage Ratio	DR	0.70	0.83	
Radius of investigation	Rinv	2953.34	3315.06	ft
Productivity Index	PI	9.7	12.02	bbl/d/Psia
Wellbore Storage	Cs	0.21	0.21	BPD/Psia
End of the wellbore storage distortion	Twbs	3.17	2	hours

Table 4.1 Comparison and summarize of the difference values estimated of well test interpretation parameters of lower Qishn Clastic S1A for Sharyoof-2

4.3.1.2 Semi-log analysis using Ecrin 4.20 software:

4.3.1.2.1 Horner Plot method

From the software, the Horner plot also can be made from semi-log plot as shown in Figure (4.11).

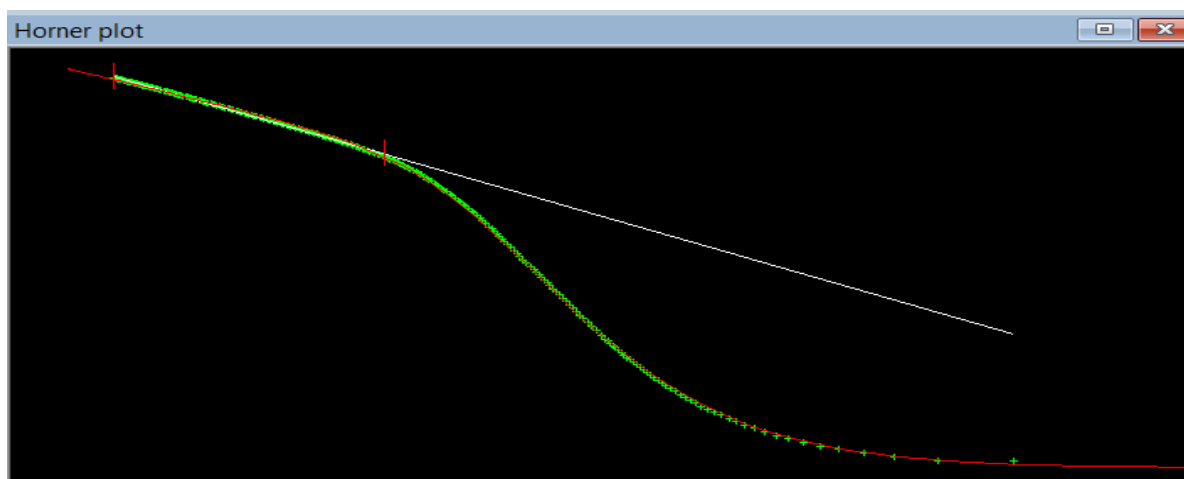


Figure 4.11 Horner Plot Using ECRIN 4.20

Based on the trend line, therefore reservoir parameters can be obtained as shown in Table (4.9)

Horner Result Using Ecrin Software							
Parameter	Symbol	Result	Unit	Parameter	Symbol	Result	Unit
Intercept Pressure	Pi	1382.6	Psia	Flow Efficiency	FE	1.15	
Pressure at one hour	P1hr	1293.04	Psia	Damage Ratio	DR	0.87	
Slope	m	62.87		Radius of investigation	Rinv	2955.16	ft
Effective Permeability	k	2440	md	Productivity Index	PI	11.08	bbl/d/Psia
Formation Transmissibility	kh	64700	md.ft	Wellbore Storage	Cs	0.21	BPD/Psia
Skin Factor	S	-1.02		End of the wellbore storage distortion	Twbs	3.17	hours
Pressure Drop due to skin factor	DP Skin	-56	psi				

Table 4.9 Horner Plot Result Using Ecrin Software

4.3.1.2.2 Miller-Dye-Hutchinson MDH Plot method

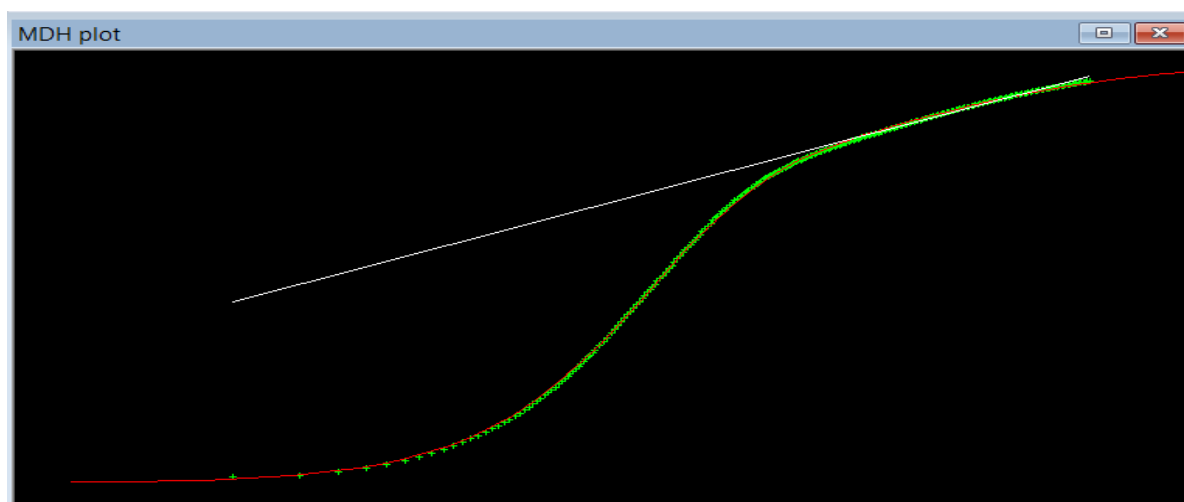


Figure 4.12 MDH plot using ECRIN software

MDH Result Using Ecrin Software							
Parameter	Symbol	Result	Unit	Parameter	Symbol	Result	Unit
Intercept Pressure	Pi	1298.12	Psia	Flow Efficiency	FE	0.21	
Pressure at one hour	P1hr	1298.12	Psia	Damage Ratio	DR	4.76	
Slope	m	50		Radius of investigation	Rinv	3320.19	ft
Effective Permeability	k	3080	md	Productivity Index	PI	17.34	bbl/d/Psia
Formation Transmissibility	kh	81500	md.ft	Wellbore Storage	Cs	0.21	BPD/Psia
Skin Factor	S	0.289		End of the wellbore storage distortion	Twbs	2.52	hours
Pressure Drop due to skin factor	DP Skin	12.57	psi				

Table 4.^ MDH Plot Result Using Ecrin Software

Semi-log Results						
Parameter	Symbol	Horner plot		MDH plot		Unit
		ECRIN	EXCEL	ECRIN	EXCEL	
Intercept Pressure	Pi	1382.6	1381	1298.12	1370	Psia
Pressure at one hour	P1hr	1293.04	1296	1298.12	1300	Psia
Slope	m	62.87	63	50	50	
Effective Permeability	k	2440	2437	3080	3070.5	md
Formation Transmissibility	kh	64700	64578	81500	81368	md.ft
Skin Factor	S	-1.02	-2.7	0.289	-1.5	
Pressure Drop due to skin factor	DPskin	-56	-146.6	12.57	-65.18	Psia
Flow Efficiency	FE	1.15	1.43	0.21	1.2	
Damage Ratio	DR	0.87	0.70	4.76	0.83	
Radius of investigation	Rinv	2955.16	2953.34	3320.19	3315.06	ft
Productivity Index	PI	11.08	9.7	17.34	12.02	bbl/d/Psia
Wellbore Storage	Cs	0.21	0.21	0.21	0.21	BPD/Psia
End of the wellbore storage distortion	Twbs	3.17	3.17	2.52	2	hours

Table 4.⁹ Is comparison semi log methods results from EXCEL and ECRIN software

From Table (4.⁹) Results analysis comparison it is clear, there is no difference between main reservoir parameters as well as there is no any indication of existing sealing fault between two wells.



Horner plot

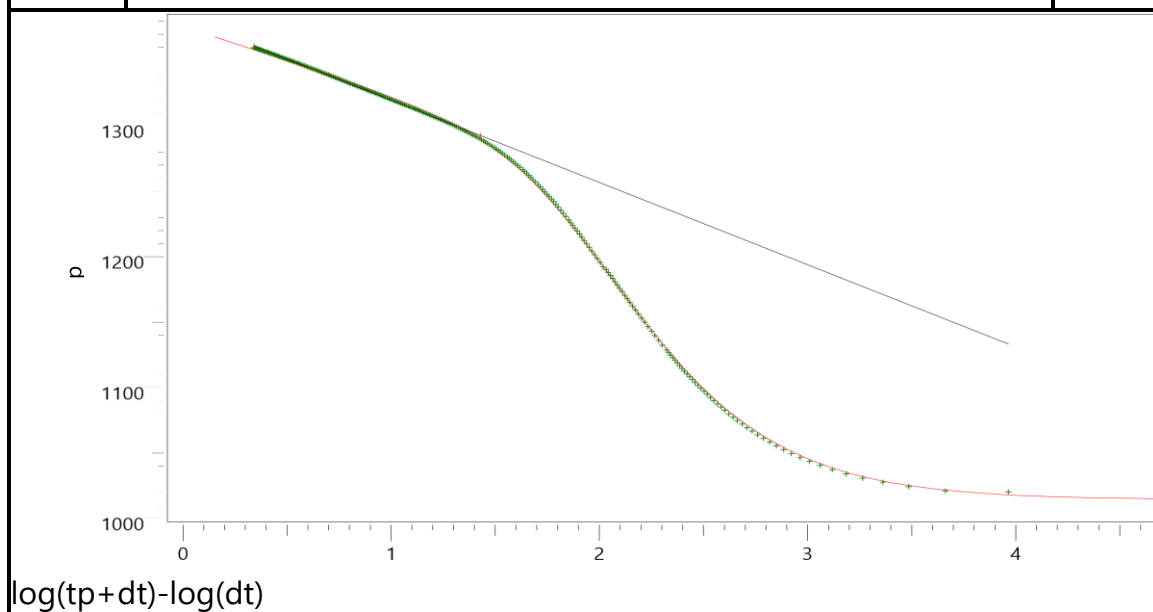
Analysis 1



Company

Field

Well Tested well :Sharyoof-2 Test Name / DST-2 lower S1A



_Line #1 (DST-2 Sharyoof-2 build-up #1)

DST-2 Sharyoof-2 build-up #1

Rate 0 STB/D

Rate change 4700 STB/D

P@dt=0 1014.55 psia

Pi 1375.76 psia

Slope -62.8702 psi

Intercept 1382.6 psia

P@1hr 1293.04 psia

k.h 64700 md.ft

k 2440 md

Skin -1.02

Figure 4.13 Horner Plot Results Using Ecrin 4.20

4.3.2 Pressure Buildup Analysis Using derivative method

Pressure buildup analysis using derivative method is a technique that we used in this project to characterize the behavior of a reservoir after a well has been shut in for a period of time. In this project we make some scenarios of models such as infinite, single sealing fault, and intersecting fault because we want to understand and diagnostic the reservoir. The derivative method is a common approach used in pressure transient analysis to interpret pressure buildup data. The derivative method usually called is diagnostic model because from the model we can interpret and explain what is happening in the reservoir. This pressure derivative method curve arises because the final determination of the wellbore storage effect by using the Horner analysis method cannot provide the accurate results,

In pressure buildup analysis using the derivative method on kappa Ecrin Software to interpreted some models, which can provide insights into the reservoir and well behavior. However, the pressure derivative is calculated by taking the derivative of the pressure data with respect to time.

From this log-log plot results can be used to determine the reservoir boundary by matching the pressure derivative type curve model with Ecrin 4.20. After the matching value is known, then the model can be improved.

We used the derivative method to identify the flow regime in the reservoir, such as boundary dominated flow or radial flow. Moreover, we estimated important reservoir parameters like permeability, skin factor, and reservoir boundaries.

4.3.2.1 Infinite Acting Model:

This model assumes that no lateral boundaries have been observed and is the simplest possible interpretation of the well test. We made the scenario of infinite acting radial flow in pressure buildup analysis because the reservoir is considered to be infinite in extent with no boundaries affecting the pressure response during the test. (Figure 4.14) shows that the pressure derivative on log-log plot against time since the well was shut-in. In the infinite acting radial flow regime, the pressure derivative plot shows a horizontal line indicated that the pressure response is proportional to the logarithm of time. This flow regime is characterized by the pressure response being unaffected by the reservoir boundaries. However, from this model we estimated some reservoir parameters such as permeability, skin factor, and others parameters.

This model provides a compromise between the match to the early flat pressure derivative response and the late time dipping pressure points. The initial reservoir pressure extrapolated from this model is 1377.34 psia,

The infinite acting predicts a reservoir permeability of 33100 md in the S1A_Lower and a skin of 0.527. Although a significantly better match can be achieved with an infinite acting model.

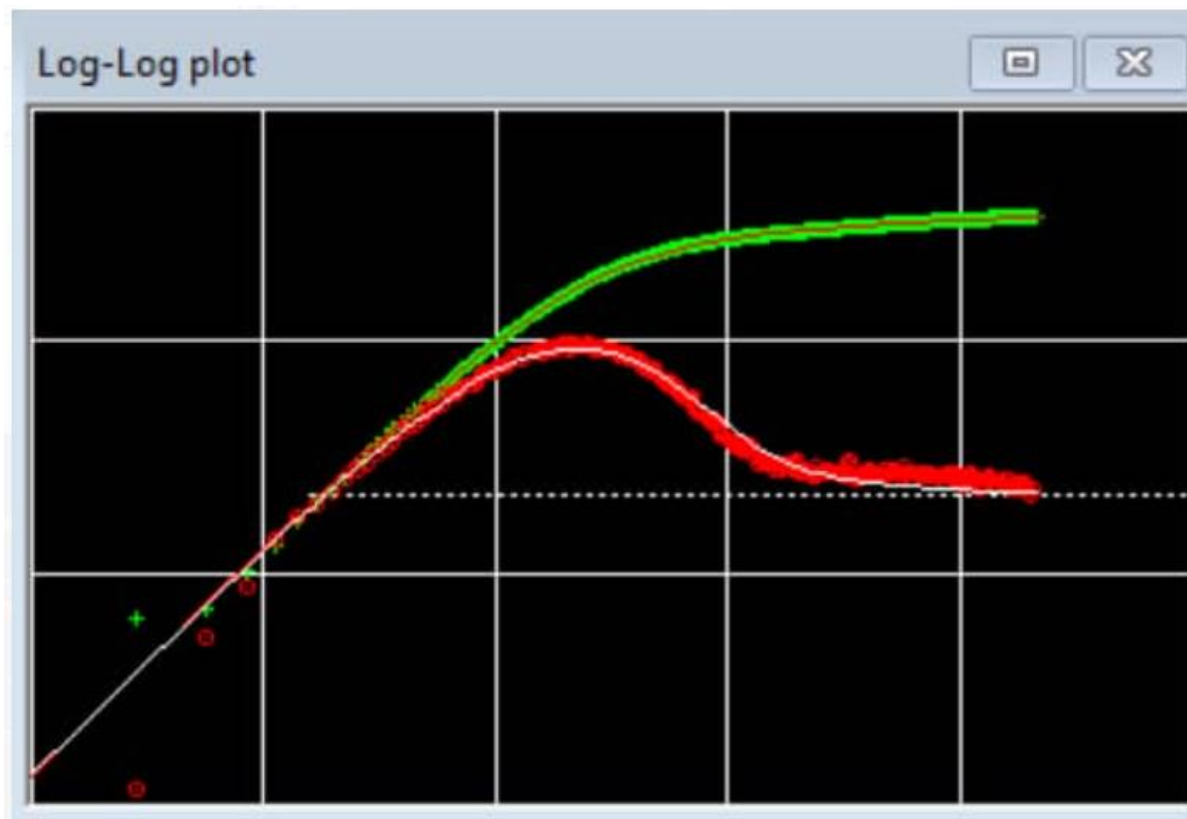


Figure 4.14 Infinte model

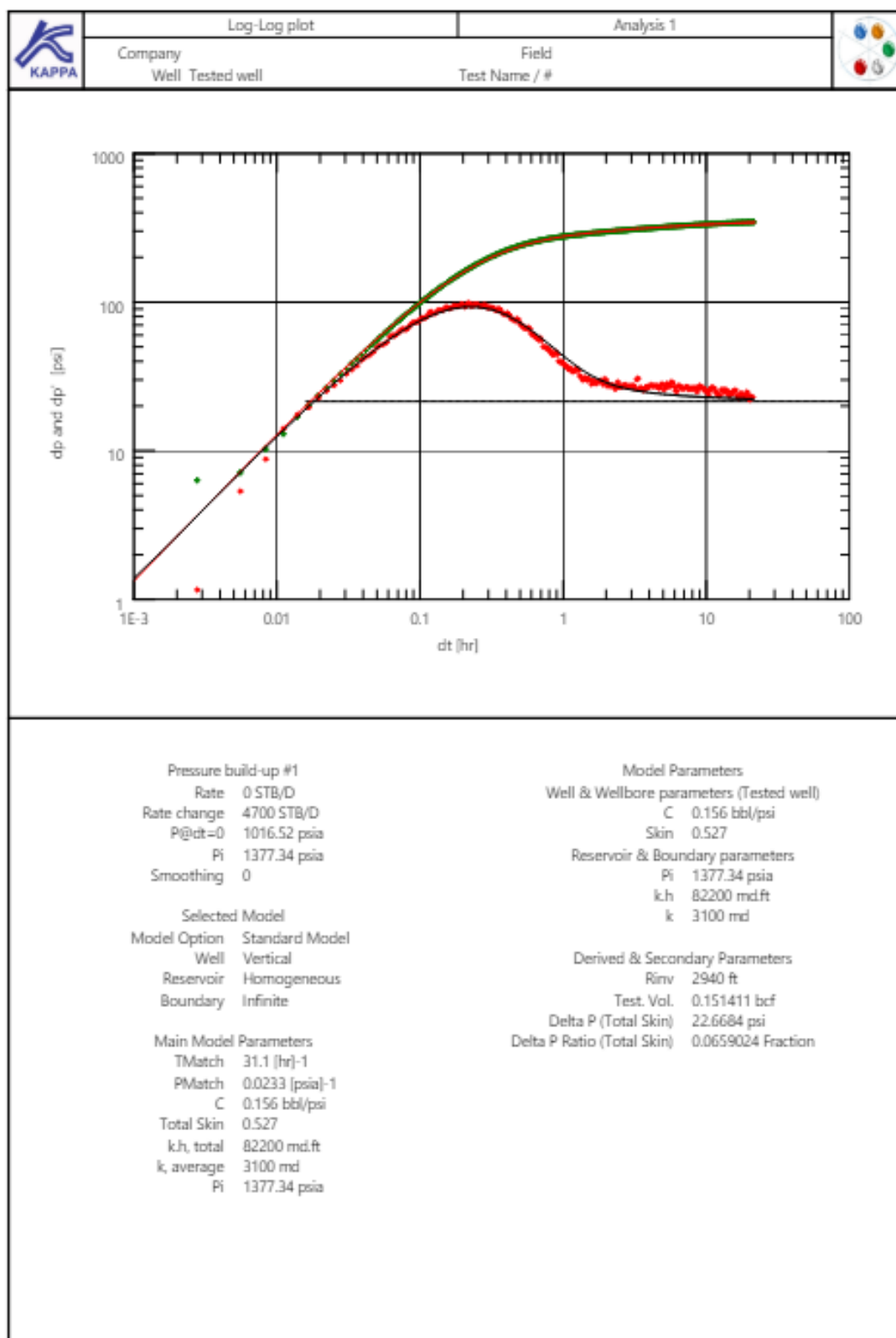


Figure 4.15 Infinte model Plot Results Using Ecrin 4.20

4.3.2.2 Reservoir boundary models:

There are different reservoir boundary models that can be considered in the pressure buildup analysis using the derivative method but we selected tow models single fault and intersecting fault boundary models based on seismic section and structure map figure 1,1. The single fault and intersecting fault boundary models are particularly useful in areas with known fault structures. In both of these models the presence of the faults introduces additional flow regimes that can be identified on the pressure derivative plot. By analyzing the characteristics of these flow regimes can determine the properties and the location of the faults. However, in this project we made both single fault and intersecting fault models but we couldn't recognize if there is a fault.

4.3.2.2.1 Single Fault boundary model:

In this model the reservoir is bounded by impermeable boundaries such as faults or sealing formations. The pressure derivative plot will show radial flow regime at early times then transition to a linear flow regime on log-log plot and the boundary dominated flow regime at late times with an upward trend on the pressure derivative plot. From the analysis of the pressure derivative plot of this model show in (Figure 4.17) we couldn't recognize if there is a fault because it is may be the absence sealing fault near Sharyoof-2 well or the shut-in period time wasn't long enough on other hand, we estimated the permeability from the radial flow regime.

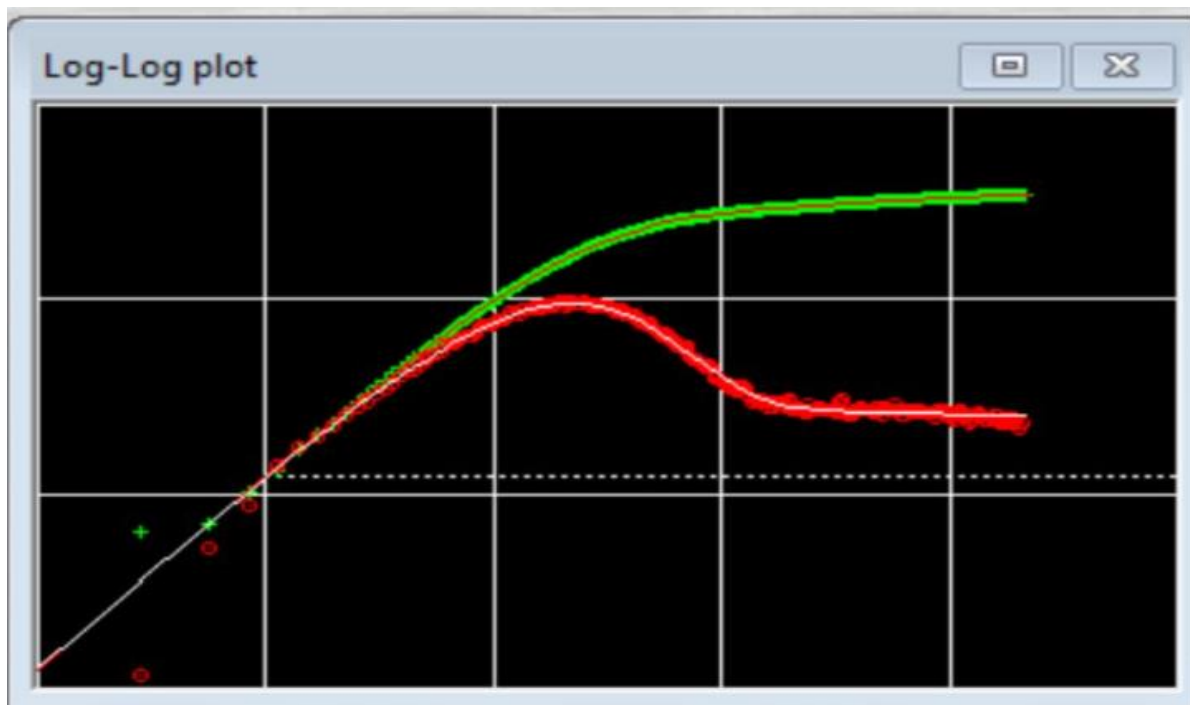


Figure 4.16 Single Fault boundary model

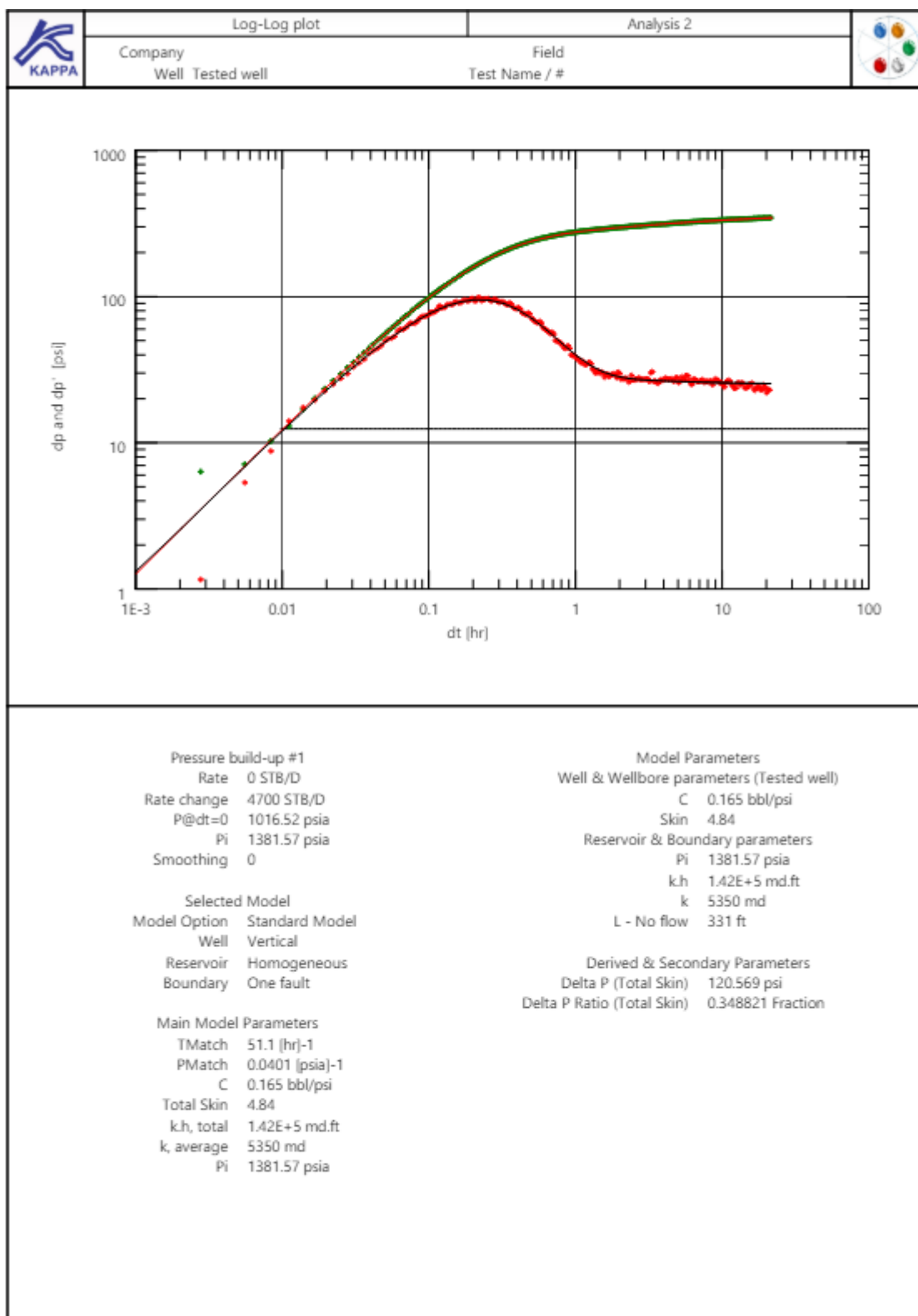


Figure 4.17 Single Fault boundary model Results Using Ecrin 4.20

4.3.2.2.2 Intersecting Fault boundary model

In this model the reservoir is bounded by two intersecting impermeable faults. The pressure derivative plot will show the radial flow regime at early times then the transition to bilinear flow regime characterized by a $1/4$ slope on the log-log plot and the boundary dominated flow regime at late times with an upward trend on the pressure derivative plot. From the analysis of the pressure derivative plot, if the shut-in time was long enough we would estimate the distance to the intersecting faults from the transition to the bilinear flow regime and fault transmissibility from the boundary dominated flow regime. However, from the analysis of the pressure derivative plot of this model shown in (Figure 4.19) we only estimated the permeability from the radial flow regime.

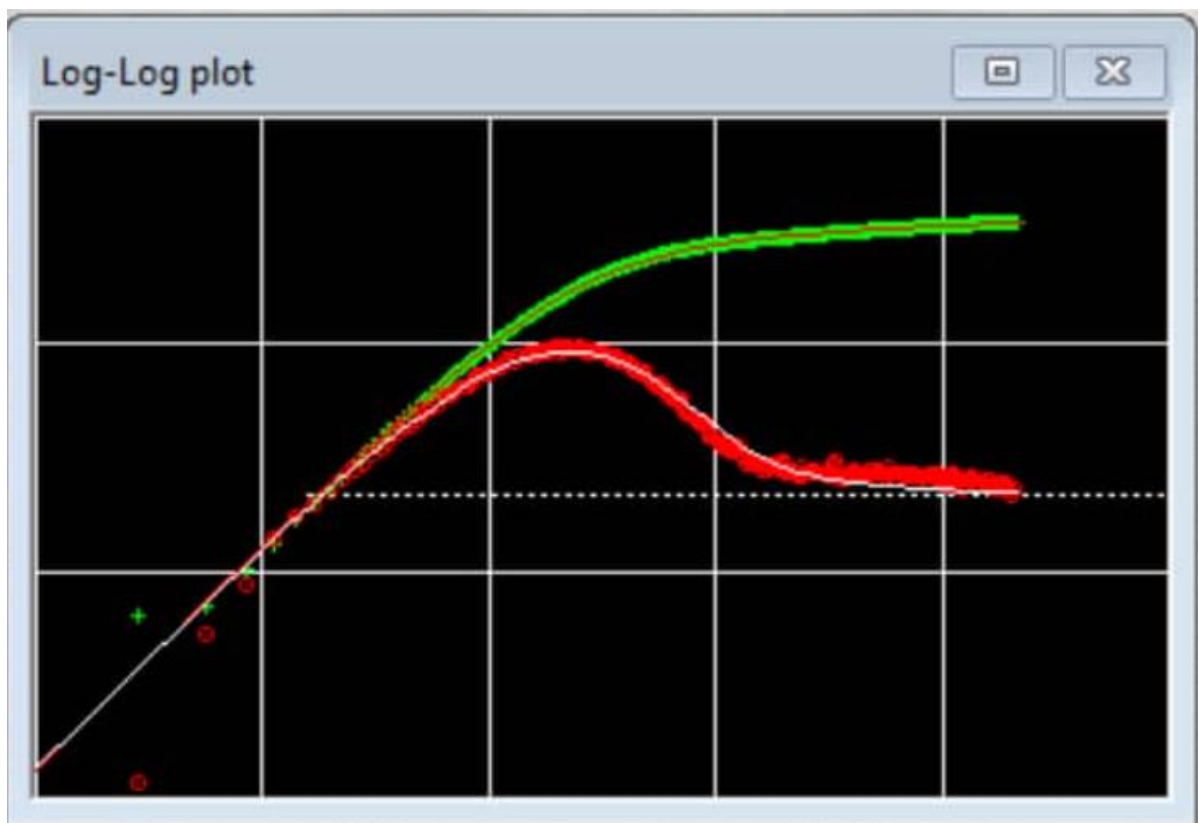


Figure 4.18 Intersecting Fault boundary model

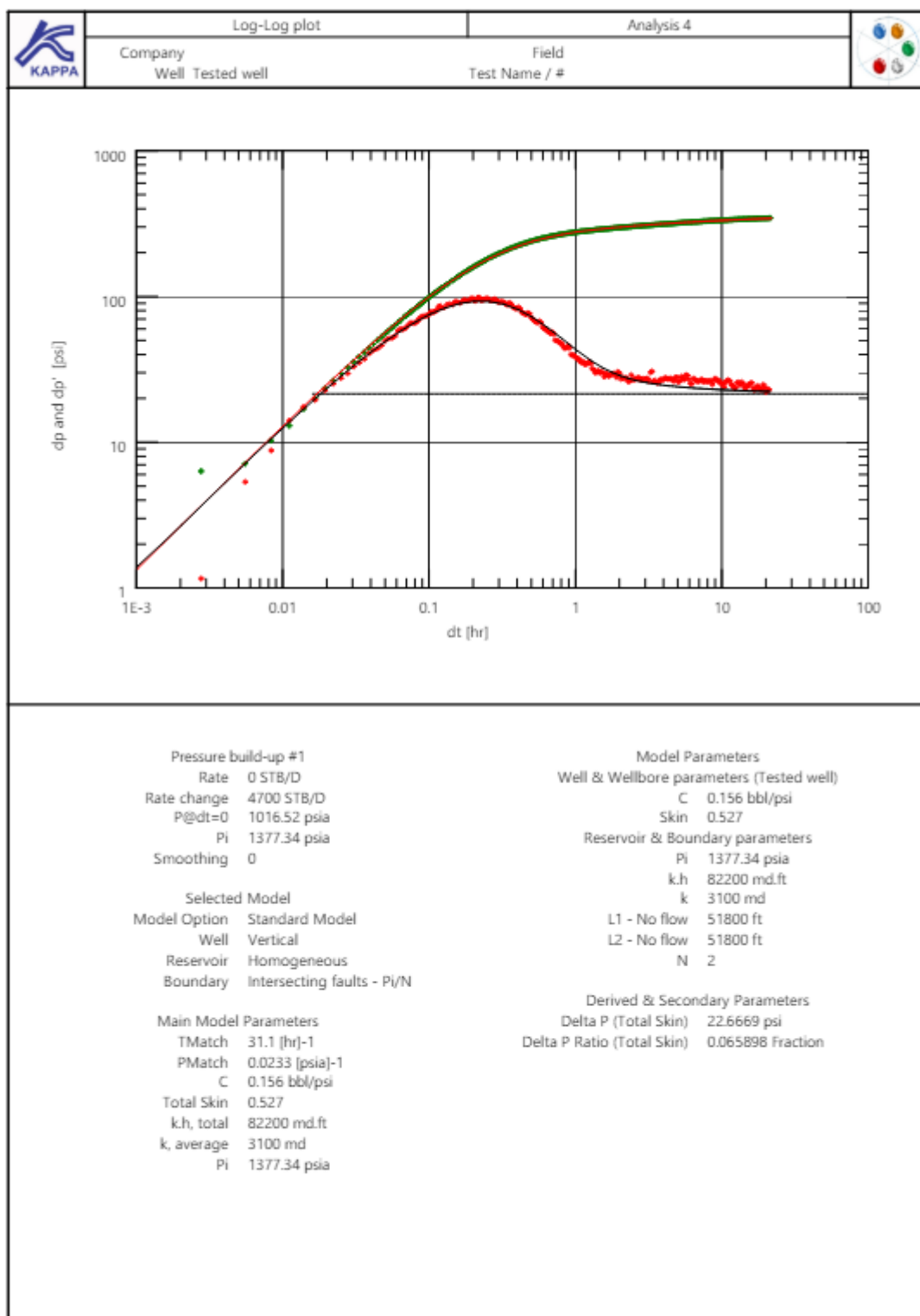


Figure 4.19 Intersecting Fault boundary model Results Using Ecrin 4.20

4.4 Summary Reservoir Characterization and Well Performance Evaluation

Reservoir characterization and well performance evaluation in general is described the reservoir and well properties by using different techniques. The main reservoir characterizations are very important to understand and identify the flow behavior of the reservoir such initial reservoir pressure, porosity, average permeability, water saturation, net pay zone, oil viscosity, formation transmissibility, formation conductivity, formation mobility, and the radius of investigation on the other hand Sharyoof-2 well performance evaluation is necessary to know its performance and determine some parameters such as skin factor, flow efficiency, and productivity index. (Table 4.10 and 4.11) summarize **reservoir characterization** of S1A lower Qishin clastic in Sharyoof field block-53

Reservoir Characterization of S1A lower Qishin clastic in Sharyoof field block-53			
Parameter	Symbol	Result	Unit
Initial Reservoir Pressure	Pi	1377.34	Psia
Porosity	Φ	21	%
Average Permeability	K	3100	md
Water Saturation	Sw	25	%
Net Pay Zone	h	26.5	Ft
Oil Viscosity	μ	4.98	cp
Formation Transmissibility	Kh	82200	md.ft
Formation Conductivity	Kh/ μ	16506	md.ft/cp
Formation Mobility	K/ μ	622.48	md/cp
Radius Of Investigation	Rinv	2940	Ft

Table 4.10 S1A lower Qishin clastic Reservoir Characterization

Sharyoof-2 Well Performance Evaluation			
Parameter	Symbol	Result	Unit
Skin Factor	s	-1.02	
Flow Efficiency	FE	1.15	
Productivity Index	PI	11.08	Bbl/d/Psia

Table 4.11 Sharyoof-2 Well Performance Evaluation

CHAPTER FIVE

5. CONCLUSIONS AND RECOMMENDATIONS

5.1. Introduction

During writing and preparing this project we have reached the conclusion that well Test Analysis is an area of reservoir engineering that deals with understanding reservoir characteristics with principles of fluid flow in porous rock using different techniques. One of them is that Buildup Test Analysis with a different technique of interpretation. There were two methods used of buildup test analysis by using Semi-log and derivative methods in this project.

The interpretation was done through manually by using Microsoft Excel sheet and by using Ecrin Software so we were able to easily and effectively interpret and analyses the data that we had and obtain the reservoir parameters and properties that are very essential to understand and making decisions in oil fields.

2.2 Conclusions

- 1- Semi log and pressure derivative methods, were used to obtain preliminary estimate of the reservoir parameters. These results were later fine-tuned using the pressure history match techniques of the test pressure data
- 2- It is observed that there is no different in the results that we obtained from both Horner and MDH Plots by using Excel Sheet on Semi-log and Ecrin Software on Semi-log
- 3- According to the models that had been used of derivative method that provided us with insights into the reservoir and well behavior as well estimated the parameters of well and reservoir.
- 4- The comparison study reveals that there is not much difference in parameters like the Permeability (k), Skin factor (S), and estimated reservoir pressure between all the methods and techniques that were used to PTA in this project
- 5- Based on the consistent results of both methods, showed that sharyoof-2 well in Sharyoof field have not formation damage, thus no further action is needed such as reservoir stimulation.
- 6- Interpretation of Pressure Transient contributes to the improvement and understanding of the Geological model and the reservoir fluid movements that contributes to improve reservoir development plans

5.3 Recommendations

There are some recommendations for future work as the following:

1. Consider long time build up test to ensure there is no boundaries
2. Interference test should be applied between Sharyoof-2 and Sharyoof -1 to confirm build up test interpretation
3. Consider a PLT on future wells to detect any crossflow between sand intervals
4. Remove seismic fault between Sharyoof-2 and Sharyoof-1 on the Sharyoof structure map
5. The skin shows that the well is not damaged and it is not recommended for stimulation
6. Compare well test results with core analysis results from the same field,
7. It is noted that the well perforation is cover all the net pay interval so ,it is recommended to Perform a cement squeeze in the lower perforations to avoid more water production,

5.4 Limitations

- 1 Difficulty of getting data of study area.
- 2 Unavailability of some well data.
 - a. Bottoms hole pressure data
 - b. Production data
 - c. PVT data
 - d. Core data
- 3 Absence of getting well test type of interference test.
- 4 Absence of drilling report data.
- 5 Absence of Geology and Geophysics data such as structure maps, boundaries, natural fracturing, layering, and fluid contacts.



References

1. Ahmed, T. (n.d.). Well Testing analysis.
2. Amanat U. Chaudhry Oil Well Testing Handbook.
3. Schlumberger Introduction to Well Testing (March 1998).
4. John Lee: “Well Testing”, Society of Petroleum Engineers of AIME – 1982.
5. Tarek Ahmed & Paul D. McKinney: “Advanced Reservoir Engineering” Gulf Professional Publishing is an imprint of Elsevier; USA – 2005.
6. Okotie Sylvester Department of Petroleum and Gas Engineering, Federal University of Petroleum Resources, Effurun, Nigeria Case study Well Test and PTA for Reservoir Characterization of Key Properties Received: 09-02-2015, Revised: 02-03-2015 Accepted: 13-10-2015.
7. 10th Biennial International Conference & Exposition P 078. Reservoir characterization through pressure transient test - A case study in India from the field of Cambay Sub – Asset.
8. Dynamic Flow Analysis, Olivier Houzé (OH), Didier Viturat (DV), and Ole S. Fjaere (OSF) KAPPA 1988-2008.